ADVANCE PER REVOLUTION CONTROL SYSTEM FOR CABLE PEELING ROBOT

by

LUCAS GABRIEL DUBOIS CAMACHO

Submitted in partial fulfillment of the requirements for the degree of
Mechatronics Engineering

Academic Area of Mechatronics Engineering

INTITUTO TECNOLÓGICO DE COSTA RICA

August, 2023

Declaro que el presente Proyecto de Graduación ha sido realizado enteramente por mi persona, utilizando y aplicando literatura referente al tema e introduciendo conocimientos propios.

En los casos en que he utilizado bibliografía, he procedido a indicar las fuentes mediante las respectivas citas bibliográficas.

En consecuencia, asumo la responsabilidad total por el trabajo de graduación realizado y por el contenido del correspondiente informe final.

Cartago, 7 de agosto del 2023

Lucas Gabriel Dubois Camacho

Céd: 305310699

INSTITUTO TECNOLÓGICO DE COSTA RICA
PROGRAMA DE LICENCIATURA EN INGENIERÍA MECATRÓNICA
PROYECTO FINAL DE GRADUACIÓN
ACTA DE APROBACIÓN

El profesor asesor del presente trabajo final de graduación, indica que el documento presentado por el estudiante cumple con las normas establecidas por el programa de Licenciatura en Ingeniería Mecatrónica del Instituto Tecnológico de Costa Rica para ser defendido ante el jurado evaluador, como requisito final para aprobar el curso Proyecto Final de Graduación y optar así por el título de Ingeniero en Mecatrónica, con el grado académico de Licenciatura.

Estudiante: Lucas Gabriel Dubois Camacho

Proyecto: Sistema de control de avance por revolución para un robot descortezador de cables

FELIPE GERARDO MEZA OBANDO (FIRMA)

Digitally signed by FELIPE GERARDO MEZA OBANDO (FIRMA)
Date: 2023.08.07 10:52:39 -06'00'

MSc. -Ing. Felipe Meza Obando

Asesor

Cartago, 7 de agosto del 2023

INSTITUTO TECNOLÓGICO DE COSTA RICA
PROGRAMA DE LICENCIATURA EN INGENIERÍA MECATRÓNICA
PROYECTO FINAL DE GRADUACIÓN
ACTA DE APROBACIÓN

Proyecto final de graduación defendido ante el presente jurado evaluador como requisito para optar por el título de Ingeniero en Mecatrónica con el grado académico de Licenciatura, según lo establecido por el programa de Licenciatura en Ingeniería Mecatrónica, del Instituto Tecnológico de Costa Rica.

Estudiante: Lucas Gabriel Dubois Camacho

Proyecto: Sistema de control de avance por revolución para un robot descortezador de cables

Miembros del jurado evaluador

JUAN LUIS CRESPO MARIÑO (FIRMA)
Firmado digitalmente por JUAN LUIS CRESPO MARIÑO (FIRMA)
Fecha: 2023.08.07 14:21:50 -06'00'

Dr. -Ing. Juan Luis Crespo Mariño

Jurado

ARYS INDIRA CARRASQUILLA BATISTA (FIRMA)
Firmado digitalmente por ARYS INDIRA CARRASQUILLA BATISTA (FIRMA)
Fecha: 2023.08.07 16:13:43 -06'00'

Dra. -Ing. Arys Carrasquilla Batista

Jurado

TEC | Tecnológico de Costa Rica
Firmado digitalmente por ANA GABRIELA ORTIZ LEON (FIRMA)
Fecha: 2023.08.07 14:14:22 -06'00'

Dra. -Ing. Gabriela Ortiz León

Jurado

Los miembros de este jurado dan fe de que el presente proyecto final de graduación ha sido aprobado y cumple con las normas establecidas por el programa de Licenciatura en Ingeniería Mecatrónica.

Cartago, 7 de agosto del 2023

ADVANCE PER REVOLUTION CONTROL SYSTEM FOR CABLE PEELING ROBOT

Abstract

by

LUCAS GABRIEL DUBOIS CAMACHO

This graduation project presents the design process of a device for detecting a 240 mm^2 XLPE type medium voltage cable. The device accurately measures the cable's position within a range of 150 to 240 mm from the cable end. The aim is to integrate this device into a cable peeling robot, controlling the advance per revolution with an on-off control system. To achieve this, the project investigates the most suitable technology for position tracking with sub-1 mm inaccuracy. The device utilizes a novel position tracking caster wheel system, rotary encoders, and presence-absence sensors. A gear-box mechanical system adjusts sensor sensitivity, while a slippage avoidance system prevents accuracy losses due to wheel-cable friction. Custom signal processing and filtering facilitates manual testing. The device underwent thorough testing and analysis for integration with the robot, achieving an impressive accuracy of 0.679 mm or 0.28% at its maximum range. Implementing this device in the industry can significantly reduce cable splicing failures and eliminate problems stemming from incorrect cutting distance measurements.

Keywords: Cable splicing automation, medium voltage cable peeling, caster wheel, novelty position tracking methods.

DEDICATION

To my family, you have always been my unwavering support and never ceased to believed in me. You encouraged me to always give it all and provided the means and values to endure this challenge. I'm very grateful for your love and care, without you not a single word would have never been written on this document. Even though I'm now living far from you, my gratitude crosses every border or ocean between us and reaches each of your loving arms. This thesis is dedicated to you, my parents and siblings as a very long and technical thank you.

To my friends, you always cheered me up in tough times and accompanied me in the happiest of moments with invaluable emotional support. A special thank you to those of you who were part of this fun and enduring five-year-long adventure as class-mates, you gave me the energy and motivation to become an engineer and have so much joy in the process. I'll never forget the endless nights of studying, coffee and laughter that we shared together and I'll always cherish the moments when eating pinto at the university cafeteria. This thesis is dedicated to you as a symbol of unity, because we were a strong team that I hope I come across again in my career.

To all my housemates, to the ones I had in Cartago that made coming home after school a family reunion, your presence in our shared space has transformed our humble abode into a sanctuary of academic growth and camaraderie, reminding me that I am not alone in this pursuit of knowledge. Also to the ones in Enschede, who received me as a student from the other side of the world and treated me like one of their own without hesitation. Thank you for sharing more than a roof but becoming the most real and cherished friends I could ever ask for. This thesis is dedicated to you as a token for eternal brotherhood.

Finally to my university teachers, who shaped my academic growth and graciously shared their knowledge. Thank you to those in my faculty who always gave the extra mile and created a friendly and entertaining learning space which encouraged me to wake up early morning to hear your pure spoken knowledge. This thesis is dedicated to all of you as a symbol of respect for your admirable dedication.

With profound love and gratitude,

Lucas Dubois

ACKNOWLEDGEMENTS

I would like to express my deepest gratitude and appreciation to the following individuals and institutions who have played a significant role in the completion of this thesis:

First and foremost, I am immensely grateful to my university supervisor Felipe Meza and my Robotics and Mechatronics supervisor Tim Elderhorst. Your guidance, expertise, and unwavering support have been invaluable throughout this research journey. Your insightful feedback and ideas have shaped the direction of this thesis and challenged me to grow both intellectually and personally.

I extend my heartfelt thanks to the faculty and staff of the RAM group, for creating an environment conducive to learning and research. The resources, facilities, and opportunities provided have been instrumental in the successful completion of this study. I am grateful for the academic rigor and intellectual stimulation that have enriched my educational experience.

I would like to express my sincere appreciation to the members of my thesis committee, Juan Luis Crespo, Gabriela Ortiz and Arys Carrasquilla. Your expertise, scholarly input, and valuable suggestions have significantly contributed to the development and refinement of this thesis. I am grateful for the time and effort you have dedicated to reviewing my work and providing thoughtful guidance.

I am indebted to the participants who generously gave their time and shared their experiences, perspectives, and insights, making this study possible. Their willingness to participate and contribute has enriched the findings and added depth to the research. I am deeply grateful for their valuable contributions.

To all those who have contributed, directly or indirectly, to the completion of this thesis, I extend my heartfelt appreciation. Your support, encouragement, and belief in my work have made this achievement possible. Thank you for being part of this journey and for shaping me into the person I am today.

With utmost gratitude,

Lucas Dubois

TABLE OF CONTENTS

LIST OF TABLES

LIST OF FIGURES

LIST OF ABBREVIATIONS

F_N Normal force between cable and mechanical switch. 82

F_f Friction force. 77

F_w Friction force on wheel. 77, 78

T_{1mm} Typical time for the device to advance 1 mm. 30, 31

$T_{s,d}$ Distance tracking sensor delay. 30, 31

$T_{s,z}$ Zero detection sensor delay. 30, 31

T_{total} Total delay. 30, 31

V_{DC} DC value of a signal. 86

X_D Sensed value. 96

X_R Real measured value. 96

ΔS Linear distance travel. 53, 69

$\Delta\theta$ Change in angle at the wheel axis. 53, 69

$\Delta\,\mathbf{y}$ Ruler deviation from the cable axis center at the maximum point of measurement. 14

α Reliability. 11

α Wheel angular displacement. 70, 71

$\hat{p}$ Estimated proportion. 11

$\hat{q}$ Estimated complement of proportion. 11

μ Friction coefficient. 77

θ_{max} Maximum angular error sensed by the swivel. 71

θ Inclination angle. 77

θ Swivel angle. 70, 71, 91, 92

A Additive error. 96

A Displacement along the cable axis. 70, 71, 91

ADC Analogue-Digital Converted. 110, 138

D Rotational displacement around the cable. 70, 71, 91

DC Direct current. 56, 86, 128

DPI Dots per Inch. 48

E Error. 14, 30, 31, 71

e Relative error. 11

F Spring force. 79

FFT Fast Fourier Transform. 128

FGP Final Graduation Project. 2

FOS Factor of safety. 119, 121, 122, 127

GHG Green house gases. 1

k Hooke's constant. 79

L Caster wheel lead distance. 78

M Multiplicative error. 96

M Torque. 77, 78

N Normal Force. 77, 78

N Sample number. 86

n Number of samples. 11

PLA Polylactic acid. ix, 34, 51, 52, 76, 80, 107

R Reaction force. 82

r Radius. 53, 69–71, 77, 78

RAM Robotics and Mechatronics. 1, 28, 47, 113, 115, 137

RF Radio frequency. 74

ROI Return of Investment. 136

RPM Revolutions per minute. 99

UT University of Twente. 1

V Sample Value. 86

x Spring compression. 79

XLPE Cross-linked polyethylene. 1–3, 5, 23

z Area under the normal curve. 11

Chapter 1

INTRODUCTION

1.1 Environment

This project was developed at the Robotics and Mechatronics (RAM) group in the University of Twente (UT) premises, localized in Enschede, Overijssel, The Netherlands. Resources were given by the Alliander organisation, which is a group of companies that provide innovative and sustainable solutions and services for the Dutch energy industry [1].

The energy generation industry in the Netherlands is experiencing an important transition [2]. This is due to the efforts to reduce the current high amount of greenhouse gases (GHG) that energy production currently emits in The Netherlands, ranking as the second most GHG emitting industry in said country, greatly contributing to climate change [3].

In this energy transition, Alliander group has to perform the installation of new cable infrastructure, for which cable splicing is one of the most important processes [4]. Another reason for the increase in demand for cable installation is the housing crisis that is nowadays present in the Netherlands, creating the need to install cable infrastructure for new real estate and not enough electricity technicians can satisfy that demand [5]. This increase in demand can be seen in Alliander's investment plan, where it is expected that the total amount of medium voltage cables will double in the next 50 years [6]. On top of that, the current cable splicing process requires 125 thousand employee hours annually and its connector failure costs over 14 million euros annually.

For the reasons previously depicted, Alliander has taken the decision to modernize its processes through the use of automation. This way, according to data collected by Alliander and summarized by MSc. Elderhorst [4], it was deemed that from the total cable splicing process failures, 66% were from the installation process and from that percentage, 21% is attributed to shrinking, 13% to peeling the semiconductor, 11% to measurement and 10% to sanding the outer layer and also that the most common cable is the Cross-linked polyethylene (XLPE) medium voltage cable of size 240 mm^2. Using this data and discussing with Alliander employees it was determined that the peeling of the semiconductor part of the process may be the most automatable sub-process of the entire

cable splicing procedure, which accounts for an estimated 8 hundred thousand euros loss annually with a failure rate of 0.1%. Therefore the project of creating a device that automatically peels the semiconductor layer of a 240 mm^2 XLPE cable type with 100% success rate surged, from which this Final Graduation Project (FGP) is a part of as it was determined that in order to increase the success rate, better distance of cut measurement methods have to be used.

To automate this process a robot containing various subsystems is in development. This subsystems were previously defined by MSc. Elderhorst and they are: A drive-train or movement system, a cutting tool height control system, a computer vision for depth of cut monitoring and a relative positioning along the axis measuring system for feed per revolution control. This FGP elaborates on the design of the latter mentioned and it is crucial to accomplish the reduction in fail rate to 0%.

1.2 Problem definition

The problem in study is to measure the position of a cable splicing rotating and displacing device along an XLPE 240 mm^2 cable axis, as this process is currently done by hand and it was found that human contribution in the process leads to a low success rate.

The aim is to create a system that in the future will be implemented in a robotic system composed by various subsystems and for this reason correct integration is needed. This means that the along the cable positioning measurement must be performed without physically altering the cable and that the device dimensions and physical principle should enable the system to work both when turned by hand and when automated in the future without too many modifications.

Finally, while performing the distance measurement, the along-the-axis movement of the robot must be controlled only by changing the feed per revolution between the positions stop or move; the move position has one speed in one direction, and these are the only two positions available. The device should also be able to tell once the cable reaches the cutting tool as this is important for other subsystems within the robot.

1.3 Problem summary

Measuring and controlling the shielding-layer-peeling device's position along the cable is currently done by hand, which makes it too inaccurate and causes a loss in success rate. A device that calculates said device's position and detects the cable has to be designed in order to control the feed per revolution of a cable peeling robot in future implementations.

1.4 Objectives

1.4.1 General Objective

To design an automatic control system capable of tracking the relative position of an insulation layer peeling robot along the XLPE 240 mm^2 cable type axis and sending signals to control the feed per revolution to move and stop the robot at a selected distance.

1.4.2 Specific Objectives

- Execute different experiments with the already available measuring technologies at the University of Twente and select the most suitable.
- Using the winning measuring technology from the previous objective, design the sensing portion of the system responsible for directly measuring the position of the device along the cable axis and automatically setting the zero position at the cable end.
- Build an automatic control program able to change the feed per revolution of the robotic system.
- Design a mechanical structure that integrates adequately with the rest of the robot subsystems.
- Validate the correct operation of the control system using a real-life usage simulation on the final prototype.

Chapter 2

THEORETICAL FRAMEWORK

2.1 Medium-voltage cable splicing process

Splicing refers to the junction of two or more conductors using a suitable connector, then re-insulated, re-shielded and re-jacketed with compatible materials and applied over a properly prepared surface [7].

The steps reported by Alliander technicians in the whole cable installation process are [4]:

1. Transport to the project site.
2. Digging a hole to lay the cables bare.
3. Preparing the workplace.
4. Cutting cables and cable splicing.
5. Installing the cable connector.
6. Putting cables back into the ground.
7. Disassembling the workplace.

From the previous list, the main step developed in this project corresponds to step 4. This process is straightforward and repetitive as follows[4]:

1. Cutting the cable.
2. Cleaning the outer PVC layer.
3. Sanding the outer PVC layer.
4. Heating the outer PVC layer.
5. Peeling away the outer PVC layer.

6. Peeling away the paper swelling tape.
7. Bending the copper ground wires.
8. Peeling away the plastic swell band.
9. Peeling away the semi-conducting layer.
10. Peeling away the insulation and second semi-conducting layer.

This project revolves around the "peeling away the semiconductor layer" step, seen in figure 2.1 which must be performed adequately to ensure an homogeneous electric field around the cable. Small holes in the cable can create an unstable electric field that after continuous use may render the holes bigger or further damage on the cable [8].

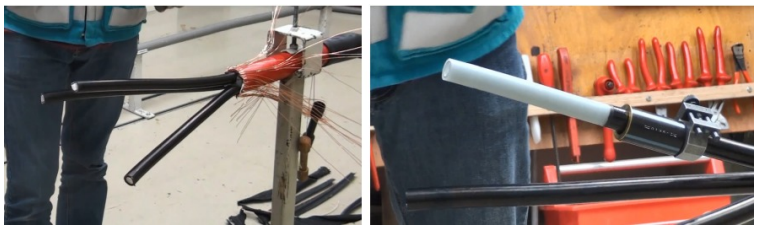

Figure 2.1: Before and after performing the peeling of the semi-conductor layer step [4]

Finally, different tools can be used to perform this step, namely: the diaphragm peeler gr1, diaphragm peeler gr.2 and the US02-7000 [4]. The latter one is used throughout the design of the product in this project.

2.2 Twenpower 240 mm² medium-voltage XLPE cable

The cable used for the development of this project corresponds to a medium-voltage, circular and single-cored cross-linked polyethylene (XLPE) type cable of 240 mm² cross-section area rated for voltages between 12 and 20 kV, made by the cable manufacturer BV Twentsche Kabelfabriek. This type of cable is used for public utilities, industry, non-residential construction and related fields [9].

Using figure 2.2 as reference, from top to bottom the layers of the cable are [9]:

1. **Conductor:** Circular conductor made of stranded copper wires or soft aluminum. The one used for the development of this project used solid soft aluminum.

2. **Conductor screen:** 0.5 mm thick semi-conductive XLPE layer.
3. **Insulation layer:** Thin high-quality XLPE.
4. **Insulation screen:** Semi-conductive polymer layer. This layer is covered by a bedding of a conductive swelling tape.
5. **Earthing screen:** Copper wires with an open pattern counter-wound copper strip.

Figure 2.2: XLPE cable layers [9]

It is worth noting that from the previously described layers, the conductor screen, the insulation and the insulation screen are applied in a single three-layer extrusion process and vulcanized under nitrogen pressure at one go [9].

The relevant physical characteristics of this cable are:

- **Nominal core cross-section area:** 1x240 mm ^{2}.
- **Earthing screen cross-section area:** 25 mm^2.
- **Minimum diameter for conductor layer:** 17.1 mm.

- **Minimum diameter for insulation layer:** 30.4 mm.
- **Minimum diameter for earthing screen:** 35.3 mm.
- **Minimum diameter for cable:** 42 mm.
- **Weight:** 1.8 kg/m.

2.3 Ripley US02-7000 tool

The Ripley US02-7000 bonded semicon shaving tool seen in figure 2.3 is used in this project.

Some relevant features of this device include [10]:

- Blade depth adjustments in increments of 0.1 mm.
- Its design is adjustable for cables from 18 mm to 60 mm.
- A revolving ergonomic handle and accessible adjustment knobs.
- Multiple advance per revolution positions, where stop position enables for completing the shaving operation without the need for an additional clamp.
- Its cutting blade is easily replaceable.

Figure 2.3: Ripley US-7000

The following are the instructions to use this tool according to the manufacturer [10] and also a workshop received by the author of this document [11]:

1. Retracting the cutting blade to the highest position turning the yellow knob counterclockwise.
2. Open the tool with the other knob to locate the middle line of the cutting tool in line with the cable end and secure the cable in the tool.
3. Turn the blade adjusting knob clockwise until the blade barely touches the semiconductor screen.
4. Set the feed lever into first position to ensure minimal feed.
5. Rotate the tool and observe the chip. As it moves, adjust the height of the cutting tool until the insulation layer is of one third of the total chip width.
6. Move the feed lever to its second position. Continue with the peeling and observe the chip to make sure the strip does not get caught under the cable rollers, as this will disturb the shaving result.
7. Once the cable is shaved to a desired length, the feed lever is to be moved to the stop position.
8. Perform a visual inspection in search for irregularities.

2.4 Cable peeling robot

The cable stripping robot that is being developed and from which this project is a part of, consists of an automated adaptation of the Ripley US02-7000 stripping tool. The main goal of this automatic system is to have a higher accuracy than the system operated by a human and therefore a lower failure rate [4].

In order to do this the entire robotic system has been divided into 4 other automation subsystems, briefly explained as follows according to the latest advancements [4].

1. Drivetrain: This system will allow the cutting tool to propel itself over the cable. The friction force on the wheel should have a sufficient magnitude to overcome the maximum cutting force as well as the inertia of the tool and other energy losses. This system will also allow

for modifying of the feed per revolution according to the signals received by the feed per revolution control system.

2. Tool height control: In order to get a high quality result, it is important that the tool blade is set at the right height throughout the cutting procedure. This system receives signals from the feed per revolution control system in order to know when to start the cutting procedure.

3. Computer vision chip inspection: A computer vision system is in charge of monitoring the ratio of insulation vs shielding layer and using said data as feedback for the tool height control.

4. Feed per revolution control system: This system is in charge of monitoring the position of the robot along the cable and detecting the presence of it. It outputs the position in which the feed per revolution lever of the tool should be.

2.5 Sensor calibration

The accuracy of a sensor or system can be lower than the required for a certain application, in said occasions a calibration of the sensor or a combination of the sensor and its interface circuit is required for minimizing the error values [12].

A calibration requires the application of precisely known stimuli and reading the sensor responses called calibration points, whose input-output values are the point coordinates. Typically between 2-5 points are preferred in order to characterize a function with higher accuracy. Another very important factor that directly plays a role in the sensor accuracy is using highly accurate reference sources for the input stimuli, preferably traceable to a national standard [12].

Before performing calibration, a mathematical model of the transfer function has to be obtained or a good approximation of the sensor's response. Once that has been done, the calibration can be performed in several ways, including [12]:

1. Modifying the transfer function or its approximation to fit the experimental data.

2. Adjustment of the data acquisition system to trim its output by making the outputs signal to fit into a normalized transfer function. For example modifying the gain and offset.

3. Modification of the sensor itself and its properties to fit the predetermined transfer function.

4. Creating the sensor-specific reference device with the matching properties at particular calibrating points.

2.6 Accuracy of a sensor

The accuracy of a sensor (or combination of sensors) in reality means inaccuracy, because it measures the highest deviation of a value represented by the sensor from the ideal or true value of a stimulus at its input. The true value is attributed to the input stimulus and accepted as having a specified uncertainty [12].

The inaccuracy of a system must be obtained by repeating an experiment in multiple occasions as a random component is always present. Therefore to obtain the systematic inaccuracy of the system, the error should be represented as an average or mean value of multiple errors [12].

Due to material variations, workmanship, design errors, manufacturing tolerances, and other limitations, a real function rarely coincides with the ideal, or even two real functions might not be the same even if the experiment is performed under presumably identical conditions. In order to improve the accuracy, the error-contributing factors should be identified and reduced. Often this includes the calibration of every sensor of a system in order to more closely follow the real sensor's accuracy [12].

Some of the forms to represent the inaccuracy of a system are [12]:

1. Directly in terms of measured value of a stimulus: This form is used when error is independent on the signal magnitude, usually used when there's only additive noise or systematic bias. For example in a temperature sensor the accuracy could be stated as 0.15 ^{o}C.

2. In percentage of the input span: This form closely relates from the last mentioned, but in this case the input span must be specified and the error is always associated to this maximum value. It is worth noting that this form is only useful for linear-transfer-function sensors.

3. In percentage of the measured signal. It is useful for a sensor with a non-linear transfer function. The error is always associated with the current given value.

4. In terms of the output signal. This is useful for sensors with a digital output format so the error can be expressed, for example, in units of LSB.

2.7 Choice of sample size for validation

In order to determine if the amount of samples taken is enough to obtain a certain level of confidence in the accuracy of results, statistics have to be used. In this section a brief explanation of a common approach for sample selection will be explained.

First, using $\hat{p}$ as an estimate of a given proportion p, where a proportion is the amount of samples that fall under a given number and $\hat{q}$ is the estimate of q, which is the compliment of p, one can be $100(1-\alpha)\%$ confident that the error will not exceed $z_{\alpha/2}\sqrt{\hat{p}\hat{q}/n}$ for a sample size of n [13].

Therefore, from what has been previously explained the sample size can be calculated as seen in equation 2.1, where e is the error of the predicted value. Said equation should be used after a given experiment to determine if the amount of samples taken is good enough or if further experimenting is necessary or to obtain the estimated possible error [13].

$$n = \frac{z^2_{\alpha/2}\hat{p}\hat{q}}{e^2} \tag{2.1}$$

Chapter 3

METHODOLOGY

The product design methodology described in [14], known as the Ulrich and Eppinger method is used as base, nonetheless some changes have been done to it as this is a specific design for a proof of concept and not a final commercial product. The base method consists of the following phases: Planning, concept development, system-level design, detail design and production ramp-up in that timeline order.

In this case, as the system to be designed will be used as a proof of concept, the only phase followed from this method to come up with a solution is the concept development phase. From this concept developing stage, the following steps will be executed in this project:

1. Identifying the customer needs.
2. Defining the product's specifications.
3. Generating concepts.
4. Concept selection.
5. Concept Testing.
6. Final concept selection.

It is important to remark that all the previously depicted steps are in an initial chronological order, but once a step is completed, one has to look back to the previous steps and do modifications if found necessary. Also as the project was done at a university with many already-available technologies, testing of these technologies was performed after the concept generation step for the measuring technology, as it helped grasp a better idea of what can be done with the current available tools, which ultimately saves time and money.

3.1 Determination of needs

3.1.1 Initial data acquisition

Initially a first statement from the customer was obtained in the form of a meeting, in which the principal requirements for the device to design were obtained. The client's statement summarizes as follows: The system to design is an innovative proof of concept and it has to measure the relative position of the robot along the cable with 0.5 millimeter accuracy without the need for any human participation. The distance to measure varies from 150 to 240 mm depending on the cable connector to be used later and said distance and a start command should both be the only human inputs once the robot is correctly placed. There is still uncertainty on whether or not the robot is going to be used in field applications, so for now resistance to the elements is considered a plus but not necessary. Finally, the robot is going to be an automated adaptation of the device currently used by the company (Ripley US02-700) for which the main thing that is to be controlled by the system being developed in this project is the feed per revolution position, and only two are going to be used, positions "2" and "stop", but the system should also be capable of outputting when the cable end has been detected so the depth of cut controller knows when to start working.

Apart from the client's statement, a hands-on cable splicing workshop was experienced by the author of this project as a way of better understanding the problem, paying special attention to the peeling of the semiconductor step [11]. It was observed in this step that the point where the cut to the cable end is done has an irregular shape, but when the client was asked, the answer was that the cable end is to be retouched in the next step of the cable splicing process so the irregularity would be removed. It was also noticed that the shielding layer chip that comes out when the cutting process is done can get in the way of the measuring to be performed, but to solve this, one of the other systems is going to manage the chip handling.

Videos of the process being done by professionals were also received from Alliander [8], where the peeling of the semiconducting layer was analyzed. It was observed that currently the measuring process is done in a completely manual manner, where a stopping device is placed by hand using a measuring tape like observed in figure 3.1, which has many potential error sources, mainly human involuntary movements while observing, and the cable is not perfectly straight so measuring with a straight ruler or tape loses accuracy due to the ruler not being parallel to a plane that contains

the axis of the cable. This suggests that the current process has an accuracy of more than 0.5 millimeters, even though guidelines recommend this maximum error. It is worth mentioning that once this matter was brought up to the client, he acknowledged that this may be one of the most important errors in the distance measuring process and that the maximum error recommended in guidelines might not be accurate, but research for a better approximation of the maximum error from which problems might occur is necessary.

Figure 3.1: Current distance of cut measuring [8]

Making an estimation of the error from current technique is possible by looking at the current process videos. Assuming a worst case scenario, where the distance is of 240 mm which is the longest distance for cable peeling that is performed in this types of cable, the actual distance measured by the technician can be estimated using Eq. 3.1 using figure 3.2 as reference. Assuming that Δy is around half of the diameter of the cable that's around 31 mm of diameter, the error is of 0.5 mm, therefore it is likely that the current error is of more than 1 mm as other variables such as cable curvature have to be taken into account.

$$E = |240 - \sqrt{\Delta y^2 + 240^2}| \tag{3.1}$$

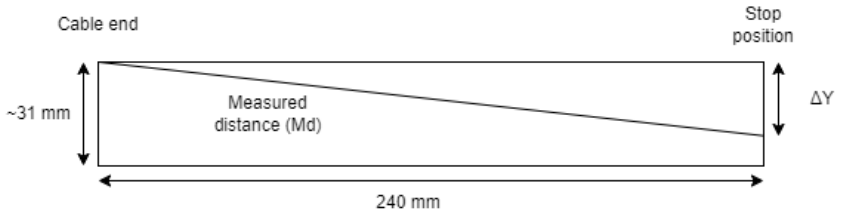

Figure 3.2: Current error by not placing the measuring tape properly on the cable

Another point taken from the videos [8] was the total duration of the peeling of the semiconducting layer process of around 12 minutes, from which around 1 minute (8.3%) of the total time is dedicated to the measuring of the cutting distance and placement of the stopping device. When the client was asked, an increment in the speed of the process is not so important.

Finally interviewing to field technicians was performed by MSc. Elderhorst with questions designed by the author of this project. This had the objective of grasping a better understanding of the problem and were also questions that came from the need interpretation process. The following are the questions with the answers reported back by MSc. Elderhorst from an Alliander cable splicer technician:

1. Have you or any colleagues had problems in any of the stages of the cable installation because of a bad measuring of the cutting distance of the insulation layer?
   Yes, two and a half percent of all insulation defects are due to measurements. This represents 250 thousand euros in damage. Four defects a year due to measurement but it's hard to determine which portion of that can be just for the shielding layer alone.

2. How often is the total distance of cut revised as a quality control method after making the cut?
   That depends on the technician. Usually not, just measuring beforehand.

3. Under what types of weather conditions can the cable splicing process be executed? Can it be performed while raining?
   It can be performed while raining, but we put a tent to shield ourselves and the cable from any weather condition. It can also be performed when is really cold and temperatures make it so that cutting the cable requires more force.

4. How often is the cable splicing process done? Is the cable splicing process usually done in waves (more than one cable spliced after the other)? If yes, around how many times is the process repeated per wave?
   Yes, it is usually done in waves, 3 times per cable as each cable has 3 cores and each of those waves is performed around 4 times a day, so in total the cable splicing process is done 12 times a day.

5. Is there anything specifically annoying about the measuring process?
   No, not any particular detail.

3.1.2 Need interpretation

The needs were obtained for the measuring, automating and mechanical structure components of the total system by separate, as these are the main mechatronic fields of the system to design, it allows for a view of the clients needs in greater detail. Nonetheless, once this is done by separate, the final result will be analyzed by joining all the needs and considering new ones for the entirety of the system.

For the importance of each interpreted need, a form was made by the writer of this document and later filled by interviewing the client. This way, the importance was categorized from one to five, the scale is as follows for all future importance categorizing of the needs:

1. Undesirable. Wouldn't consider a product with this function.
2. Not important. Not a need, but having it wouldn't mind me.
3. It would be useful to have this function, but it is not necessary.
4. Highly desirable, but I would accept a product without it.
5. The function is of critical importance. I wouldn't consider a product without it.

Measuring portion of the device

This is the most important portion of the device to design, as the needs gathered here will allow to correctly choose a measuring technology.

First, it was expressed by the client, that the main goal of the system to design should be to stop the along-the-axis movement of the robot at a certain distance from 150 to 240 mm with 0.5 millimeter accuracy 100% of the times. Nonetheless, in later steps of the design, once the behaviour of the system was studied and after technical discussion with the client, it was recognized that as this is a first design proposal for a non-existing device (with no previous state of the art), this requirement was changed to a more realistic value for a first iteration that can be later improved by other students in future assignments and also taking into account that for validation in further

steps of the design, there are no tools that can guarantee that said level of accuracy is achieved. Therefore, the following need is recognized: **The designed system is very accurate calculating the position of the device along the cable axis.**

Next, the device should also output when the cable is detected. This is so that the cutting tool control can receive a signal that indicates when to start the cutting procedure. Therefore, as this has to be contemplated in the needs for the measuring part of the system, the following need is added to the list: **The designed system is very accurate detecting the presence of the cable end.**

Also, as the client said in the initial statement, the designed system should be completely automated, and the reason for this is that failure is not accepted and as it was discussed in section 3.1.1, human interaction is one of the main contributors to loss of precision and accuracy. For this reason the designed device should **eliminate human actions in the measuring process**.

Even though time concerns were never expressed by the client, during the study of the process it was discovered that the total duration of the overall operation was around 12 minutes. Therefore considering the environment of the project (not enough technicians in The Netherlands), the need **the system works very fast** was interpreted.

Following the same idea, to reduce employee hours using the robotic system, preparation should be minimal, suggesting that the system to be designed should not be calibrated very often and its calibration needs to be simple. This creates the needs: The designed system is **easy to calibrate** and **requires infrequent calibration.**

From the interview with the technicians, it was discovered that the conditions in which the device will work may vary, and as the device might be used in field applications, this brings the need for the system to be **resistant to the environment.**

Also, as the system is to be used on top of a cable that must not get damaged and as it is to be carried by humans, there is the need for a **lightweight and compact system.**

As the measuring subsystem is to be connected to a more complex system, there was the question of whether or not the client perceived as requirement that the **designed system must be easily detachable**.

Finally, as different cable connectors require different distances of cut, the final requirement encountered for the system was for it to **measure all the distances used for the different cable connectors**.

This way, the interpreted needs for the sensing part of the system were separated into first and second order hierarchy, namely:

1. The designed system is efficient and reliable
    - The designed system can make the drive-train stop at the ending position as accurately as possible.
    - The designed system is very accurate detecting the presence of the cable end.
    - The designed system eliminates human actions in the measuring process.
    - The designed system adds minimum delay to the rest of the process.
    - The designed system requires infrequent calibration.
    - The designed system is resistant to the environment.
    - The designed system measures all the distances used for the different cable connectors.
2. The designed system is easy to use and handle.
    - The designed system is easy to calibrate.
    - The designed system is lightweight and compact.
3. The designed system is easily detachable from the rest of the robotic system.
    - The designed system is easily detachable from the rest of the robotic system.

Once the hierarchy was defined, using a form to discuss the importance of each requirement with the client, the results in 3.1 were obtained.

Table 3.1: Second order needs and their importance for the sensing part of the system

#	Requirement	Importance
1	The designed system is easily detachable from the rest of the robotic system.	2
2	The designed system adds minimum delay to the rest of the process	3
3	The designed system is resistant to humidity and dust.	3
4	The designed system calibrates quickly.	4
5	The designed system requires infrequent calibration.	4
6	The designed system is lightweight and compact.	4
7	The designed system is very accurate calculating the position of the device along the cable axis.	5
8	The designed system is very accurate detecting the presence of the cable end.	5
9	The designed system eliminates human actions in the measuring process.	5
10	The designed system measures all the distances used for the different cable connectors.	5

Automatic control portion of the system

To grasp a better idea of the control system that is to be designed, a second level input-output diagram is portrayed on figure 3.3. It shows the subsystems that are part of the automatic control to design. It is worth mentioning that the drive-train is going to receive the feed position signal but nothing can be changed in its design. Another important factor to take into account is that the rest of the robotic system is still in development, so no information can be obtained from any electronic component that is not part from the system designed in this project (i.e., drive-train motors).

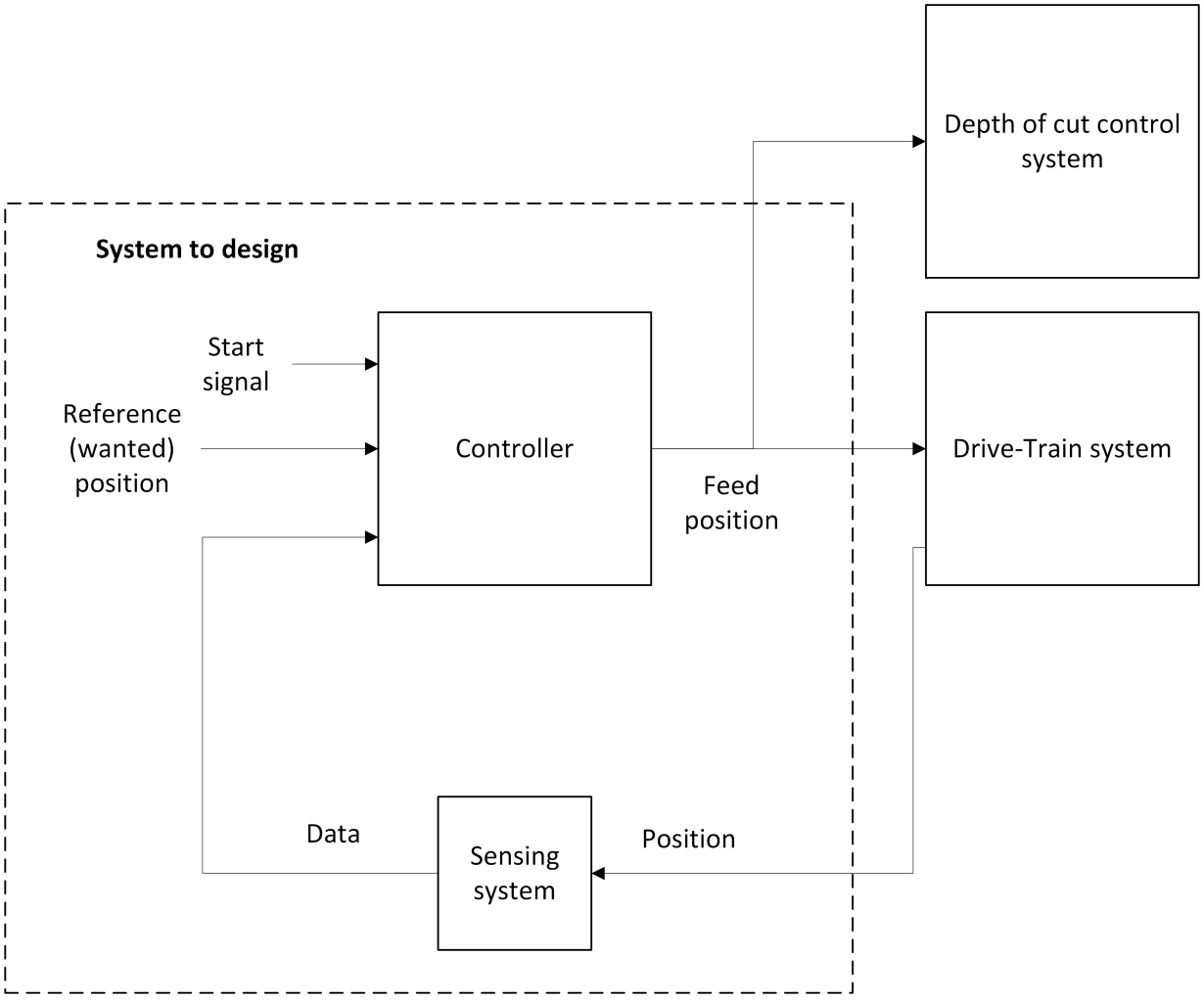

Figure 3.3: Block diagram for the automatic controller main connections

To correctly measure distances, the automatic control should be able to receive signals from the sensing system and adequately **set the robot's position relative to the zero** at the cable end.

The output of the system is another important factor to consider, as the system is connected to the drive-train which as explained by the client, will only have 2 feed positions and this cannot be changed. Therefore the designed system must **output the feed option in which the robot should be** (Stop or position '2') and **output the detection of the cable end** when it reaches the cable tool.

Finally, as the system is going to be subjected to a wide range of distances, the reference distance of cut should be modifiable in this system. This way a new requirement is discovered as: the designed system's total **distance to measure can be easily modified.**

In this case, only one first order requirement is found:

1. The controller is capable of automating the robotic system.

    - The designed system automatically sets the start position of the relative measurement in the zero position.
    - The designed system outputs the feed option in which the robot should be (stop or 2) and the detection of the cable end.
    - The designed system's total distance to measure can be easily modified.

The importance found for each of these second order needs can be seen on table 3.2

Table 3.2: Second order needs and their importance for the controlling part of the system

#	Requirement	Importance
1	The designed system automatically sets the start position of the measurement in the zero position.	5
2	The designed system outputs the feed option in which the robot should be (stop or 2) and the detection of the cable end	5
3	The designed system's total distance to measure can be easily modified.	5

Mechanical structure of the system

Regarding the mechanical structure, a few things must be mentioned. First of all, as the design should only validate a proof of concept and is not going to be distributed as a final product, life expectancy is not considered important. This was brought up to the client and he stated that all he wants is to guarantee that the system is not going to break while its being used for demonstrations. This means that there is the need to **maintain structural integrity with typical usage.**

As it was explained for the measuring portion of the device, the system should not be very bulky. This is also very important for the mechanical structure that is going to carry the measuring system. Therefore, the need for a system that is **lightweight and compact** is reiterated (as it was previously brought up for the measuring needs).

The subsystem in discussion is part of a bigger robotic system, so there's the requirement to not interfere with any other subsystem of the robot. This applies both in terms of space and physical interference such as force of friction or inertia increase. Nonetheless in further steps of the design, the rest of the robot was still not developed enough and therefore there was no way of knowing for

sure if there is no interference, so this need was discarded as a requirement for the design when discussed with the client, but communication was constant between designers to ensure that in later implementations this device can be coupled to the robot as seamlessly as possible, giving various options to the client.

Finally, some possible solutions in which the cable is covered or visibly obstructed emerged later in the concept creation stage. Real time observation might be preferred to show the instant results of the cutting, specially considering this is proof of concept. For this reason it was to be determined if **cable visibility** as the process is executed is a requirement.

Putting all the interpreted needs in hierarchy results in the following:

1. The designed system's structure does not affect other subsystems of the robot.
    - The designed system's structure does not add significant inertia to the movement of the system.
    - The designed system's structure does not add significant friction force to the movement of the system.
2. The designed system's structure withstands typical usage.
    - The designed system maintains structural integrity with typical usage.
    - The designed system is lightweight and compact.
3. The designed system's structure facilitates real-time observation of the cutting process.
    - The designed system allows for already-cut cable visibility during the process.

The second order needs were asked in the form of an in person survey in order to obtain their importance, the results are shown in table 3.3. It is worth noting that the need regarding a lightweight and compact system had its importance defined already in previous discussion.

Table 3.3: Second order need importance for the mechanical structure of the system

#	Requirement	Importance
1	The designed system's structure adds minimum inertia to the rotational movement of the system	3
2	The designed system's structure adds minimum friction force to the movement of the system	3
3	The designed system is compact and lightweight	4
4	The designed system allows for already-cut cable visibility during the process	4
5	The designed system maintains structural integrity with typical usage	5

Entire system and overview

Finally, all the elements are jointed and analyzed. During this analysis, it was found that a very important need was being left out, that is the integrity of the cable. This was asked to the client and he agreed that this is indeed one of the most important aspects of the design. Therefore the requirement for **maintaining the integrity of the inner white XLPE insulating layer** was added to the list.

The final list of requirements for the design of the system in discussion can be seen in table 3.4, this list was checked several times throughout the design process and changes were done accordingly.

Table 3.4: List of requirements for the project's system

#	Requirement	Importance
1	The designed system is easily detachable from the rest of the robotic system.	2
2	The designed system adds minimum delay to the rest of the process.	3
3	The designed system's structure adds minimum inertia to the rotational movement of the system.	3
4	The designed system's structure adds minimum friction force to the movement of the system.	3
5	The designed system is resistant to the environment	3
6	The designed system calibrates quickly.	4
7	The designed system requires infrequent calibration.	4
8	The designed system is lightweight and compact.	4
9	The designed system allows for already-cut cable visibility during the process.	4
10	The designed system is very accurate calculating the position of the device along the cable axis.	5
11	The designed system eliminates human actions in the measuring process.	5
12	The designed system measures all the distances used for the different cable connectors.	5
13	The designed system automatically sets the start position of the relative measurement in the zero position.	5
14	The designed system outputs the feed option in which the robot should be and the detection of the cable end.	5
15	The designed system's total distance to measure can be easily modified.	5
16	The designed system maintains structural integrity with typical usage.	5
17	The designed system maintains the integrity of the XLPE insulating layer.	5

3.2 Specifications

Once the needs were obtained for the different mechatronic systems within the solution to design, metrics to measure the fulfillment of the requirements were researched and also obtained by studying the process and asking the client directly. Comparisons with similar products were made at a high-level because the only similar product [15] does not have a publicly available data sheet with numerical values.

3.2.1 State of the art

As mentioned earlier, the only other similar device currently in the market is the Medium Voltage Electric Cable End Preparation System by ULC Technologies and Con Edison. This device is

currently a prototype that performs a type of splice used during adverse system conditions to expedite feeder restoration [15].

It performs the 4 following operations [15]:

1. Short field end of cable: The machine first creates a short between the flat strap neutrals and conductor to ensure field end is grounded.

2. Cut feeder cable: A specialized saw on the machine is used to cut through the cable.

3. Prepare cable end: A complex array of tooling on the mechanism is used to cut and remove each layer of the cable.

4. Install pre-molded end cap: The cold shrink cap / live end cap is pushed onto the cable until the end cap is fully engaged. The core of the cable cap is then removed.

It can be seen that this robot is capable of performing the whole cable splicing process, not only the peeling of the insulation layer. Nonetheless, as seen in figure 3.4 this device is very bulky and requires a whole industrial set-up in order to function. This is very different from the idea behind the robot that is being designed for this project, where a relatively small device is placed on the cable to perform the peeling operation only.

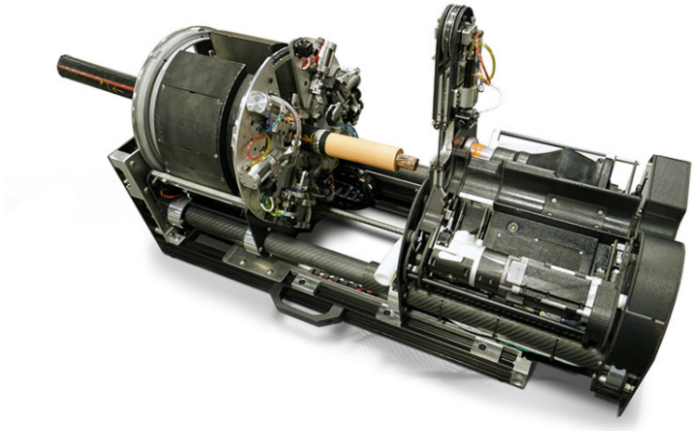

Figure 3.4: Medium Voltage Electric Cable End Preparation System [15]

Also, as no numerical values or specifications of this prototype are available, there is no way of using the current state of the art to obtain goal and marginal values for the specifications of the device to design in this project. This means that initial estimations were made using the current

technique used by the technicians and their guidelines, which is not always achievable, and therefore some changes had been made throughout the design process as more information was obtained and as the behaviour of the system was observed.

3.2.2 Determination of metrics and goal and marginal values

As well as for the needs, the determination of metrics was done for each mechatronic subsystem by separate. Also, to simplify the understanding of where do each of these metrics come from, the thought process and research behind them is separated by requirement.

Measuring portion of the device

In the following paragraphs the explanation behind the measuring portion's specifications can be seen.

The designed system is easily detachable from the rest of the robotic system: This perceived need is of low importance and for this reason no more thought is going to be given to this requirement in order to focus on more important factors.

The designed system adds minimum delay to the rest of the process: As the importance level of this requirement is a 3, having rapid measurements is not a priority. Through discussion with MSc. Elderhorst, an improvement on current speeds is desired but not needed. For this, the total duration of one measuring cycle will be used as metric as it is commonly used to measure the efficiency of automated systems [16]. As goal value, live measuring will be looked for. Nonetheless an added time of 2 minutes is still accepted as it is around double of the current manual measuring time and the client deemed this as a limit of time that does not interfere too much with the workers time.

The designed system is resistant to the environment: As this need is of importance 3, it is also not a priority. This is because the system corresponds to a proof of concept and it is still uncertain whether or not the device is going to be used in the field. After discussion with the client, it was considered that it is enough if the system's sensors work properly in usual temperature ranges. This creates the metric of system's working temperatures, and as temperature in the Netherlands usually varies from 0.71 ^{o}C to 23.08 ^{o}C [17] this temperature range is used as marginal value, while a broader range for atypical temperatures ranging from -5 ^{o}C to 30^{o}C is used as goal.

The designed system calibrates quickly: Calibration should happen without further delaying the cable splicing process. Considering that every sub-process before the peeling of the shielding layer lasts around 15 minutes according to videos of the process done by Alliander [8], and using the metric of total calibration time, less than 15 minutes will be accepted as marginal value and no calibration time is taken as goal, where the system virtually requires no calibration. This number comes from the fact that while one of the technicians may be preparing the cable for the rest of the process, another technician could calibrate the device in the meantime.

The designed system requires infrequent calibration: As in the last one, the frequency of calibration may also negatively influence the process as according to the interviews performed to technicians, the splicing process is often done for various cables one after the other. This indicates that if calibration must be performed between cables, more time than necessary would be consumed. After discussing this with the client, he suggested that calibration once a day would not impact significantly the overall time consumed for the process, but that he would prefer an entire week without calibration. This way, marginal value is of more than 12 cycles (daily amount of cycles reported by employees) and more than 60 cycles is the goal value.

The designed system is lightweight and compact: As the measuring subsystem is part of a bigger and more complex robotic system, the weight needs to be considered so that it does not interfere with other robot operations in future implementations or with the cable's integrity. This was directly asked to the client and the answer was that less than 1 kg is acceptable but he would prefer less than 500 grams, creating a weight metrics with said values as marginal and goal values respectively.

The designed system is very accurate detecting the presence of the cable end: This requirement also has an importance of 5 because the output signal that indicates the presence of the cable end on the cutting tool is going to be used to activate the depth of cut system. As metric the average absolute error of the cable detection is used and 0.5 mm is set as marginal value and 0.25 as goal value, as this two are considered acceptable to start the peeling process.

The designed system is very accurate calculating the position of the device along the cable axis. For this metric the method to measure accuracy was the first question, as it is often defined as a maximum, or typical or average error [12]. Initially using the maximum error only was considered, but later it was discovered that using the average error value would be more representative for

the large range of measurements and would also help eliminate atypical values and the random component of the experiments, therefore giving a systematic accuracy value. As for the accepted values used in this regard, it was initially considered according to the guidelines used by current Alliander employees using a maximum error of 0.5 mm (which in reality is never achieved), nonetheless this value did not take into account that calibration patterns to get to this value are not obtainable within the RAM premises and also the special characteristics of the cable (i.e., the cut at the end of the cable is not perfectly straight or the curvature of the cable). So these two discussed reasons lead to the conclusion that the metrics used should be the average absolute error and maximum absolute error as through discussion with the client and taking into account that this is a proof of concept, the goal value is set as 0.5 mm of average error and 1 mm as marginal value for the average error, as this is considered enough to encourage future investment from Alliander and render the system perfectly usable and 3 mm and 1 mm as marginal and goal values as maximum absolute error because more than 3 mm of error would be unacceptable in any reading.

The designed system eliminates human actions in the measuring process: It is expected for the robot to completely eliminate non-required human interference. This is understood as having as only human input for this system the desired distance of cut. For this reason the metric is a list of sub-processes where human interaction will be required. Both goal and marginal values are a list of one item: Selection of distance to measure. Note that this may include more than one action (i.e., typing the value and then pressing enter).

The designed system measures all the distances used for the different cable connectors: As discussed with the client, the typical distance for cable connectors range from 150 to 240 mm, therefore those are the distances that the system needs to be able to cut. This creates 2 metrics, the first one is the distance selection resolution and the second is the range of measurements. For the first one, resolution should be of less or equal to 1 mm both for marginal and goal values. For the second one, the range should be at least 150 to 240 mm as marginal and goal values.

To ensure that all needs have a metric that validates them, correspondence between each requirement and metric can be seen on figure 3.5.

#	Requirements	Metric	Total delay produced by the measuring cycle	Range of working temperatures	Total calibration time	Number of cycles before a calibration curve adjustment is needed	Weight	Accuracy of the cable end detection	Average absolute error when tracking the robot's position	Maximum absolute error when tracking the robot's position	Subprocesses where human interaction is required	Resolution of the distance selector	Range of measurements that can be sensed
2	The designed system adds minimum delay to the rest of the process		•										
3	The designed system is resistant to the environment.			•									
4	The designed system calibrates quickly.				•								
5	The designed system requires infrequent calibration.					•							
6	The designed system is lightweight and compact.						•						
7	The designed system is very accurate detecting the presence of the cable end.							•					
8	The designed system is very accurate calculating the position of the device along the cable axis.								•	•			
9	The designed system eliminates human actions in the measuring process.										•		
10	The designed system measures all the distances used for the different cable connectors.											•	•

Figure 3.5: Correspondence between metrics and specifications for the sensing part of the system

The list of specifications with the marginal and objective values can be seen summarized in table 3.5.

Table 3.5: List of specifications for the sensing part of the system

#	Metric	Importance	Units	Marginal value	Goal value
1	Total delay produced by the measuring cycle	3	s	<120	0
2	Working temperatures	3	Celsius degrees	[0.71,23.08]	[-5, 30]
3	Total calibration time	4	s	<900	0
4	Number of cycles before a calibration curve adjustment is needed	4	Cycles	>12	>60
5	Weight	4	kg	≤1	≤0.5
6	Maximum absolute error when tracking the robot's position		mm	<3	<1
7	Average absolute error when tracking the robot's position	5	mm	<1	<0.5
8	Average of the cable end detection absolute error	5	mm	<0.25	<0.5
9	Subprocesses where human interaction is required	5	List	Distance selection	Distance selection
10	Resolution of the distance selector	5	mm	≤1	≤1
11	Range of measurements that can be sensed	5	mm	[150,240]	[150,240]

Automatic control portion of the system

Now for the automatic control, the specifications sheet metric was created as explained in the following paragraphs.

The designed system automatically sets the start position of the measurement in the zero position: According to the inputs received from the measuring system, the distance used for control should be automatically adjusted to correspond with the precise distance from the cable end to the cutting tool. The correct detection of the zero needs to have as little delay as possible in order to keep the error low. The system will experience two important delays that affect its precision for stopping, which are: The delay when detecting the zero and the delay from measuring the distance shouldn't enable the system to reach the maximum marginal value of absolute error. The sum of these delays should not let the robot stop with an error greater than the settled as marginal value for absolute error of the system. This can be mathematically seen in Eq. 3.2. Where T_{total} represents the total delay, $T_{s,z}$ the delay from the zero detection sensor, $T_{s,d}$ the delay from the distance tracking sensor, T_{1mm} the typical time it takes the device to advance 1 mm and finally E_{avg} represents the

average error value obtained.

$$T_{total} = T_{s,z} + T_{s,d} \leq T_{1mm} * (1 - E_{avg}) \tag{3.2}$$

The designed system outputs the feed option in which the robot should be: According to the client, it is important that the final digital output of the system in discussion is very simple. This means that the amount of output bits should be 2, one that indicates the feed position and one that indicates the presence of the cable.

The designed system's total distance to measure can be easily modified: As the easiness to do a process is mostly subjective, a survey shall be conducted, where 5 random persons with a background of at least high-school education should scale from 0 to 4 the easiness to modify the total distance after doing that process. The metric should be the mean easiness obtained and the goal and marginal value should be 4 and 3 respectively, as this would mean the distance selecting is a very easy-to-do process. The survey is based off [18] as it explains in depth different questions that can be used in a survey to determine the ease of use of a system.

Finally, correspondence between metrics and needs on the topic discussed in this subsection can be seen in figure 3.6.

#		Metric	Sampling time	Output bits	Level of easiness to modify the distance to measure
	Requirements				
1	The designed system automatically sets the start position of the measurement in the zero position.		•		
2	The designed system outputs the feed option in which the robot should be (stop or 2) and the detection of the cable end			•	
3	The designed system's total distance to measure can be easily modified.				•

Figure 3.6: Correspondence between metrics and needs for the automatic control portion of the system.

Once it had been confirmed that every need has a metric to measure its fulfillment, the importance and acceptance values were added and the specification sheet for the automatic control of the system this time. This can be seen on table 3.6.

Table 3.6: List of specifications for the automatic control of the system

#	Metric	Importance	Units	Marginal value	Goal value
1	Sampling period	5	s	Eq. 3.2	Eq. 3.2
2	Output bits	5	bits	2	2
3	Level of easiness to modify the distance measure	5	subj. survey Lickert scale	3	4

Mechanical structure of the system

For the mechanical structure of the system, the specification sheet was obtained for each necessity as it is explained in the following paragraphs.

The designed system's structure adds minimum inertia to the rotational movement of the system and **the designed system's structure adds minimum friction force to the movement of the system**: The force required to start the rotational motion of the system is used as metric for

this two requirements, using figure 3.7 as reference . 148 Newtons is determined as a safe value to apply this force [19], and even though the robot is going to use motors to do this motion, for testing human force will be used so this is still considered for the design for safety reasons.

Figure 3.7: Force applied to the device

The designed system is compact and lightweight: This was previously addressed in the needs for the measuring portion of the device.

The designed system allows for already-cut cable visibility during the process: To make sure this is fulfilled, the metric minimum percentage of longitude of cable visible is used. It is a minimum because the longitude of the cable is variable depending on the distance selected. It is considered that being able to see half of the cable is enough to perform quality control on the process while it is being done, but 90% of cable visibility is aimed for. Apart from this metric, after discussion with the client, he mentioned that the most important part to see is what has just been cut. For this reason, the following metric was also added: Distance of cut from which the part of the cable that has just been cut can be seen; goal value is 0 mm and marginal value is 150 mm (at the minimum cutting distance). This is because in later stages of the design methodology some solutions were found to only be able to provide visibility in a limited range of distances.

The designed system maintains structural integrity with typical usage: This is going to be verified using simulation analysis in Solidworks software. The nominal forces to which the system is going to be subjected are going to be defined and the minimum safety factor of the mechanical structure obtained in simulation is going to be used as metric. Considering the principal

manufacturing material that is going to be used for the proof of concept is PLA under not severe loading and environmental conditions, Machinery's Handbook [20] recommends a safety factor from 2 to 2.5. A conservative approach is followed, so the goal and marginal values are of a safety factor greater than 2.5.

The correspondence between needs and metrics just discussed can be seen in figure 3.8.

#	Requirements	Metric	Force required to start moving the device when in feed position 2	Weight	Percentage of visible already-cut cable	Distance of cut from which the most recently cut cable can be seen during the process	Safety factor for the mechanical structure
1	The designed system's structure adds minimum inertia to the rotational movement of the system		•				
2	The designed system's structure adds minimum friction force to the rotational movement of the system		•				
3	The designed system is compact and lightweight			•			
4	The designed system allows for already-cut cable visibility during the process				•	•	
6	The designed system maintains structural integrity with typical usage						•

Figure 3.8: Correspondence between needs and metrics for the mechanical structure

Finally, the resulting specification sheet for the mechanical structure is the one shown on table 3.7.

Table 3.7: List of specifications for the mechanical structure

#	Metric	Importance	Units	Marginal value	Goal value
1	Force required to start moving the device when in feed position 2	3	N	148	148
2	Weight	4	kg	0.5	0.5
3	Minimum visible already-cut cable from 150 to 240 mm distance of cut	4	%	>50	>90
4	Minimum distance of cut from which the most recently cut cable can be seen during the process	4	mm	<150	0
5	Safety factor for the mechanical structure	5	non-dimensional	>2.5	>2.5

Entire system and overview

As it was done previously for the system needs, everything is jointed together as a way of making sure that nothing is being left out for the entire integration of the mechatronic system. Some needs had very similar or identical specifications, so in order to have clearer metrics, the needs were updated and adapted accordingly.

The system specifications can be seen in table 3.8. This table has been revised multiple times throughout the process in order to make sure that it is comprehensive enough.

Table 3.8: List of specifications for the entire system

#	Metric	Importance	Units	Marginal value	Goal value
1	Total delay produced by the measuring cycle	3	s	<120	0
2	Force required to start moving the device when in feed position "2"	3	N	<148	<148
3	Working temperatures	3	Celsius	[0.7,23.1]	[-5,30]
4	Total calibration time	4	s	<900	0
5	Number of cycles before a calibration curve adjustment is needed	4	Cycles	>12	>60
6	Weight	4	Kg	≤ 1	≤0.5
7	Minimum visible already-cut cable from 150 to 240 mm distance of cut	4	%	>50	>90
8	Minimum distance of cut from which the most recently cut cable can be seen during the process	4	mm	<150	0
9	Maximum absolute error for position tracking the robot	5	mm	<3	<1
10	Average absolute error for position tracking the robot	5	mm	<1	<0.5
11	Average absolute error for zero detection	5	mm	≤0.5	≤0.25
12	Sub-processes where human interaction is required	5	List	Distance selection	Distance selection
13	Output bits	5	bits	2	2
14	Resolution of the distance selector	5	mm	≤1	≤1
15	Range of measurements that can be selected	5	mm	[150,240]	[150,240]
16	Sampling period	5	s	Eq. 3.2	Eq. 3.2
17	Level of easiness to modify the distance measurement	5	subj. survey Lickert scale	>3	4
18	Safety factor for the mechanical structure	5	non-dimensional	>2.5	>2.5
19	The cable's XLPE layer is unharmed during the process	5	Binary	Yes	Yes

3.3 Concept generation

In this section, the problem in discussion will be decomposed in as many features as it is necessary to ensure that all sub-problems are manageable enough to obtain solution strategies for each of them.

First, the diagram in figure 3.9 was constructed, where the general solution will be described in terms of the inputs and outputs of the system. It is worth pointing out that the current state output signal has been added because after reflection on the process to be done, it is necessary to indicate the current output as a visual safety implementation. This will allow for the user to know the current feed position and act accordingly.

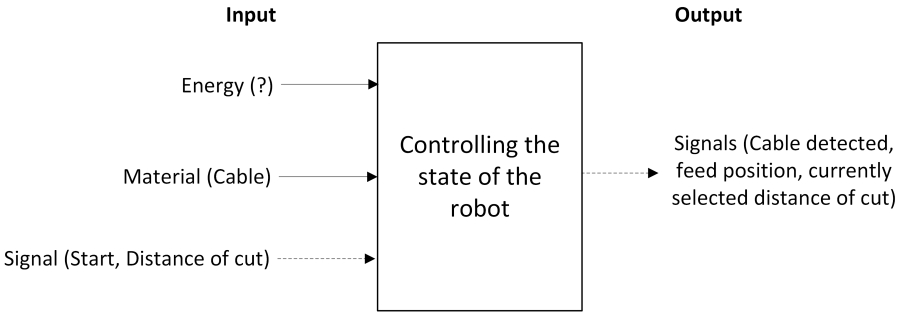

Figure 3.9: Black-box diagram for the designed system

The main problem to solve in this project has been divided in 8 different sub-problems to be solved. This division diagram can be seen in figure 3.10. A brief explanation of each of these sub-problems is on the following subsections as well as the possible solutions that were found through external and internal research. As it can be seen, none of these sub-problems include resistance to weather considerations, however as said need is of low importance it is taken into account for the design steps and selection throughout the process but not treated as a separate problem.

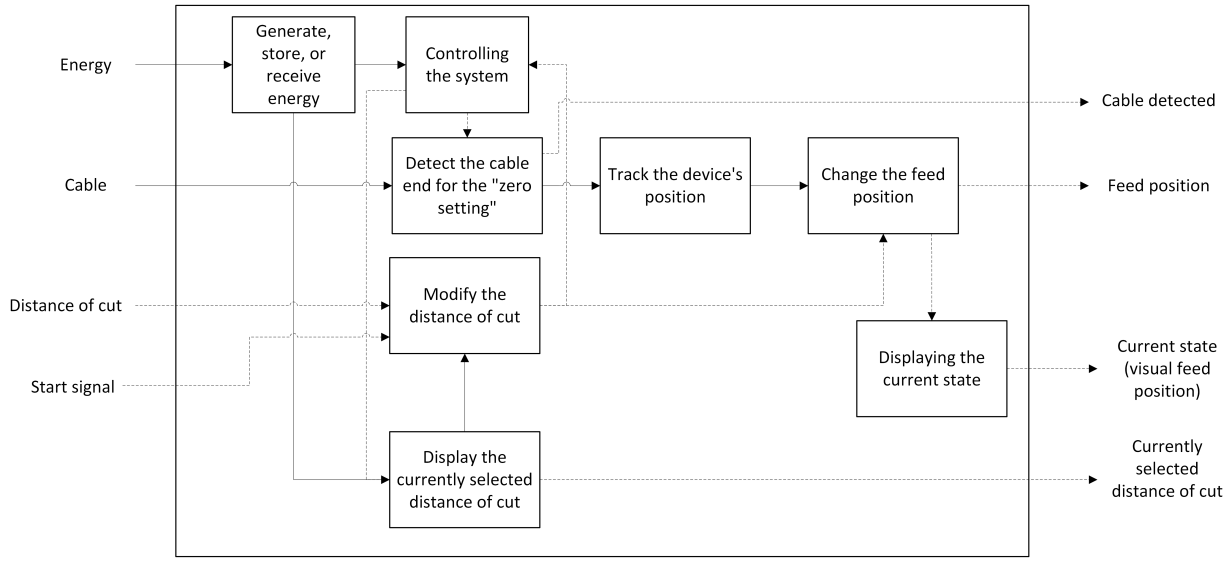

Figure 3.10: Division of design problem in sub-problems

3.3.1 Track the device's position

One of the main goals of this project is to measure the relative position of the cable peeling device accurately enough to output a signal that could stop it at a given distance with an average absolute error of 0.5 mm as goal value. For this reason, special attention is payed to this sub-problem and additional testing is going to be performed to select a good concept in the next design step of the method.

Most of the solutions created for this sub-problem come from internal investigation as the designer is very familiar with sensor equipment. Nonetheless, some solutions explained in the following paragraphs come from external investigation.

Computer vision based solutions were already thought of, nonetheless, only image segmentation was considered at that point. For this reason, more research into ways to obtain the current position of the robot in relation to his environment were made and ego-motion came up as a possible solution [21].

Other direct distance measuring technologies that were part of the external research are the optical LED, the optical laser, and the linear variable differential transformer or transducers [22]. Distance measuring can also be made using magnetic sensors [23]. Finally, another less conventional method of measuring linear position was found to use a magnetostrictive linear position sensor [24].

The result from internal and external research for the sub-problem in discussion can be seen in figure 3.11.

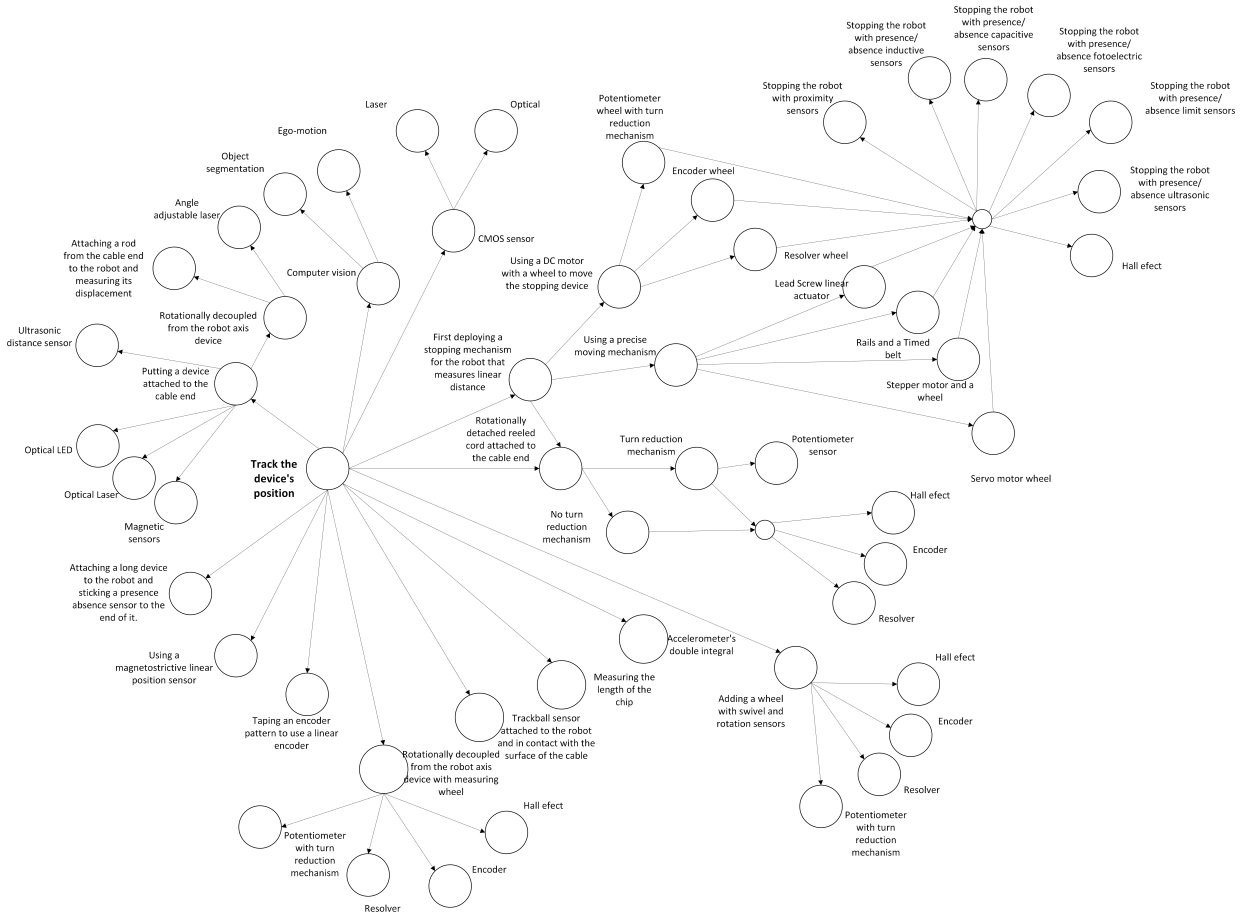

Figure 3.11: Solutions results from internal and external research for the sub-problem “track the device’s position”

As it can be seen in figure 3.11, there are too many solutions for this sub-problem, nonetheless only the available technologies or easily obtainable are going to be taken into account and experimenting is performed in later steps in order to select the best one with the resources at hand.

The technologies that may be used for position tracking according to the research done in this section are the following:

- Optical LED distance sensor.
- Optical laser distance sensor.
- Ultrasonic distance sensor.
- Computer vision camera.

- Rotational potentiometer.
- Linear transducer.
- Rotational encoder.
- Linear encoder.
- Hall-effect rotary sensor.
- Magnetometer.
- Capacitive presence/absence or inductive sensor.
- Hall effect proximity sensors.
- Presence/absence inductive sensor.
- Presence/absence switch sensor.
- Presence/absence photoelectric sensor.
- Presence/absence ultrasonic sensor.
- Accelerometer.
- Trackball sensor.
- Magnetostrictive linear position sensor.
- Lead screw linear actuator.
- Rails and timed belt.
- Stepper motor.
- Servo motor.

3.3.2 Detect the cable end for relative zero setting

This sub-problem refers to the setting of the zero that is going to be used for the relative measurements and is deeply related to the previously discussed, for this reason, later when selecting the concepts compatibility between this two has to be greatly taken into account. All of the solutions depicted on figure 3.12 are from internal investigation only as when later doing the external research, no new useful solutions were found.

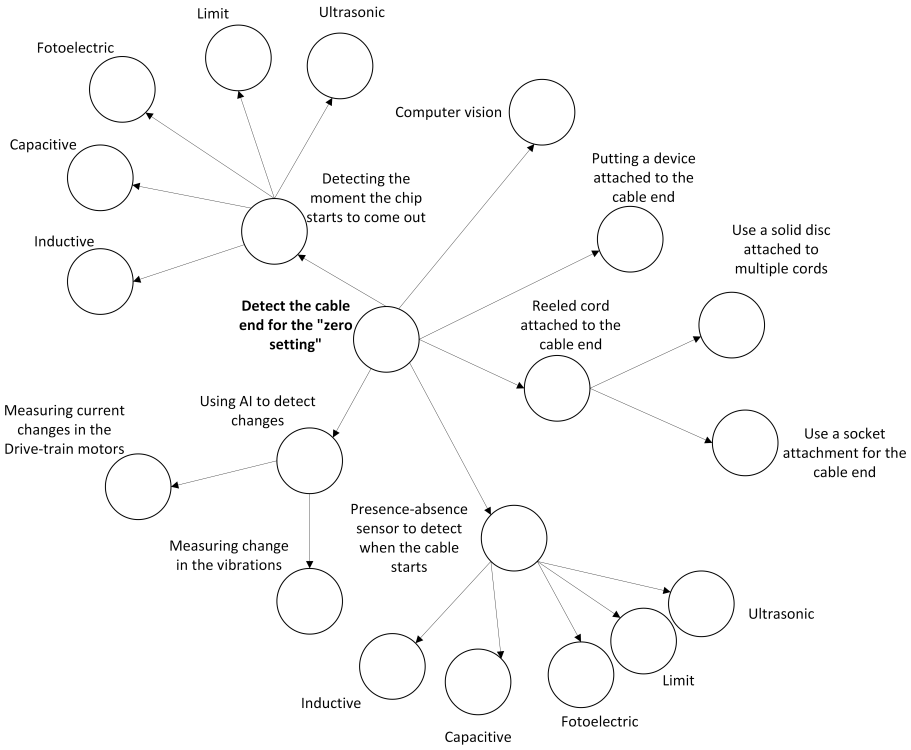

Figure 3.12: Solutions resulted from internal and external research for the sub-problem "detect the cable end for zero setting"

3.3.3 Generate, store or receive energy

This refers to the way the electronic components of the system are going to be powered. Internal research yielded a satisfying amount of results, nonetheless through research it was found that the device which rotates enabling cable tangling, could also receive energy from a stationary point (such as a power outlet) using a slip ring that rotationally decouples the cables [25]. Results can be seen in figure3.13.

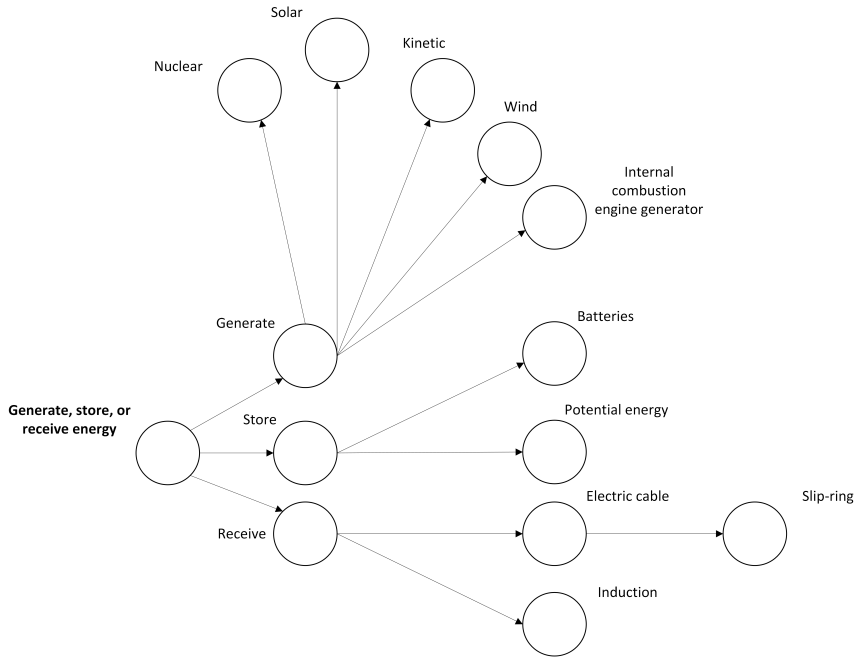

Figure 3.13: Solutions resulted from internal and external research for the sub-problem "generate, store, or receive energy"

3.3.4 Controlling the system

The designed system needs to have a way of controlling the electronic components within itself as well as having a way to save memory values and perform mathematical calculations. The different ways to control this were figured by internal research as external research did not bring any relevant solutions. This can be seen in figure 3.14.

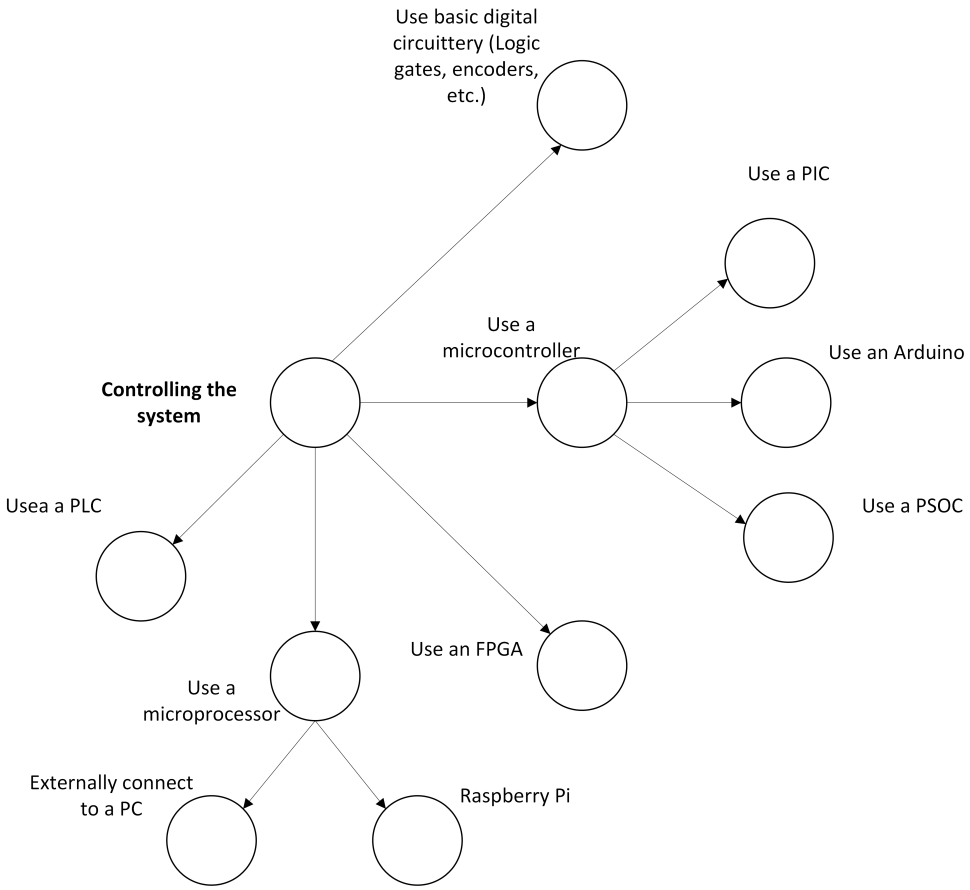

Figure 3.14: Solutions resulted from internal and external research for the sub-problem "controlling the measuring system"

3.3.5 Change the feed position

Another sub-problem to solve is the automatic control function. There are different automatic control methods, some of the most important that may be used to solve this are showed in figure 3.15. They are the result from internal and external research [26].

It is worth noting that in an on-off control system the control signal can only be set as two different values, so gradual speed control is not possible and this will be most likely the case for this problem as there are only 2 speeds that can be selected. For this reason, in future implementation on the actual robot, it might be useful to consider a different approach to also control the motors speed, but that is outside the scope of this project. For now, these other ideas are left as part of the design process so in future optimization of the design, going back and making changes to this step can be easily done.

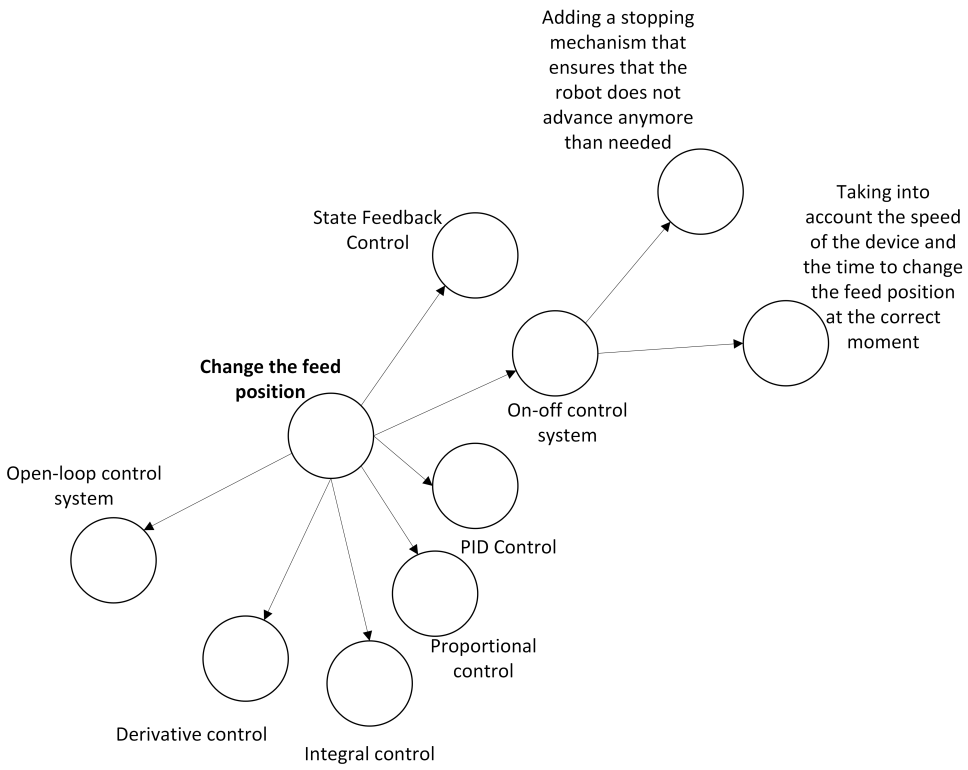

Figure 3.15: Solutions resulted from internal and external research for the sub-problem "change the feed position"

3.3.6 Modify the distance of cut

The distance of cut is variable and depends on the cable connector to be used and the clearance it requires. For this reason, the way this variable is going to be modified is to be figured out. Internal research gave results, but external research also gave major input to solve this issue. The externally found solutions are namely: Positioning devices (such as mouses), Styli, Gaze control and Gestures [27]. The results from this investigations can be seen in figure 3.16.

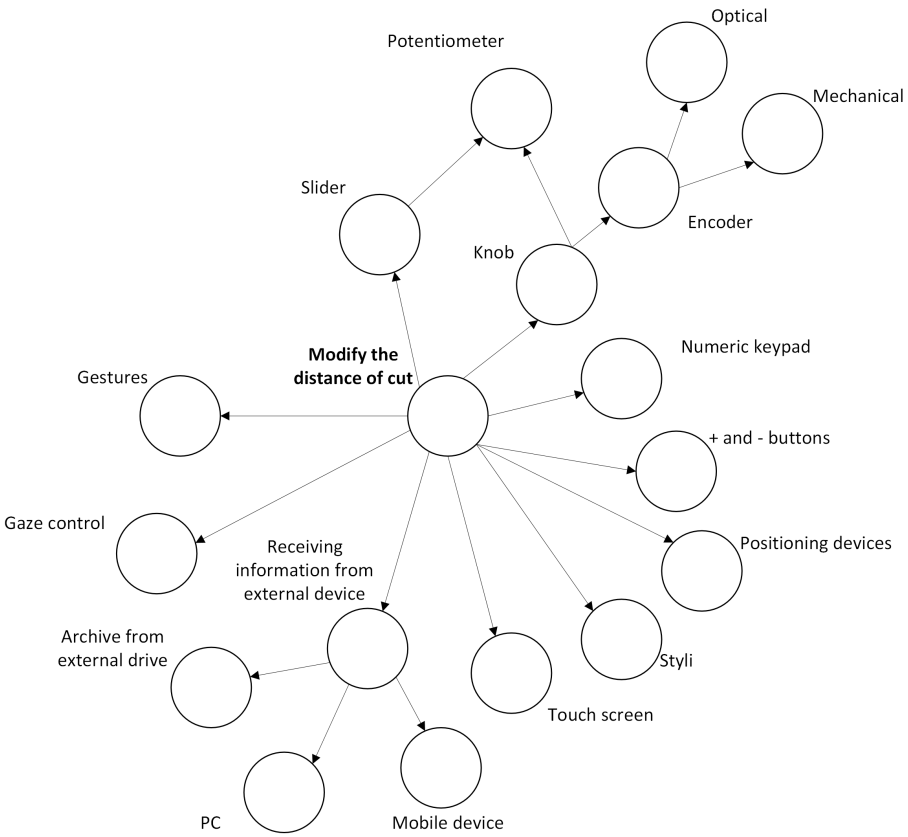

Figure 3.16: Solutions resulted from internal and external research for the sub-problem "modify the distance of cut"

3.3.7 Display the currently selected distance of cut

For this sub-problem, only internal investigation was done as external research did not provide useful solutions. The results can be seen in figure 3.17

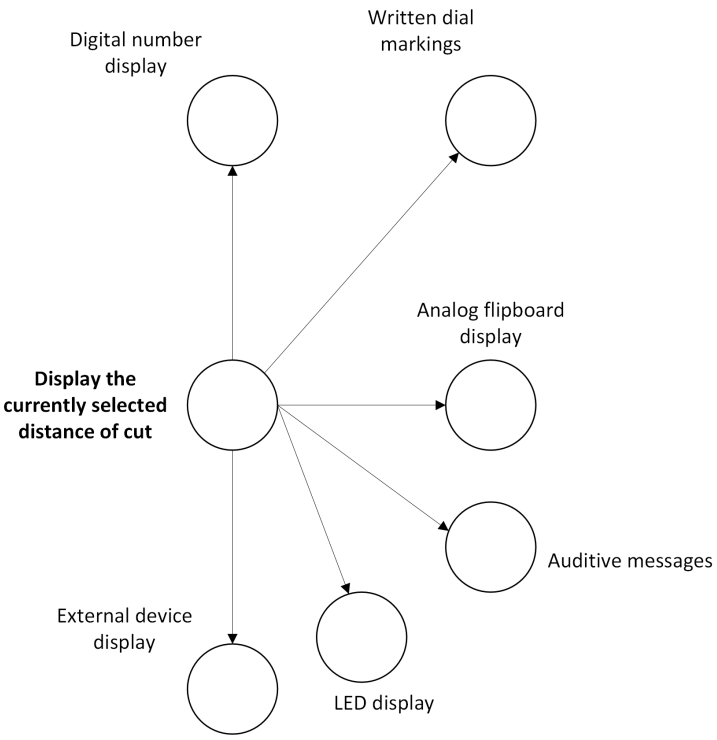

Figure 3.17: Solutions resulted from internal and external research for the sub-problem "Display the currently selected distance of cut"

3.3.8 Displaying the current state

This is a sub-problem that needs to be solved as an information giving safety measure for the device. It is very useful to know when the device is going to move as it might hurt somebody in that process, this can be seen as an alarm system. The most important thing to keep in mind for a solution to this sub-problem is that alarm conditions must be easily distinguished from normal conditions [27]. Using this information, the research yielded the results in figure 3.18.

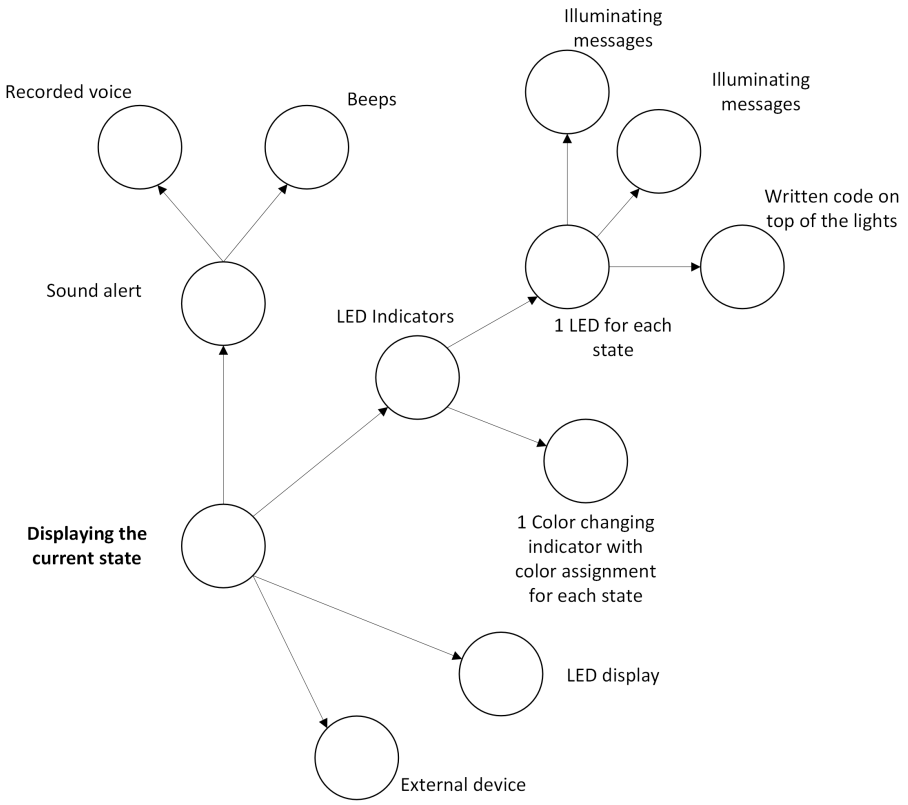

Figure 3.18: Solutions resulted from internal and external research for the sub-problem "displaying the current state"

3.4 Experimenting with the available technologies

It was expressed at some point by the client that already-available at the university premises is strongly preferred, for this reason an inventory of the available technologies out of the ones obtained from the research for the sub-problem "track the device's position" was made by asking RAM group staff members.

The available position measuring technologies at the university premises are:

- Computer vision camera: CMOS with laser sensor from Microsoft basic mouse.
- Rotary potentiometer: 2000 Ohm unlimited turns rotary potentiometer, unknown brand.
- Encoder: 24 step EC16E20-24P24C mechanical incremental encoder.
- Encoder: 2000 step optical incremental encoder.

Presence/absence technologies were also available:

- Magnetometer: Hall sensor KY-003.
- Mechanical switch: Switch WLK-4MINI.
- Photoelectric: Laser with light sensor module LM393.
- Inductive sensor: OMRON E1A-M12KS04-WP-B1.

3.4.1 Computer vision camera: CMOS with laser sensor

Many factors contribute to the loss of precision in mouse sensors. The most important are: the measuring surface, chip selection and irradiance on the sensor [28]. These points were studied via experimentation as explained in the following paragraphs.

The measuring surface can either be the already-cut white XLPE insulation layer or the black semi-conductive layer. It is known that rough surfaces and diffuse reflecting is preferred [28], for this reason, it is expected that the white XLPE will perform better as it has a glossy machined texture, contrary to the shiny black semi-conductive layer. Experiments were performed on both surfaces to obtain precision values depending on the surface.

As for the chip selection, a Microsoft Basic laser mouse sensor, rated 800 dots per inch (DPI) was used. The reason for this is availability, as there was a mouse no longer needed and could be taken apart.

There are important things that have an effect on irradiance on the sensor, namely: diffuse reflection efficiency and distance from the lens to the object [28]. This was studied by varying the distance from the optic sensor to the cable in two different test benches and by changing the enclosure of the system to allow more light to get in and out.

For all the experiments done with this technology, a computer software that tracks the mouse cursor position was created, it can be seen in appendix H.1. The cursor is placed at the highest position of the screen and the total displacement downwards was measured. The goal of this was to obtain the precision, accuracy was not a concern because repeatability was found crucial while accuracy would have been fixable through calibration. Precision is calculated by taking 5 measures

and subtracting the lower value obtained minus the higher. Relative precision is calculated as the resulting precision divided by the average value obtained.

Test 1: Initially a rapidly 3D printed test-bench (figure 3.19) that enabled a mouse to be attached to it directly was used. It is worth noting that by design, this test-bench added 1 mm to the distance from the lens to the object. Another thing worth pointing out is that in this case a Genius GM-04003A mouse was used instead of the Microsoft Basic, but it has the same working characteristics and that was not deemed to affect this experiment. A distance of travel $(55.00 \pm 0.025)mm$ was measured using a caliper and then marked using a marker to put tape so that the test-bench stops at after the same displacement every time.

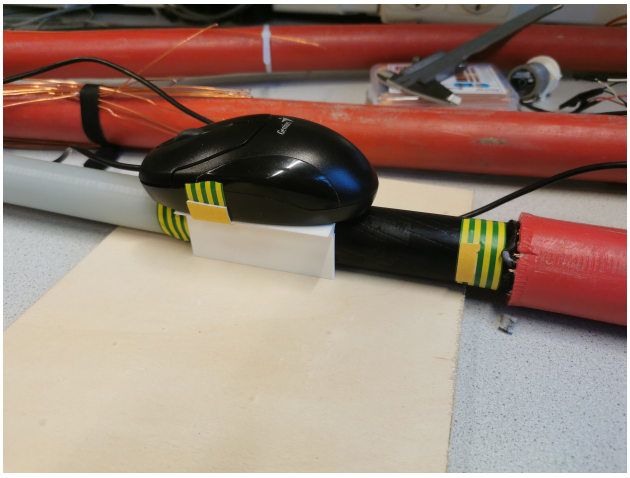

Figure 3.19: Set-up used for test 1 of the CMOS with laser sensor experiment

Test 2: The distance from the lens to the object was changed to nominal with this second design. The mouse was a Microsoft Basic, like initially intended. The outer carcass was removed making sure the parts that involved optical sensing were not damaged in the process (as it can be seen in figures 3.20 and 3.21). Other thing worth mentioning is that this time instead of using tape to set the start and end of the measurements, 3D printed stoppers were taped to ensure more reliable readings. The distance of travel also changed to $(121.00 \pm 0.025)mm$, mainly because the new test-bench is shorter and allows for more movement on the available cable.

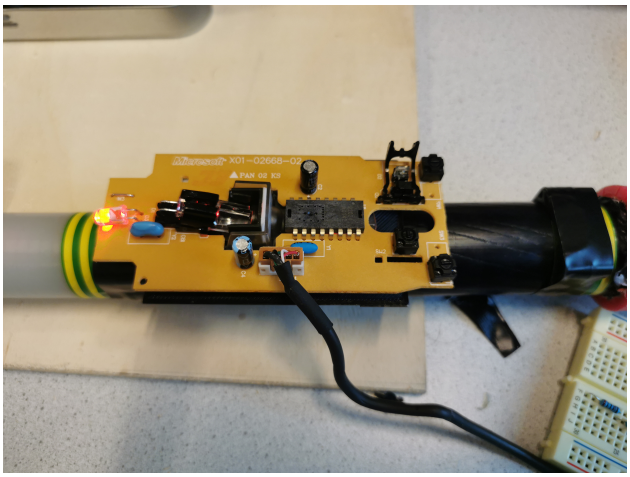

Figure 3.20: Set-up used for test 2 of the CMOS with laser sensor experiment (top view)

Figure 3.21: Set-up used for test 2 of the CMOS with laser sensor experiment (view from under)

Test 3: The amount of light that can get out or in of the system was reduced using electric tape to cover all the gaps in the device (figure 3.22). This was the only significant difference from test 2.

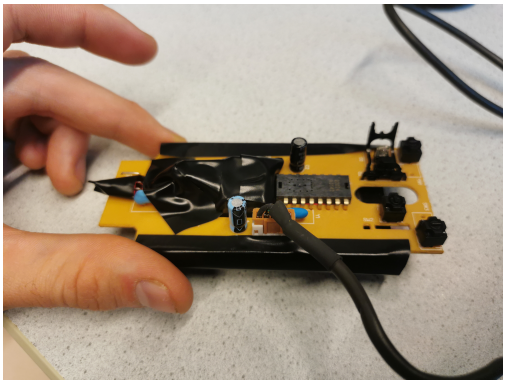

Figure 3.22: Set-up used for test 3 of the CMOS with laser sensor experiment

Test 4: Using the same set-up as the one described in the previous test, the experiment was repeated but this time on the white XLPE-layer.

The results from the previous tests can be seen in subsection 6.1.1.

3.4.2 Rotary potentiometer

A $(2000 \pm 3\%)\Omega$ linear rotary potentiometer was used. There were two different experiments performed in 2 different test-bench set-ups, the data for both was taken using an Arduino Nano sampling at 100Hz and the code can be seen in appendix H.2. The tests performed were the following:

Test 1: The first test was performed using the PLA 3D printing test bench shown in figure 3.23. The wheel is placed on top of the cable by applying forward hand pressure to the potentiometer's case. The real distance of travel was measured with a caliper to be $(55 \pm 0.025)mm$ and the start and ending points were set using tape. The data was taken using an Arduino Nano at 100Hz, which is well above the Nyquist frequency for this set-up (where the rotation of the wheel is the main frequency and it does not reach more than 1 Hz).

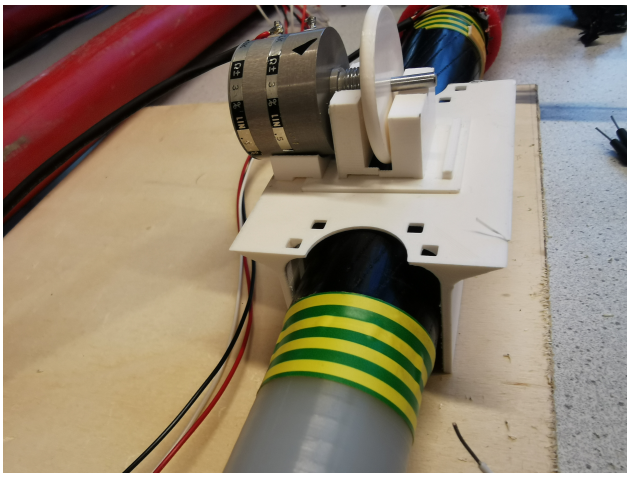

Figure 3.23: Rotary potentiometer experimental set-up for test 1

Test 2: The second test was performed using a Tough PLA 3D printed wheel with the shape of the cable to help with alignment and also a moving parallel-to-the-ground base to ensure that there is no rotation from involuntary hand movement (as seen in figure 3.24). 3D printed stoppers were also used instead of directly using tape as this allows for a better experiment.

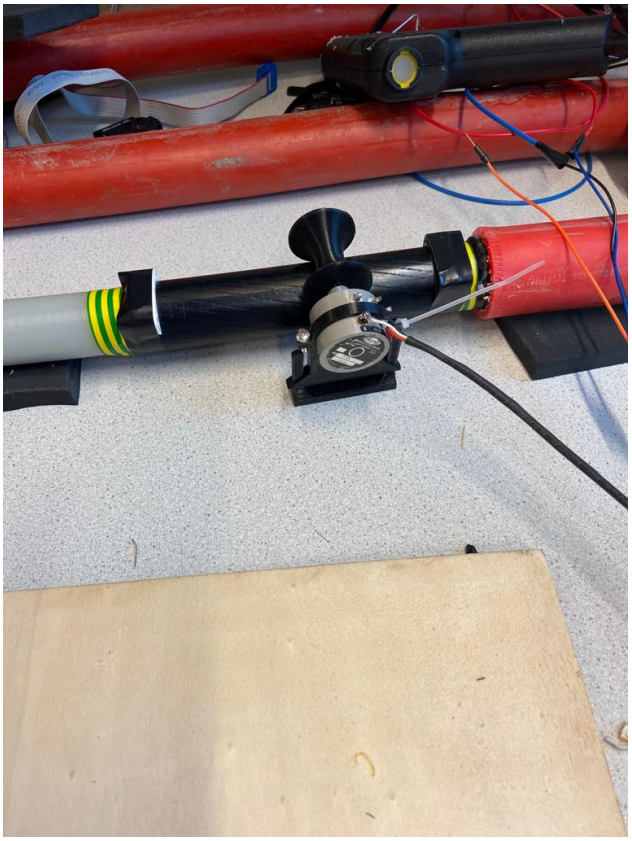

Figure 3.24: Rotary potentiometer experimental set-up for test 2

The results obtained in the tests previously described can be seen in subsection 6.1.2.

3.4.3 Encoder

For the experimenting with the encoder, a two thousand step incremental encoder was used. Two thousand steps translate to a resolution of $\pi/1000$ radians. Knowing that, it can be calculated using equation 3.3 (where ΔS is the linear distance travelled, $\Delta\theta$ is the change in angle and r the radius) that the maximum radius of the wheel in order to obtain a theoretical resolution of $0.5mm$ is $r = 159.15mm$. Therefore, the tests in this section were performed using a metallic $(80.0 \pm 0.5)mm$ diameter wheel found at the university premises. Data was taken using a sampling frequency of 100 Hz with an Arduino Nano; the code can be seen in the appendixes.

$$\Delta S = \Delta\theta r \tag{3.3}$$

Two experiments were done, the procedure and reasoning behind each of them is explained in the following paragraphs.

Test 1: The set-up for this experiment can be seen on figure 3.25, tests were mainly performed to see if there were slippage issues between the encoder's axis and the wheel attached to it. This was measured with the precision values, as good precision would most likely indicate that indeed there is minimum slippage. The test done by manually moving the set-up a linear distance of $(180.0 \pm 0.5)mm$ 5 times.

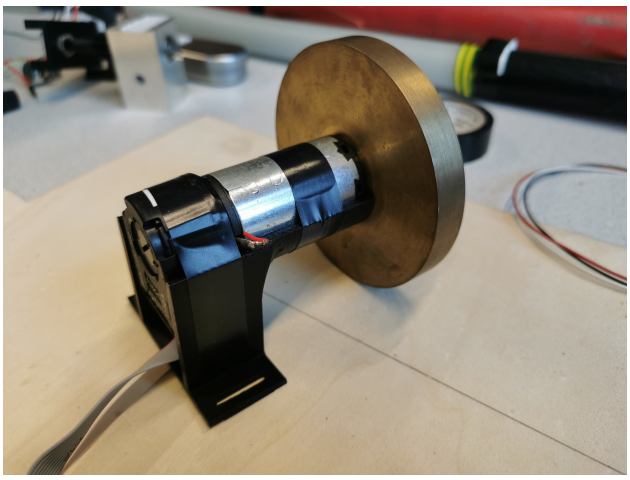

Figure 3.25: Set-up for experiment with encoder wheel

Test 2: Another test-bench was built for this experiment (figure 3.26), for which a reel that goes attached to a wheel was built. Testing was performed to see the variables that should be taken into account if this method is used later. It is worth noting that the linear displacement uncertainty is also defined by the radius of the reel attached to it, as expressed in Eq. 3.3. The test was performed by attaching a string to a stationary object and manually rotating the reel to add significant tension to it, then displacing the set-up a total distance of (180.0 ± 0.5) mm. The diameter of the reel is $(83.0 \pm 0.5)mm$ and is attached to the metallic wheel, which is enough to avoid cable winding considerations as less than one turn is needed to move the maximum distance of 240 mm.

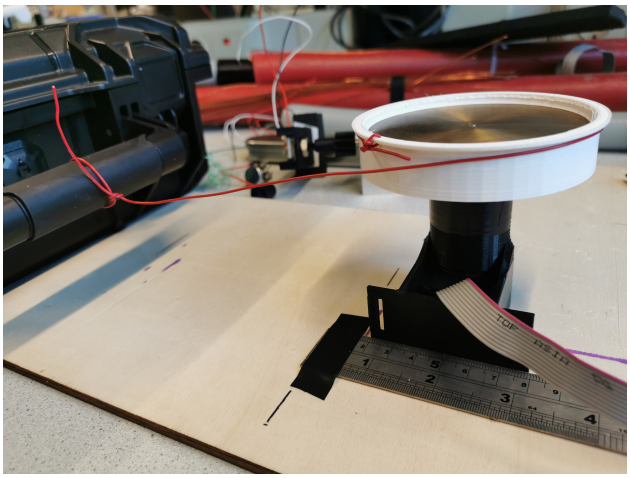

Figure 3.26: Set-up for experiment with encoder measuring reel

The results from the tests performed can be seen in subsection 6.1.3

3.4.4 Presence/absence detection technologies

For these technologies, the tests were performed by using them in the different objects which they could eventually detect. This means in general, on the robot and on the cable. All of the available technologies were tested with the exception of the mechanical switch as it will most likely work on any solid object. The specific procedure for each technology is briefly explained in the following paragraphs.

Magnetometer: With the magnetometer the main question was whether or not the ferromagnetic content of the objects was enough to trigger a response, so it was placed in contact with the cable peeling machine to see the response. The data was taken using an Arduino Nano on a KY-003 hall sensor.

Photoelectric: As for the photoelectric LM393 sensor, a through beam set-up was set in place and the main goal was to observe if the ambient light played an effect on the detection of the laser signal. The experiments were performed on the side of a window on a sunny day. The data was taken using an Arduino Nano.

Inductive: Using an OMRON E1A-M12KS04-WP-B1 sensor, the sensing capability was tested on the metallic components; namely the cable core and the cable peeler, as detection varies depending on the metal. The data was taken using an Arduino Nano. The maximum distance for detection was also tested in these two components.

The results from the previously described tests can be seen in subsection 6.1.4.

3.5 Concept Selection

In this section the process behind the concept selection is explained for each of the sub-problems found at the concept generation step. An effort was made to ensure that all solutions can be fabricated using already available technologies, but technologies that are easily obtainable via the preferred suppliers RS-Online and Farnell were also considered.

In order to obtain a final concept, the concept selection was separated into the following 2 different categories: Measuring method sub-problems and other sub-problems. This way, the sub-problems that involve major changes in the design and working of the system can be addressed first and the solution to the rest of sub-problems, which are independent of each other is to be selected later.

3.5.1 Concept selection for the measuring method sub-problems

Initially the principle of measuring sub-problems are to be assessed, these involve which technology is used and the way it is going to be used for both the zero-setting and the tracking of the robot.

Solutions A, B, C and D involve the use of already available technologies while concept E uses technology obtainable through the University suppliers, but not readily available, their description can be seen in table 3.9; to help understand the concept a Solidworks high-level representation was rendered. The testing performed on the technologies was used determine which concepts were not

useful and allowed for solutions that would most certainly work, as this project is of an exploratory nature, experimenting helped the designer in the creative process of making concepts.

Table 3.9: Concepts created for the measuring principle sub-problems

Solution	Zero setting	Track robot	Figure
A	Photoelectric to detect cable ends	First deploying a stopping mechanism with a DC motor attached to encoder wheel. Stopping the robot with presence/absence sensors.	3.27 & 3.28
B	Detect cable ends using a photoelectric sensor	Rotationally decoupled from the robot axis device with encoder measuring wheel	3.29 & 3.30
C	Use a socket attachment for the cable end	Encoder with a rotationally detached reel cord attached to the cable end	3.31 & 3.32
D	Presence-absence	Adding a caster wheel with swivel and rotation encoders	3.33 & 3.34
E	Detect cable ends using a photoelectric sensor	Using a precise moving mechanism	3.35

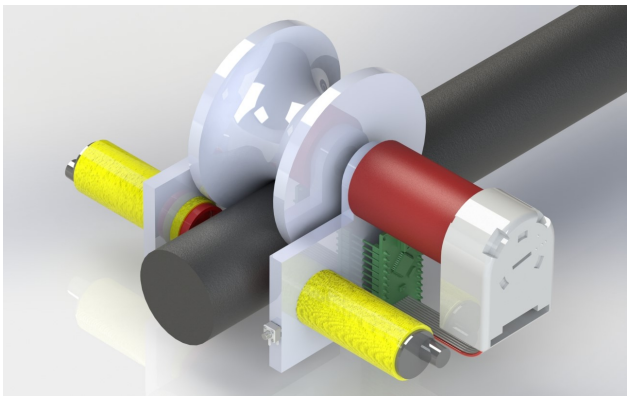

Figure 3.27: Isometric render of concept A

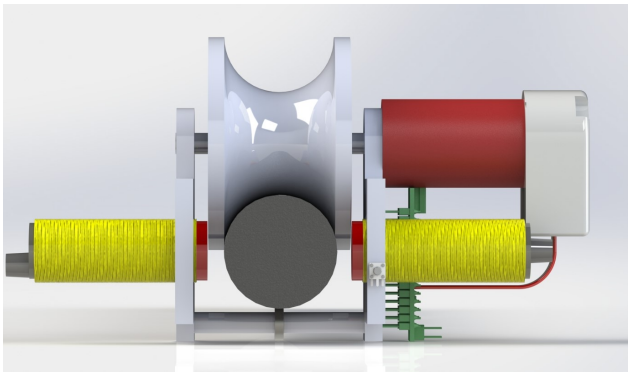

Figure 3.28: Frontal render of concept A

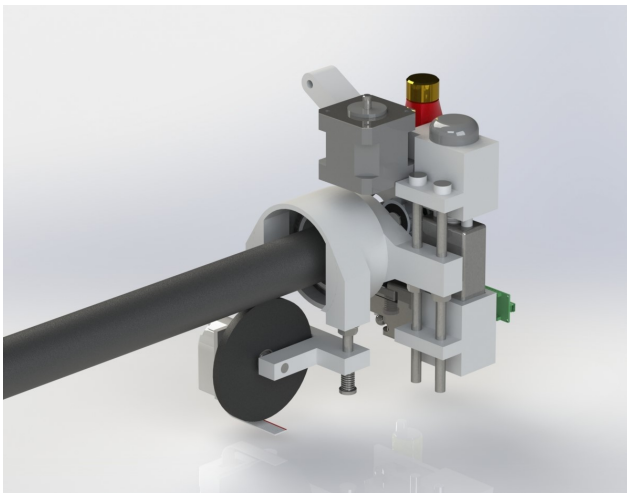

Figure 3.29: First render of concept B

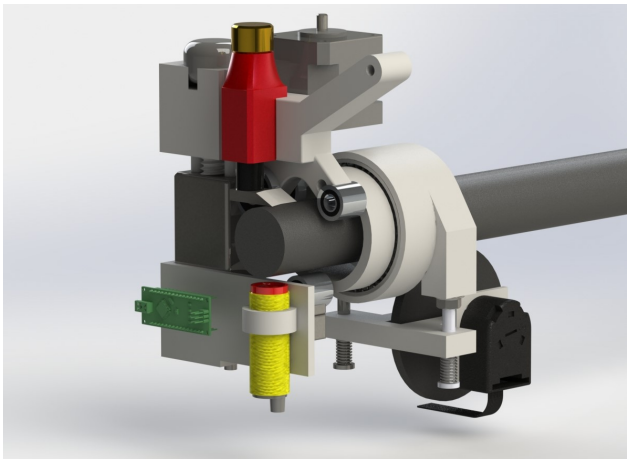

Figure 3.30: Second render of concept B

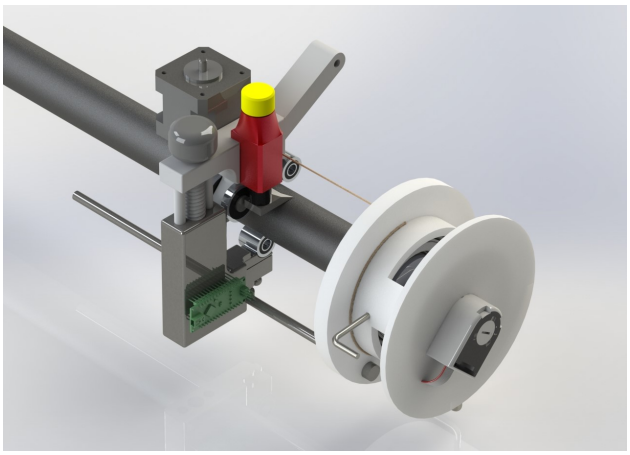

Figure 3.31: Render of concept C

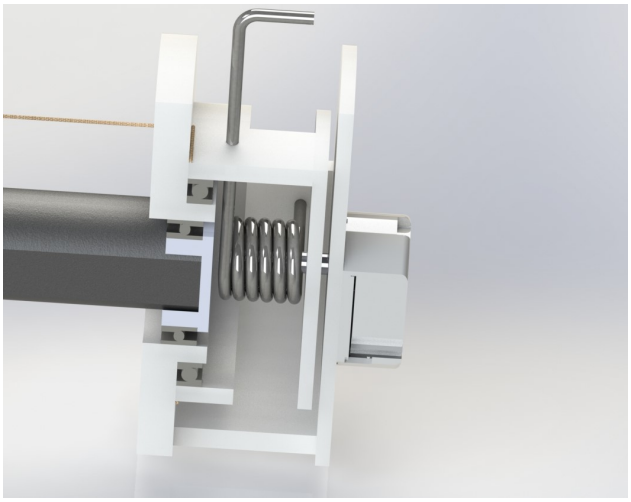

Figure 3.32: Sliced view render of concept C

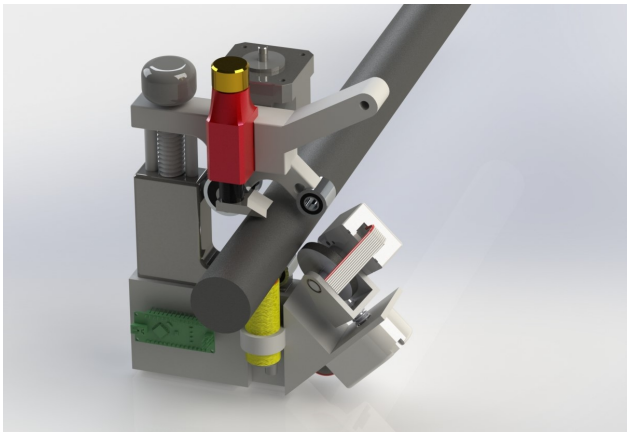

Figure 3.33: Isometric render of concept D

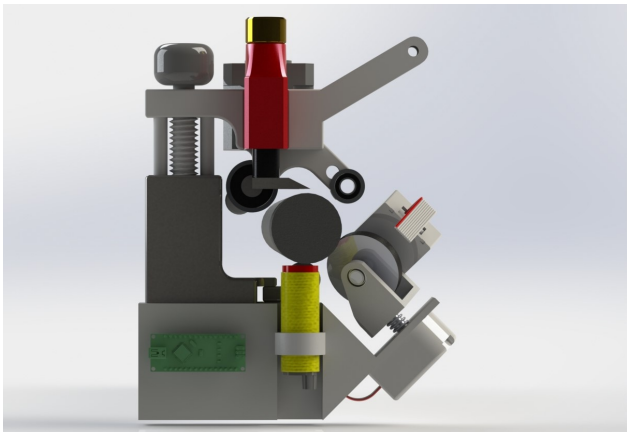

Figure 3.34: Frontal render of concept D

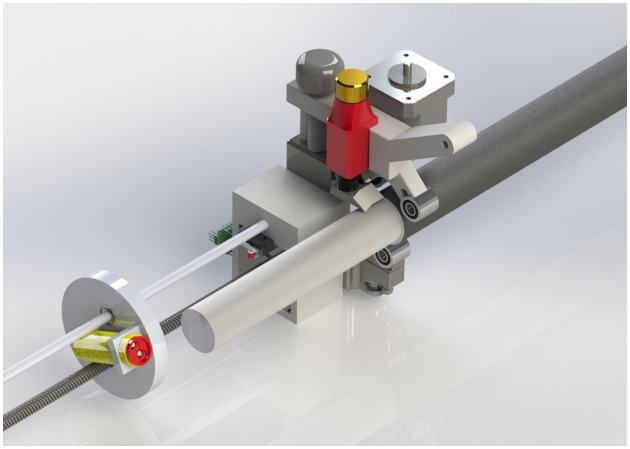

Figure 3.35: Render of concept E

Using these concepts, a comparison between them was made with a selection matrix that uses the needs as selection criteria and concept D as reference, as the process was repeated using each solution as reference and concept D was found to be the most middle-scored. This revealed the results in table 3.10. It is worth noting that concepts B and C are taken out and no combinations were done as no advantageous combination possibilities were found due to the very different nature of each concept.

Table 3.10: Selection Matrix for the selected concepts

	Concepts				
Selection Criteria	A: Self deploying robot	B: Rotationally decoupled wheel	C: Reel system	D: Extra wheel (REF)	E: Lead screw
Efficient and reliable					
Precision	+	+	-	0	+
Lack of human intervention	-	0	0	0	0
Does not add delay	-	0	0	0	-
Period between calibrations	0	0	0	0	-
Fast calibration	0	0	0	0	-
Resistance to the elements	+	0	0	0	+
Easy to use and handle					
Easy to calibrate	0	0	0	0	+
Compactness	-	-	-	0	-
Automation					
Easiness to set zero	0	0	+	0	+
Integration					
Doesn't add rotational inertia	+	-	-	0	-
Doesn't add friction force	+	-	+	0	+
Cable visibility	+	-	-	0	-
Easy to make					
Available technologies	+	0	0	0	-
Easiness to manufacture	+	-	-	0	+
Score	4	-4	-3	0	-1
Rank	1	5	4	2	3
Continue?	Yes	No	No	Yes	Yes

To choose a winner concept a selection criteria with weighted values was created using the importance of each need as well as expert criteria. Iterations of this process were made in order to see the effect of changing the weight of each criteria. The results can be seen on table 3.11

Table 3.11: Winner concepts according to weighted criteria

		Concepts					
		A: Self deploying robot		D: Additional wheel		E: Lead screw	
Selection Criteria	Weight	Rating	Weighted score	Rating	Weighted score	Rating	Weighted score
Efficient and reliable							
Precision	18%	5	0.9	4	0.72	5	0.9
Lack of human intervention	14%	2	0.28	5	0.7	5	0.7
Does not add delay	3%	2	0.06	5	0.15	3	0.09
Fast calibration	5%	4	0.2	4	0.2	5	0.25
Resistance to the elements	4%	5	0.2	3	0.12	4	0.16
Easy to use and handle			0		0		0
Easy to calibrate	4%	4	0.16	4	0.16	5	0.2
Compactness	5%	3	0.15	5	0.25	2	0.1
Automation			0		0		0
Easiness to set zero	8%	3	0.24	4	0.32	5	0.4
Integration							
Doesn't add rotational inertia	4%	5	0.2	5	0.2	1	0.04
Doesn't add friction force	4%	5	0.2	3	0.12	5	0.2
Cable visibility	3%	4	0.12	5	0.15	2	0.06
Easy to make			0		0		0
Available technologies	15%	5	0.75	4	0.6	1	0.15
Easiness to manufacture	13%	5	0.65	2	0.26	5	0.65
Score	100%		4.11		3.95		3.9
Rank			1		2		3
Continue?		No		Develop		No	

Finally as the system in discussion is to be implemented with other systems, the process was explained to the client and the best concepts were explained in depth to make a final decision on the winner concept. Through a long lasting and comprehensive discussion with the client, it was decided that adding an attached system (instead of a separated system) would give a better image of the product to investors. This way the winner concept to develop as design proposal is concept D (Additional wheel), the process of detail engineering design over this concept can be seen in chapter 4.

3.5.2 Other sub-problems concept selection

Once the solutions were selected for the sub-problems which define and significantly change the project development, the rest of concepts were figured out and selected. The list of concepts for this sub-problems can be seen in table 3.12. These were mostly based on availability of components and following a "is this enough?" philosophy to avoid over-complicating the final concept.

Table 3.12: Concepts created for the non-measuring principle sub-problems

Concept	Energy	Controlling the system	Change feed	Modify distance of cut	Display distance	Displaying state
A	Receive from electric cable using a slip-ring	Use an Arduino	On-off control system	Potentiometer	Digital number display	Sound alert (beeping)
B	Store in batteries	Use an Arduino	On-off control system	Numeric keypad	Digital number display	1 LED for each state
C	Receive from electric cable	Use a Raspberry-Pi	On-off control system	PC	PC	Sound alert (beeping)

As an initial filter, the concepts were compared using concept B as reference. This process yielded the results in table 3.13. It was noticed that both concepts A and B had qualities that might be considered beneficial to combine, resulting in table 3.14, with the new concept AB.

Another influential factor is the use of external devices, as it was thought that it might discourage investors as it may look like extra work. Safety concerns are also deeply taken into account during the whole process, but specially in this critical step. All those considerations are discussed in chapter 5.

Table 3.13: Selection matrix for the non-measuring principle concepts

	Concepts		
Selection Criteria	Concept A	Concept B (REF)	Concept C
Error detection			
Error detection success	0	0	-
Easy to use and handle			
Easy to change distance of cut	-	0	-
Information easily readable	0	0	-
Current state is evident	+	0	+
Practicality			
Experience with technology	+	0	-
Availability of technology	0	0	0
Size	+	0	-
Score	2	0	-4
Rank	1	2	3
Continue?	Combine	Combine	No

Table 3.14: Second iteration of secondary concepts

Concept	Energy	Controlling the system	Change feed	Modify distance of cut	Display distance	Displaying state
A	Receive from electric cable	Use an Arduino	On-off control system	Potentiometer	Digital number display	Sound alert (beeping)
B	Store in batteries	Use an Arduino	On-off control system	Numeric keypad	Digital number display	1 LED for each state
AB	Store in batteries	Use an Arduino	On-off control system	Potentiometer	Digital number display	Sound alert (beeping) + 1 LED for each state

It is worth noting that the type of control does not vary between concepts but it's left as a design choice for future iterations on the device.

Another important thing that was discovered in next steps of the design process is that I/O availability is one critical limitation, specially considering that a compact product is one of the client needs. Therefore, having big micro-controllers is to be avoided and human-machine interfaces should be simple and require little I/O whenever possible.

Taking the discussed factors into account and the needs gathered before, table 3.15 was created and repeated until each of the weights assigned represented adequately the importance of each

factor.

Table 3.15: Winner selection of non-measuring principle concept

		Concepts					
		Concept A		Concept B		Concept AB	
Selection Criteria	Weight	Rating	Weighted score	Rating	Weighted score	Rating	Weighted score
Error detection							
Error detection success	15%	4	0.6	5	0.75	5	0.75
Easy to use and handle							
Easy to change distance of cut	15%	3	0.45	5	0.75	3	0.45
Information easily readable	15%	4	0.6	4	0.6	4	0.6
Current state is evident	15%	3	0.45	2	0.3	5	0.75
Practicality							
Little I/O required	10%	5	0.5	2	0.2	5	0.5
Experience with technology	10%	4	0.4	4	0.4	4	0.4
Availability of technology	15%	5	0.75	3	0.45	5	0.75
Size	5%	5	0.25	3	0.15	4	0.2
Score	100%		4		3.6		4.4
Rank			2		3		1
Continue?			No		No		Yes

3.6 Concept testing

Using the winning concept from both concept selection categories, an in depth design process was performed where the device was tested in order to grasp a better understanding of the system's behaviour, as little research was available on similar systems due to this being a novelty device.

In this step the selection process of the main components is also discussed if deemed necessary to understand the working principle of the device.

All of this crucial information to understand the design process can be seen in chapter 4, as all testing and study of the system forms part of the same concept where optimization based on new discoveries was performed.

Chapter 4

DESIGN PROPOSAL

Using the winner concept, an in-depth design was done taking into account the specifications to create a product that adequately solves the client's concerns. The following sections explain the development of the final design proposal in detail, explaining also problems found in the way and the solutions taken.

The proposed design uses a caster wheel (seen in figure 4.1) to measure movement. This type of wheel can be seen in shopping carts trolleys and that's where the original inspiration comes from. Said wheels have the characteristic that in ideal conditions and steady state, the direction of the wheel faces the direction of the velocity of the system. Previous analysis has been performed on the transient behaviour of this wheel and it was determined that the repeatability of the system is very high for low angle changes on the swivel [29] which makes it ideal for this design as only small changes in the advance per revolution are expected. So the angle of the swivel can be used to indicate the direction of the movement and the rotation of the wheel itself can be used to calculate displacement, so together it is possible to obtain a displacement vector on the movement of the system.

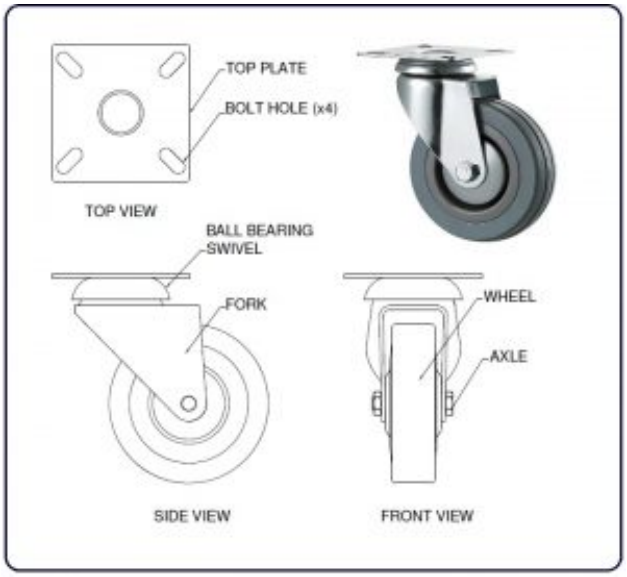

Figure 4.1: Main components of a caster wheel [30]

4.1 Sensing components selection

There are 3 components which mainly define the precision and accuracy of the entire system: The absolute encoder, the incremental encoder and the presence-absence sensor. Said components selection process is explained below.

4.1.1 Presence-absence sensors

The presence-absence sensors used corresponds to a WLK-4MINI, seen in figure 4.2.

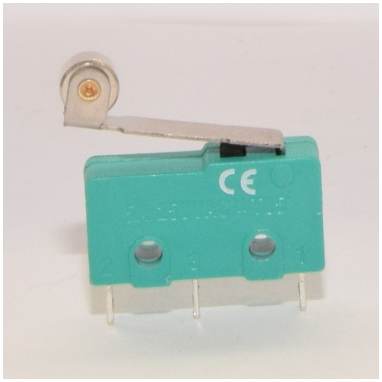

Figure 4.2: Presence-absence mechanical switch WLK-4MINI used in the final design. [31]

This sensor requires minimum I/O (one ground cable and one signal cable when used in a pull-up resistor configuration), it is small and easy to mount using a set of 2 mm screws [31]. The only potential problem found with this method of detecting presence absence is that there was a small wiggle from side to side, which might decrement the accuracy of the system. Nonetheless in practice it was observed that the cable detection always happened within a 0.25 mm difference from one measurement to the other or less when measuring with a caliper in 5 different occasions, therefore this error was not taken into account.

It is worth noting that initially the use of photo-electric sensors were thought to be used in this regard, but none of the providers had said sensors with the required range readily available. Apart from this, no testing was performed on these types of sensors, which in some cases depend on the light reflection properties of the material, adding to the uncertainty of whether or not they work for this application. Nonetheless, it might work as a possible solution in future iterations of this device.

4.1.2 Incremental encoder

The use of HEDS-550X/HEDM-550X/HEDS560X and HEDS-554X/HEDS564X series or similar encoders were strongly preferred, as experiments were carried out using similar technology in previous steps of the methodology and they're readily available using the preferred distributors of the University [32].

Taking into account the physical dimensions of the encoders to use (shown in figure 4.3), a measuring wheel attached to the axis should have a diameter greater than 30 mm to avoid collision between the encoder and the cable. Therefore a wheel of 35 mm of diameter is going to be used accounting for possible bending of pieces.

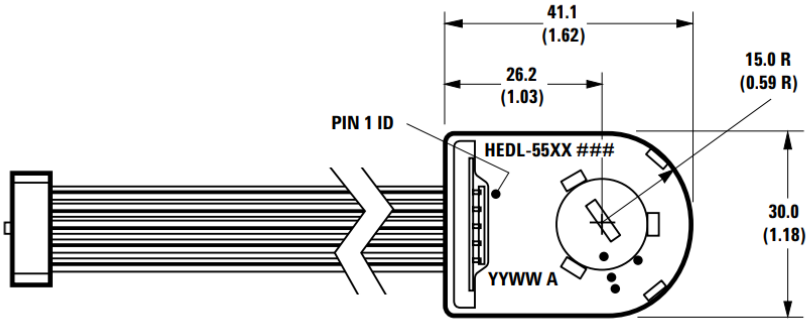

Figure 4.3: Physical dimensions of the incremental encoder used for the system [33]

Using figure 4.4 as reference to calculate a minimum angular resolution, where r is the radius of the wheel, Δs is the tangential displacement and $\Delta\theta$ is the angular displacement. Using Eq. 4.1 the total displacement per degree of rotation can be calculated.

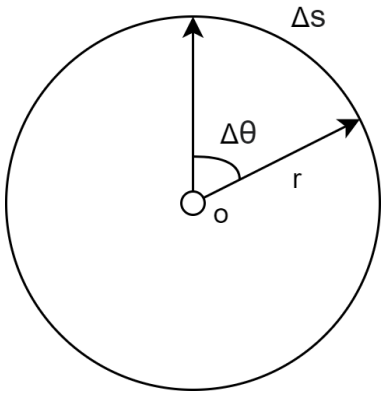

Figure 4.4: Angular to linear displacement conversion

$$r\Delta\theta = \Delta S \tag{4.1}$$

Using $\Delta S = 0.5$, assuming a movement parallel to the cable as worst case scenario. It can be seen that maintaining a constant $\Delta\theta$, the linear resolution can be incremented by reducing the radius, therefore a minimal radius is considered optimal. Now substituting the known values, $\Delta\theta = \frac{5}{35} = 0.1428rad$. It must be taken into account that the resolution of a rotary encoder is usually given in steps per revolution. This means the minimum resolution of the encoder should be of at least 44 steps per revolution.

Therefore the HEDL-5540#A12 was chosen, with an axis diameter of 6 mm which is easily obtainable from the university preferred electronic distributors and 500 physical steps per revolution (2000 virtual steps) [33] which enables for a safety factor of $f_s = 11.36$. There are no less-expensive and less-accurate optical incremental encoders that fulfill this resolution requirement within the available providers, so this was considered the best option at the time of realization of this graduation assignment.

4.1.3 Absolute encoder

To choose the absolute encoder 2 main factors were taken into account, namely: the price and the resolution of the sensor. Even though a budget was never set for the realization of this project, it was explicitly expressed by the client to invest in components as cheap as possible without jeopardizing the fulfillment of the project's objectives.

In order to find an acceptable value of resolution, the following calculations and experiments were made: Initially the advancement per revolution along the axis was studied to determine if it was constant or variable and it was found that it varies depending on the clamping force. To do this the device was turned 5 times and the distance traveled was marked using a pen; this was repeated 10 times at different clamping forces (seen in figure 4.5). The lowest feed per revolution was noticed to be around 3.5 mm/rev, nonetheless 3 mm/rev is going to be used as a conservative design value as this would mean a need for more accurate angle of movement sensing.

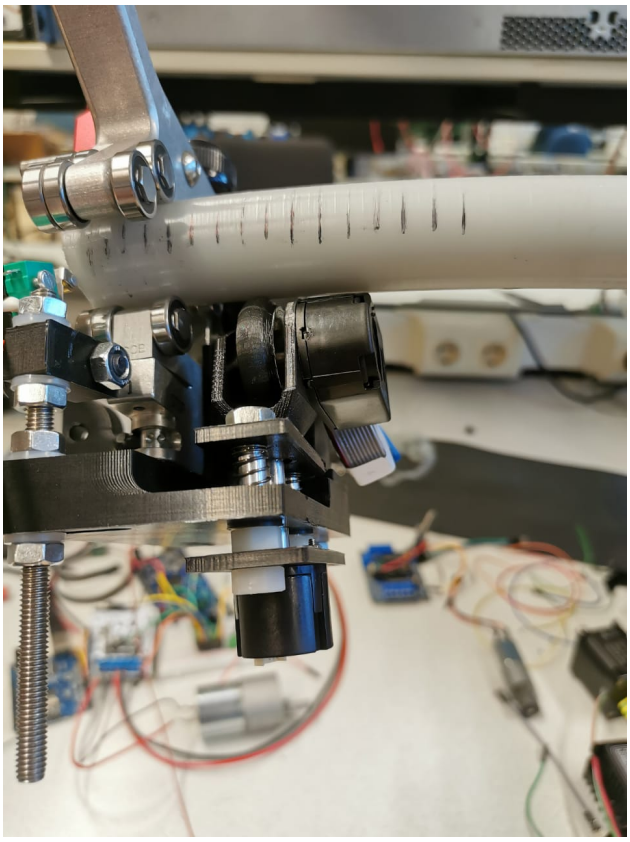

Figure 4.5: Experimenting to observe the effect of clamping force on the advance per revolution using the first version of the prototype

Therefore starting with equation 4.2.

$$A = \alpha r sin(\theta) \tag{4.2}$$

Where A is the displacement along the cable axis, αr is the total displacement sensed by the incremental encoder as seen in figure 4.6 and θ is the angle sensed by the absolute encoder. Using an advancement per revolution of 3 mm/rev and knowing that the cable's diameter is of 31 mm (in reality is slightly less, but this also serves as a conservative value), therefore its perimeter (one revolution) is $D = 31\pi = 97.389$ rendering equation 4.3 that gives the ratio for a worst case scenario movement of the robot, with an angle sensed by the absolute encoder of $\theta = 0.03079$.

$$\frac{A}{D} = \frac{3}{97.389} = 0.0308 \tag{4.3}$$

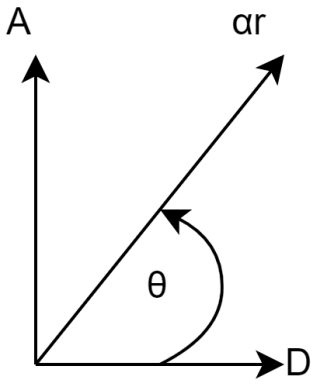

Figure 4.6: Trigonometry used to calculate the displacement along the axis, r is the radius of the measuring wheel, θ is the angle of the absolute encoder, α is the angle of the incremental encoder, D is the distance travelled by rotating around the cable and A is the position along the axis.

Continuing, using the maximum distance the device is going to measure ($A = 240$ mm), equation 4.3 gives $D = 7791.12$ mm, therefore $\alpha r = \sqrt{7791.12^2 + 240^2} = 7794.82$ mm. The maximum angle error (θ_{max}) can be determined transforming Eq. 4.3 to Eq. 4.4.

$$\alpha r sin(\theta + \theta_{max}) = A + E_{max} \tag{4.4}$$

Where E_{max} is the maximum allowed error, in this case a goal value of 0.5 mm. Substituting in Eq. 4.4, $7794.82 sin(0.03079 + \theta_{max}) = 240.5$, living a required resolution described by Eq. 4.5.

$$\theta_{max} = 0.0000687 \tag{4.5}$$

Nonetheless, this is not the resolution required by the sensor itself as a gearbox can be implemented to increase the sensitivity of the sensor with respect to the swivel rotation and as later was found, the use of multiple sample points reduces the resolution needed.

After researching for the available absolute encoders it was found that a resolution equal or better than the required can only be obtained using industrial absolute encoders, which are too big and expensive to be used in this concept. Therefore the sensor AEAT-6012-A06 [34] was chosen and it is to be implemented using a gearbox to adjust the sensibility to the desired value. This sensor has 12 bits of resolution or 4096 steps per revolution, which translates to a resolution of $\theta_{sensor} = 0.001534$.

4.2 Electronic circuit

An Arduino Nano [35] was used as it is lightweight and compact and it was deemed to have the necessary I/O and frequency to work on this design.

The different sensors used as well as the interface components must be wired to the Arduino Nano following the designed circuit in figure 4.7. A brief description of the pin arrangement for the proposed circuit can be seen in table 4.1.

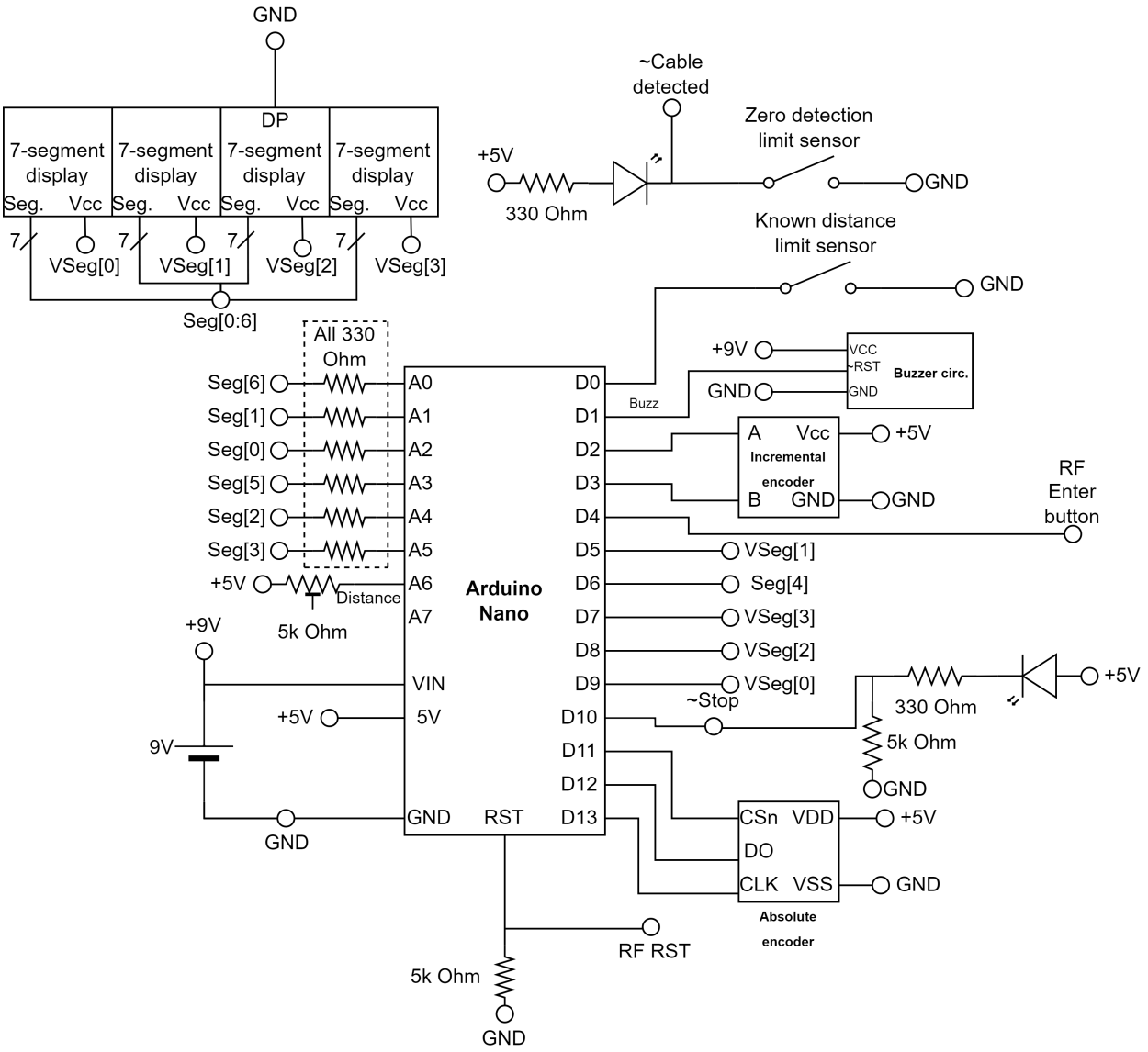

Figure 4.7: Diagram of the electronic circuit used for the project

Table 4.1: Pin description for the Arduino Nano micro-controller used in this project

Pin	Type	I/O	Name	Description
D0	Digital	Input Pullup	~Known position reached	Inverted signal, indicates cable has reached a known position to start the relative measurement
D1	Digital	Output	Buzz	Indicates when to make alarm sound
D2	Digital	Interrupt	Incremental Encoder A	Indicates movement in the incremental encoder
D3	Digital	Interrupt	Incremental Encoder B	Indicates movement in the incremental encoder
D4	Digital	Input Pullup	RF Enter Button	Button that saves the selected distance and indicates the start of the motion
D5	Digital	Output	VSeg[1]	Lights 7-segment display number 1
D6	Digital	Output	Seg[4]	Lights segment 4
D7	Digital	Output	VSeg[3]	Lights 7-segment display number 3
D8	Digital	Output	VSeg[2]	Lights 7-segment display number 2
D9	Digital	Output	VSeg[0]	Lights 7-segment display number 0
D10	Digital	Output	~Stop	Inverted signal, indicates when to change the advance per revolution to "stop"
D11	Digital	Output	Chip select	Signal that enables the reading of the absolute encoder (SPI protocol)
D12	Digital	Input	Absolute encoder position	Serial signal that sends the current position of the absolute encoder (SPI protocol)
D13	Digital	Output	Absolute encoder CLK	Clock for the absolute encoder (SPI protocol)
A0	Digital	Output	Seg[6]	Lights segment 6
A1	Digital	Output	Seg[1]	Lights segment 1
A2	Digital	Output	Seg[0]	Lights segment 0
A3	Digital	Output	Seg[5]	Lights segment 5
A4	Digital	Output	Seg[2]	Lights segment 2
A5	Digital	Output	Seg[3]	Lights segment 3
A6	Analogue	Input	Distance	Analogue value coming from a potentiometer

The signal that indicates the presence of the cable is not wired to the Arduino as it was found later that not setting the zero, but setting a known distance farther away as a starting point is more beneficial as it enables the system to collect more samples on the angle before starting the measurement process. This also makes it so that there is no further delay on the cable detection signal sent to the depth of cut controlling system of the robot.

It is worth noticing that a 9V battery is used to power the system. The use of batteries enables the system to rotate freely without cables of the system getting tangled around the XLPE cable limiting its movement, but it also means that the output voltage of the battery configuration should be checked frequently to be above 7 V in order to ensure the correct functioning of the system [35]. On the other hand, the lack of actuators in the system also means the total current draw from the batteries is considerably lower than solutions that involve the use of motors.

Another element worth mentioning is the use of radio frequency (RF signals to control the device). This is the result of considering the safety regulations for machine control. As the robot is going to be moving, the access to buttons might be limited in case of a required emergency stop, therefore wireless and remote access will be used. Details on how this helps from a safety standpoint are discussed in chapter 5. Note that this RF device is not implemented in the final prototype as said prototype is moved by hand and stopping of the device can be done by not rotating it. It is strongly recommended to use it in the final implementation.

In order to use RF signals for the emergency stop (RF RST) and (RF Enter) buttons, an RF module and a controller must be acquired. After researching into the available options from the preferred distributors, it was concluded that the FOBOEM-4S4 Remote Control System [36] was inexpensive, works for the intended purposes and also transmits at a frequency allowed by the European governments [37], therefore it was selected for this application.

This receiver uses low current and works with voltages from 1.8 to 3.6 Volts [38], which enables it to be connected directly to the 3.3V pin of the Arduino Nano. Using figure 4.8 as reference, output 1 and 2 are the digital RF Enter and RF RST signals respectively and will be connected to its respective tags in figure 4.7.

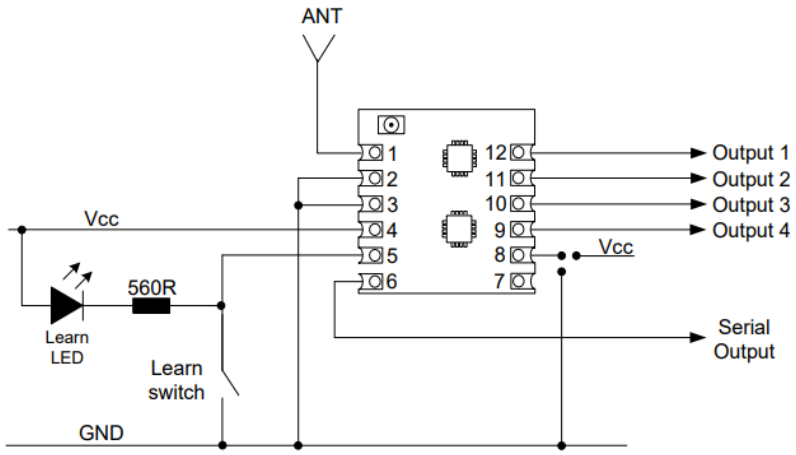

Figure 4.8: FOBOEM-4S4 receiver diagram [38]

4.3 Mechanical structure

4.3.1 Gearbox

To compensate for the lack of resolution in the absolute encoder, the sensitivity has to be changed and for this a gearbox was used, the procedure for calculating the gears to be used was as follows:

The required resolution given by Eq. 4.5 is $\theta_{max} = 0.0000687$, while the resolution of the sensor is $\theta_{sensor} = 0.001534$, therefore the turn ratio is shown in Eq. 4.6.

$$\frac{\theta_{max}}{\theta_{sensor}} = 0.04478 \tag{4.6}$$

This means that a turn relation of around 1:25 should be used for the gear-box to guarantee that the error is always lower than 0.5. Nonetheless a relation of 1:5 was first tested in a design iteration and it was found that said value is enough to comply with the specifications of the system set by the client as multiple sample points are taken and an average is used, therefore 1:5 was left as the turn ratio of the gearbox in an effort to save space and not add unnecessary weight to the system.

The use of this gear box also implies the presence of backlash [20], for this reason the best 3D printing configuration available was used to allow for 0.1 mm resolution and less loss of accuracy and the modulus used was the lower possible with that resolution (modulus of 0.5 mm). The lower the modulus the less backlash is expected in spur gears [20].

Further gear mechanical structure analysis is not necessary due to the extremely low power nature of this application, where the main goal is not to transmit power but to give very accurate positioning.

4.3.2 Slippage avoidance

One of the most important factors to account for in this section is how to avoid slippage. In the experimentation previously performed it was found that slippage happened when the friction force was not enough. For this, the proposed designed uses springs and linear bearings that clamp the measuring wheel with enough force to avoid slippage. The linear bearings made by Iglidur [39] were selected because they provide a very low friction coefficient, they are cheap and they require no lubrication.

To ensure that little to no slippage could happen, experimentation on the XLPE material was performed using the set-up in figure 4.9 to select springs that could work. An adjustable base and a block were printed. The inclination angle was changed until the block started moving. Later the inclination angle was calculated by using trigonometry and a measuring caliper with 0.05 mm resolution.

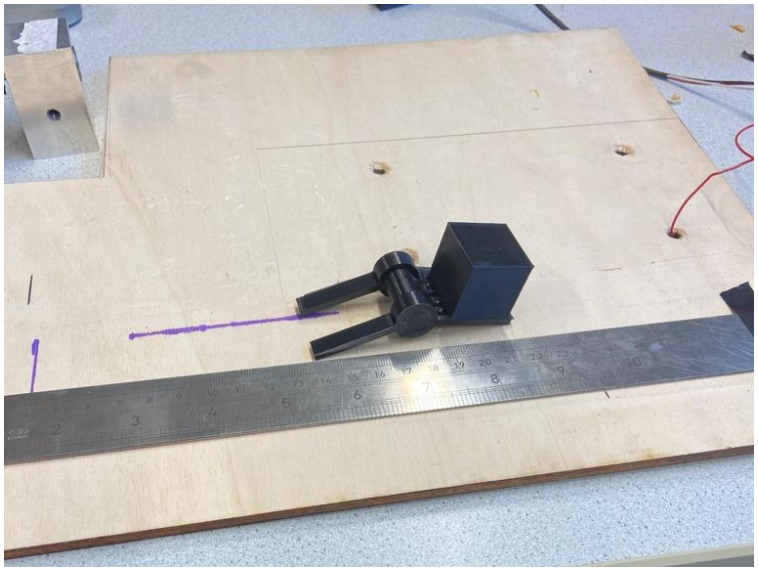

Figure 4.9: Set-up used to determine the friction coefficient between Ultimaker's PLA 3D printed material and the XLPE polymer of the cable

The experiment gave as result an inclination angle of $(12.40^{o}\ ^{+0.67}_{-0.64})$cm which can be used

to determine the friction coefficient by using Eq. 4.9, where μ is the friction coefficient and θ is the angle of inclination of the set-up.

$$\mu = \frac{sin(\theta)}{cos(\theta)} \tag{4.7}$$

Substituting the known values in Eq. 4.9 yields a friction coefficient of $\mu = 0.220 \pm 0.012$ between the PLA Tough 3D-printed material and the XLPE cable.

To figure out values for the design of the measuring wheel mechanical system, the first step was to obtain an estimation of the rotary resistance to be felt by the wheel. For this, a conservative typical starting torque of 0.63 g.cm was used [20], which translates to $6.18(E-5)N.m$ in SI units. As the measuring wheel is placed in an axis held by two bearings, the resistance is doubled, rendering a required starting torque of $M = 1.24(E-4)$ N.m. A simplified force diagram for the forces that influence on the moment around point O can be seen in figure 4.10, which renders Eq. 4.8.

$$M = rF_w \tag{4.8}$$

Using Eq. 4.8, the required friction force on the wheel to avoid slippage between the wheel and the cable while rotating is $F_w = 3.543(E-3)N$, which can be obtained using Eq. 4.8. Using the known friction coefficient and the estimated required friction force, a required normal force of $N = 0.017N$ was obtained.

$$F_f = \mu N \tag{4.9}$$

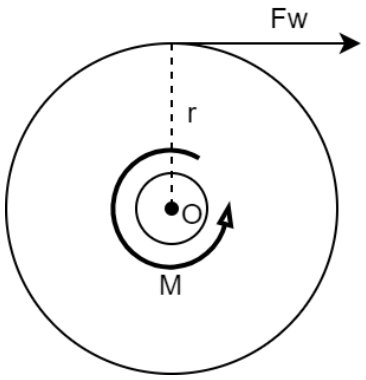

Figure 4.10: Free body diagram with forces that influence in moment around point O for the measuring wheel and its axis

It is also necessary to obtain the required normal force to avoid slippage from the swivel's perspective (ensure enough friction between wheel and cable for proper swivel axis rotation). For

this, the simplified free-body diagram from a top view of the gearbox system is used, as it can be seen in figure 4.11, where a required F_w can be obtained as a required friction to avoid slippage in the system. Analyzing body A renders Eq. 4.10, where using the gear relation designed $\frac{r_1}{r_2} = 5$, the bearing torque resistance from Machinery's handbook [20] of $6.18(E-5)N.m$.

Knowing that according to the proposed design, gear A has 3 bearings and gear B has 2, then the required torques can be approximated as: $M_1 = 3 * 6.18(E-5)$N.m= $1.85(E-4)$ N.m and $M_2 = 2 * 6.18(E-5)$ N.m = $1.24(E-4)N.m$. Therefore substituting known values in Eq. 4.10, $LF_w = 8.05(E-4)N.m$ or $F_w = \frac{8.05(E-4)}{L}N.m$. At this point it can be noted that the lead distance (L) influences on the required friction in an inversely proportional manner by changing the torque sensed by the gears, meaning a larger lead distance would also add more stability by making the required force to turn the swivel less, therefore making a more stable system.

The lead distance selected was of L = 8.58 mm. Finally, solving for F_w in Eq. 4.10, $F_w = 0.0938N$. Using the Equation 4.9 to obtain the required normal force, it yields $N = 0.45$ N. This newly obtained normal force is greater than the one previously calculated, which is why it is going to be used as the required normal force from the springs. A factor of design of 2.5 is used to ensure that the normal force will be greater in case of bending of the cable (which is expected to be minimum as the wheel is very close to the clamping point of the cable), rendering a design normal force of $N_d = 1.125$ N.

$$LF_w = \frac{r_1}{r_2}M_2 + M_1 \tag{4.10}$$

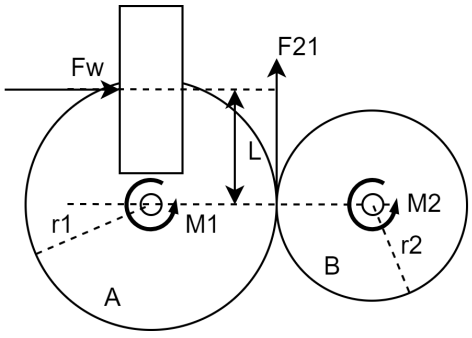

Figure 4.11: Simplified top view free-body diagram for the gearbox including only the forces that have an effect on the moment around the center of rotation of the gears.

For the selection of the springs, two 10 mm compression springs are used. In order to prevent finger clamping and require less movement of the system for greater forces the springs are going

to be pre-loaded by 3 mm leaving a 7 mm gap. Then when the cable is added and the system is clamped around it, the springs will be compressed 1 more millimeter. As 2 springs are going to be used, the normal force required can be divided by the two of them, as the multiple spring effect is additive when used in parallel [40]. Using Hooke's law [40], Eq. 4.11 can be used to calculate the required spring constant (k), where x is the spring compression or elongation and F is the resulting force. Therefore solving for k, with $x = 0.004$ m and $F = 1.125/2$ N, renders $k = 140.625$ N/m as spring constant.

$$F = kx \tag{4.11}$$

Therefore a 10 mm long compression spring with $k = 140.625$ N/m should be used, but one with a constant slightly above this value may also be acceptable, as a security factor is being used for the mechanical design.

4.3.3 Torque screwdriver adaptor

When testing was performed (results of this seen in appendix C), it was found out that the clamping force applied to the device when placing it on the cable had a deep effect in both the advance per revolution when in position 2 and the behaviour of the swivel angle signal. In general, the stronger the clamping force the more advance per revolution, but also greater oscillations on the measuring wheel and a more unpredictable behaviour. Because of this, low and constant clamping forces are preferred.

Making the clamping force constant is no easy task by hand, as a skilled worker can only try to set the same torque on a screw every time with around ±33% precision [20]. For this reason, it was necessary to create an adaptor that enables the clamping screw to be connected to a torque screwdriver which allows for much greater torque precision. This can be seen in use in figure 4.12

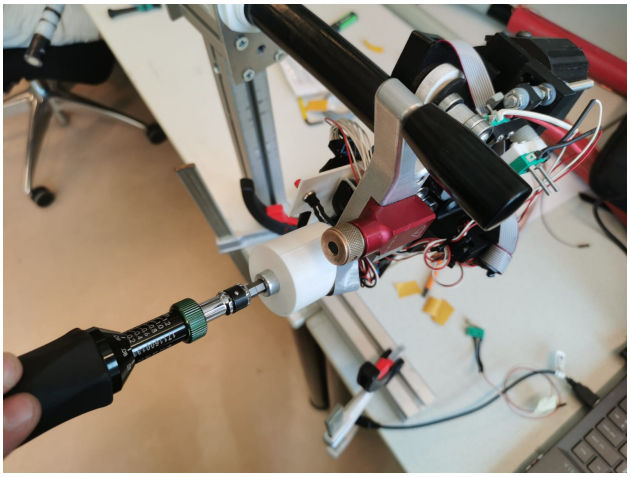

Figure 4.12: Designed torque screwdriver adaptor

The torque was set to 0.2 Nm in the torque screwdriver and a great increase in repeatability was observed, as discussed in the results chapter.

4.3.4 Structural analysis by simulation

Structural analysis was performed using Solidworks software. Different materials are used for manufacturing the pieces of the assembly, namely aluminum for the axis and Tough PLA for 3D printed designed parts. All standard components are made from a steel alloy unless otherwise specified in the list of parts, as some washers are made from nylon.

Typical values provided by Solidworks were used for the material properties in simulation, except for the tough PLA and the material used for the linear bearings by Iglidur, both proprietary but with publicly available data-sheets. For the Tough PLA, the official data sheet was used [41] and the more conservative side of values were selected to create a custom material in Solidworks as seen in figure 4.13, where all values come from the specific material's data-sheet except for the Poisson's ratio which is not there, so it is estimated to be at least the one of regular PLA material [42]. For the Iglidur bearings, all material data was extracted from its data-sheet [39], seen in Solidworks as a custom material in figure 4.14.

Property	Value	Units
Elastic Modulus	2821	N/mm^2
Poisson's Ratio	0.331	N/A
Shear Modulus		N/mm^2
Mass Density	1220	kg/m^3
Tensile Strength	19.7	N/mm^2
Compressive Strength	19.7	N/mm^2
Yield Strength	43.3	N/mm^2
Thermal Expansion Coefficient		/K
Thermal Conductivity		W/(m·K)
Specific Heat		J/(kg·K)
Material Damping Ratio		N/A

Figure 4.13: Tough PLA material properties used for simulation

Property	Value	Units
Elastic Modulus	7800	N/mm^2
Poisson's Ratio	0.3	N/A
Shear Modulus		N/mm^2
Mass Density	1460	kg/m^3
Tensile Strength	210	N/mm^2
Compressive Strength	210	N/mm^2
Yield Strength	210	N/mm^2
Thermal Expansion Coefficient		/K
Thermal Conductivity		W/(m·K)
Specific Heat	1386	J/(kg·K)
Material Damping Ratio		N/A

Figure 4.14: Iglidur bearing material properties used for simulation

The main purpose of the mechanical structure is to measure with precision, therefore as it was discussed for the gearbox design, power transfer between axis is extremely low, where the most significant resistance comes from the bearings. Considering the torque applied to said elements is negligible, it is not necessary to perform simulations or any type of resistance of materials analysis directly on the gears.

There are two main external forces that will be affecting the system in steady state; the first one comes from clamping the wheel against the cable as it can be seen in figure 4.15. This clamping force was determined in order to avoid slippage, therefore the expected normal force was already calculated earlier in this chapter as $F = 1.125N$.

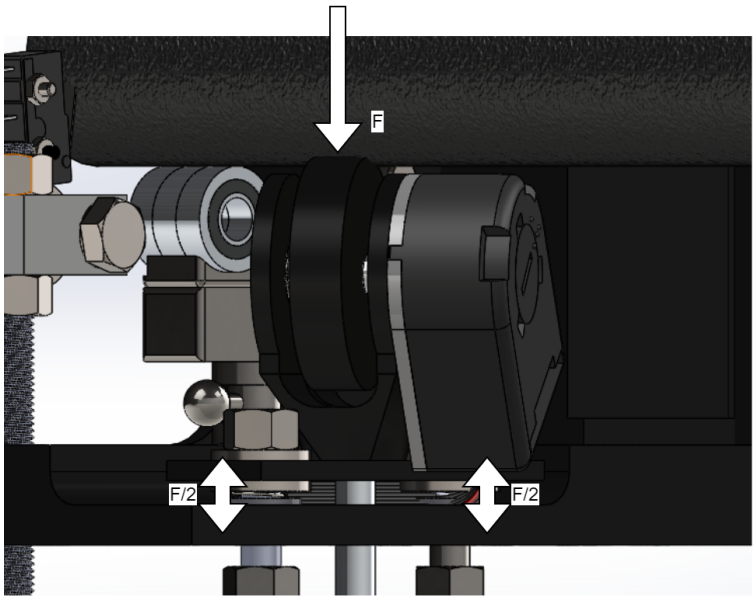

Figure 4.15: External force present from the normal force between the cable and the pressure applied by the springs

The second external force comes from the limit switches placed for cable detection. According to the data-sheet, the normal force required to activate the switch is of 1.5 N [31]. As the mechanical properties of the limit switch are unknown and the switch itself is designed to endure this conditions, for modeling purposes the normal force will be directly applied to the screw holes on the holder of the mechanical switch in the assembly.

In order to know where the forces of the mechanical switch are going to act on its holder, a static stability analysis was performed as shown in figure 4.16, showing the forces on that piece when in activated position. The reaction forces of the system can be obtained using Eq. 4.12 for the sum of forces in the tangential direction of the forces and 4.13 for the moment in point O_1. Knowing that F_N is of 1.5N, the equations in discussion are solved for R_1 and R_2. This yields R_1 = 2.132 N and R_2 = -0.631 N, meaning the initial guess of the direction of R_2 was incorrect.

$$F_N - R_1 - R_2 = 0 \tag{4.12}$$

$$F_N * 4 + F_{N2} * 9.5 = 0 \tag{4.13}$$

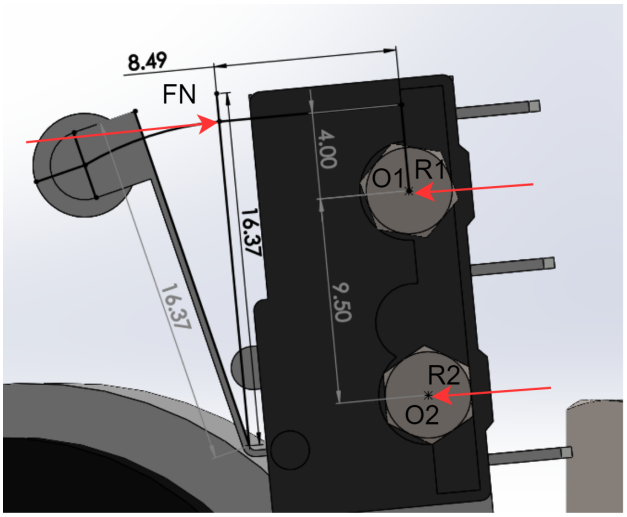

Figure 4.16: Free-body diagram for the mechanical switch.

As the system is going to be rotating around a cable, a centrifugal force was also added with a speed of 60 RPM around the cable axis and gravity was also added (with a gravity constant of 9.81 m/s^2) to account for the components weight. The device also has surfaces which are fixed to the peeling device, this are contemplated in the simulation using fixtures.

Only the elements that endure significant external forces and have an impact on the mechanical stability of the designed system are taken into account for the simulation, leaving the analysis with the elements shown in figure 4.17, enabling for a clearer view of the important to analyze elements. Results from this simulation are shown in chapter 6.

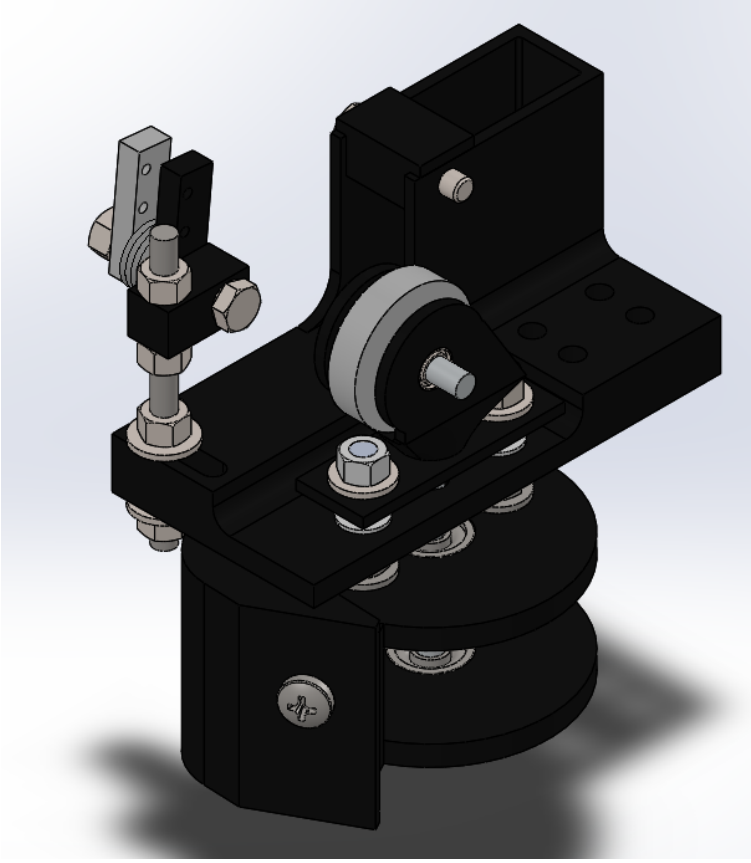

Figure 4.17: Elements included in the computer structural simulation

Other elements such as the HMI carcass that support only the weight of the perforated board and the electronic components attached to it were excluded from this analysis as it was considered that their load is so low that using expert criteria for the design and then testing in prototypes is enough to ensure the adequate structural stability of those components.

The simulations that are going to be performed are vonMises stress analysis to grasp an idea of which parts of the assembly are subjected to the most stress which might be useful in future iterations of this project, a displacement analysis to observe if there is significant shaft displacement or if the wheel is being moved too much as that might have unwanted effects on the behaviour of the system and finally a factor of safety analysis using Max Shear Stress and Max vonMises stress as this is one of the indicators for the success of this project. The most conservative value is going to be used as the FOS of the system.

4.4 Processing of sensors signals

The signals received from the sensors have to be calibrated and filtered in order to achieve the desired values of average absolute error. The steps taken in this regard are explained in the following subsections. The data-gathering circuit using an Arduino UNO seen in appendix G was used as well as the code in appendix F to obtain the data used for this section.

4.4.1 Filtering

The absolute encoder, which is attached to the swivel of the caster wheel requires extra analysis regarding both calibration and processing of the sensor output signal. Research on typical behavior of the caster wheel showed that swivel movement theoretically corresponds to an under-damped response when the angle is changed [29] and this was observed in the taken data. Analysing the signal from this sensor, it was noticed that in steady state the swivel of the caster wheel oscillates in a periodic and significant manner for each turn as seen in figure 4.18.

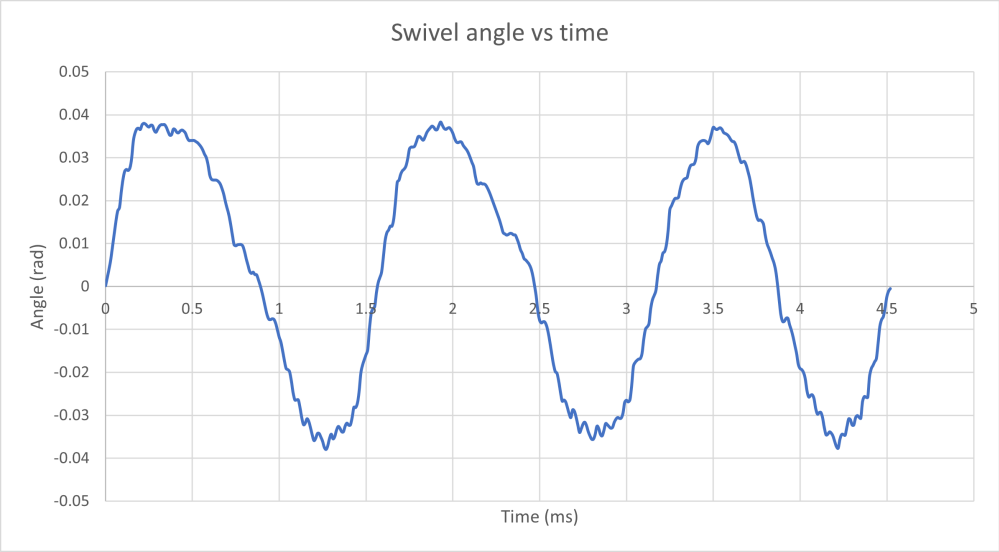

Figure 4.18: Oscillations present in the swivel angle for 3 turns around the cable in stop position.

The oscillations in steady state reduce the accuracy of the system as they deviate from the actual angle of movement, which is estimated to be the average of the signal. An FFT analysis was performed, yielding the graph in fig. 4.19. In this figure, a main frequency can be observed, which corresponds to a sine-wave with period of around the period of rotation of the system.

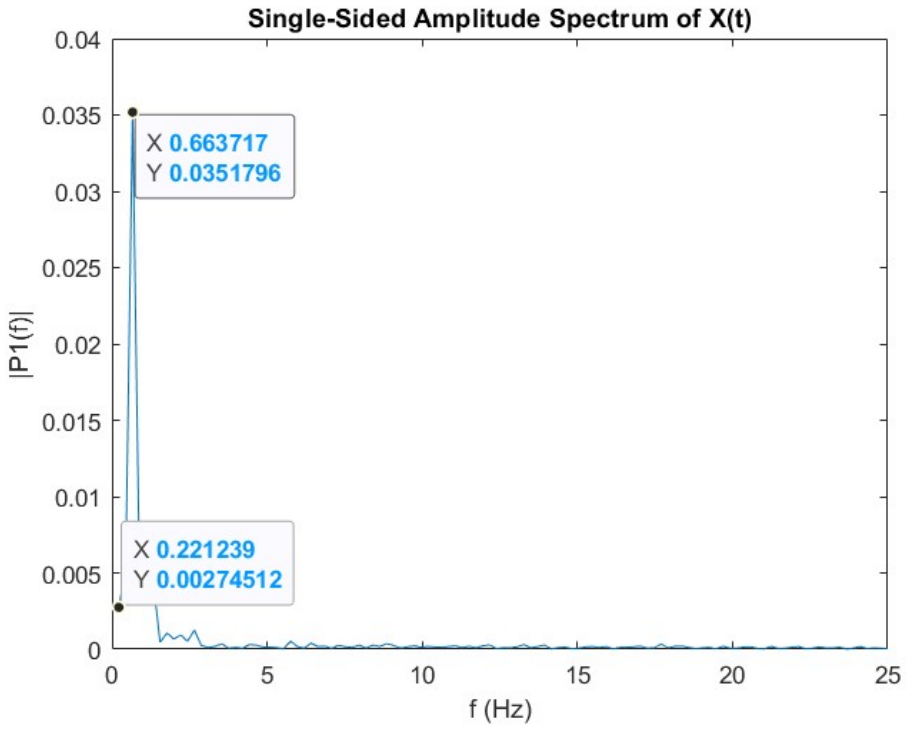

Figure 4.19: Fast Fourier Transformation of signal in figure 4.18 as X(t)

It is desired to obtain the average power of the signal (DC value) to know the angle at which the device is moving (which might be deviated, but that can be fixed later in calibration). To do this, Eq. 4.14 is used for discrete signals, where the DC value over a specific period is the average of the samples in that period of time [43]. For periodic signals the number of samples that must be used is equal to the number of samples in a period of the fundamental frequency of the signal [44]. Nonetheless, in the case of systems with unknown or variable frequencies (as in this case), it is convenient to use a very large number of samples [45].

$$V_{DC} = \frac{1}{N}\sum_{i=1}^{N} V_i \tag{4.14}$$

Different sample numbers for the average calculus of the signal were tested used on the reference unfiltered signal shown in 4.18. The observed effect can be seen in figure 4.20. It's important to point out that a higher number of samples is convenient to obtain the DC value, nonetheless doing so also implies a significant memory usage, makes the process slower for the micro-controller (as writing in memory was observed to be a time-expensive process) and also delays the signal.

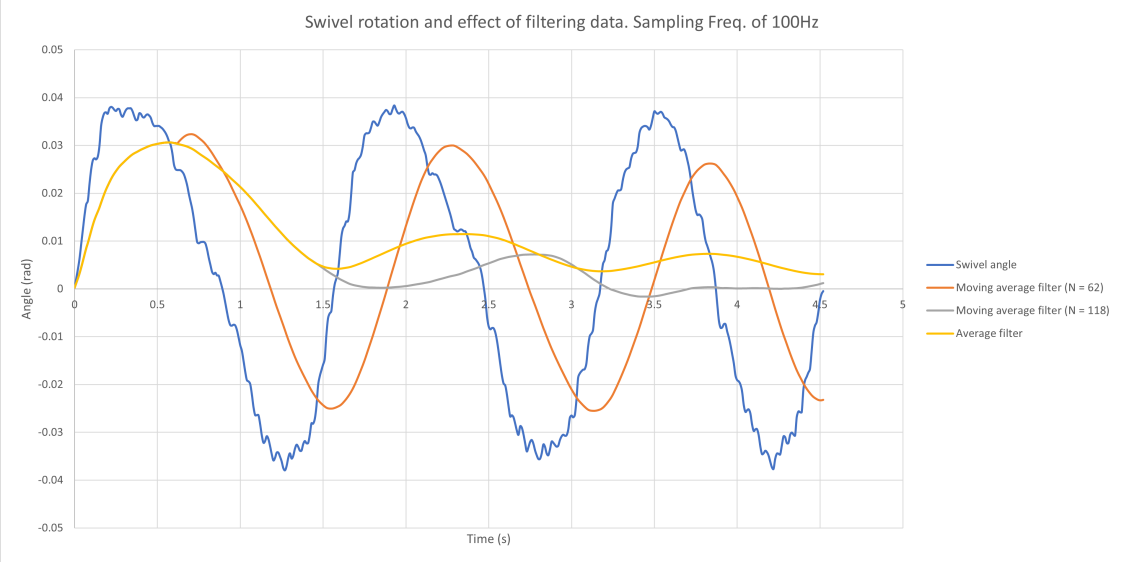

Figure 4.20: Effect of using a different number of samples. Average filter signal corresponds to using all the data previous to a given point as a way of observing the behaviour of very high number of samples

It was found as a crucial issue that the device is turned by hand when performing testing, therefore the frequency is expected to be reduced when getting close to the desired position in order to get as close to it as possible in this hand-made tests. This also changes the initial conditions of the system and makes it time variant; meaning repeatability is greatly reduced. Using a moving average filter (which works in a similar way to what's shown in Eq. 4.14), bias may be introduced to the average at low speeds as seen in figure 4.21. This newly encountered problem required a custom solution which involved the use of a variable sampling period described in detail in subsection 4.4.2. Results of filtering after implementing said solution can be seen in subsection 6.4.1. It was observed that the oscillatory behaviour was almost completely removed and that this method worked as expected.

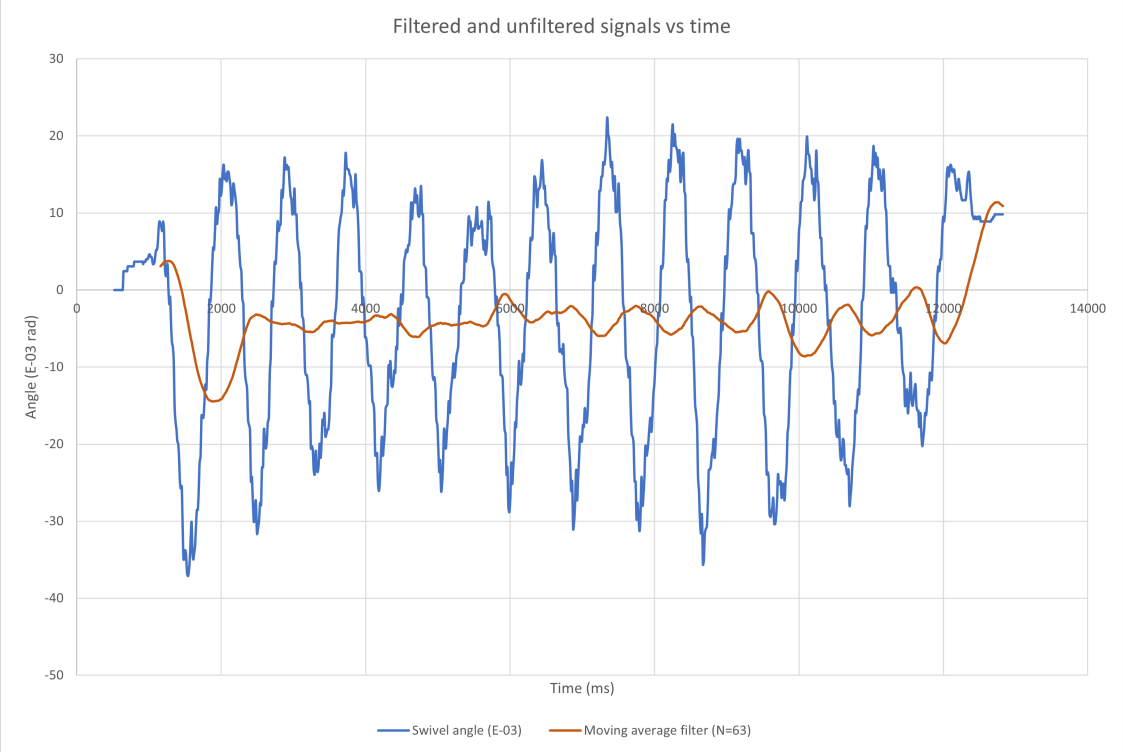

Figure 4.21: Bias seen in orange at the end of the signal, where the device turns at lower speeds and therefore the average obtained strongly deviates from the average value

Removing the remaining oscillations seen in subsection 6.4.1 would require a much larger number of samples due to the problem with moving average filters, where the transfer function is an exceptionally good smoothing filter (the action in the time domain), but an exceptionally bad low-pass filter (the action in the frequency domain) as seen in figure 4.22, some higher frequencies are left even for high sample numbers [46].

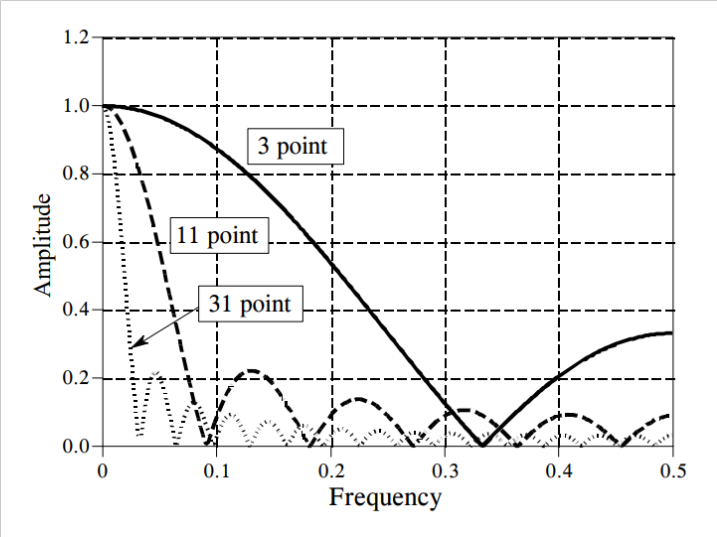

Figure 4.22: Frequency response of the moving average filter for different sample numbers [46]

4.4.2 Variable sampling period

As mentioned in subsection 4.4.1, when the device starts moving, the moving average filter is still biased to 0 because not enough samples have been taken. This also made it so that the initial conditions of the system heavily influenced the accuracy of the system, as for example, faster turning speeds meant less samples and larger displacements. A first step to solve this was to modify the physical design and add another presence-absence sensor, for which the distance to the zero is already known. Therefore, the filter will start accepting values since the program starts, but the sensed distance will be changed until the device reaches that sensor, from which point the signal is mostly stabilized and therefore the accumulative error from this deviation can be reduced.

The result of this can be seen in figure 4.23, where the distance is not updated (seen in gray) until the device reaches the new presence absence sensor. This makes it so that initial conditions play a less significant role in the accuracy of the system. Nonetheless it was found that it was still significant and the amount of samples before that point was the most significant problem.

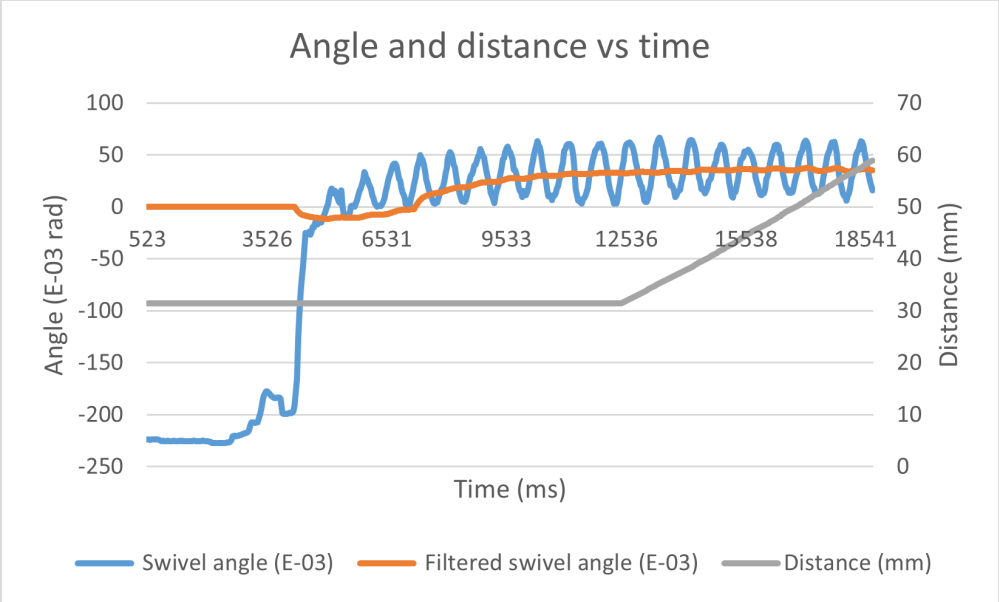

Figure 4.23: Signal filtering using 2 sensors

As the robot is still in development and the device has to be turned by hand, a solution was designed. At this point the designer thought of a way to make it so that the micro-controller treats the data as if the speed was constant. In order to do this, the data obtained was analyzed and it was discovered that at a sampling rate of 30 ms and turning the device as closely as possible to 60 RPM using a metronome, the mode step amount per sample was of 49 steps. This way, the sampling period changed from being constant (of 30 ms), to variable and it would take a sample every-time the amount of steps taken by the incremental encoder counted 49 more steps.

Using this new variable sampling period made the system much less susceptible to human error and initial conditions as seen in figure 4.24, and now the settling time of the step response was observed to always be less of the time it takes the robot to reach the presence-absence sensor that activates the position tracking which is what was being looked for. It can also be noted that the response to modifying the angle from a starting position corresponds to an under damped second order step response.

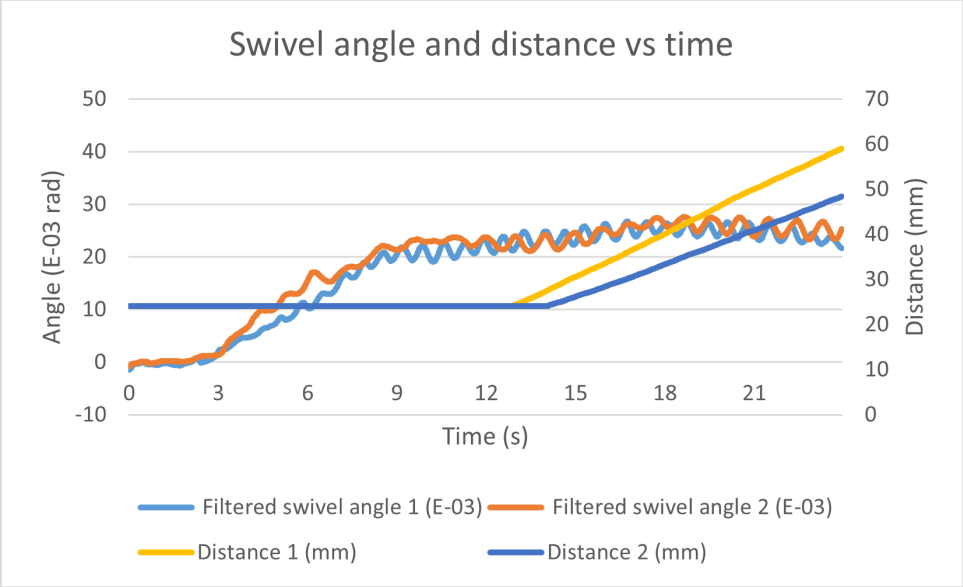

Figure 4.24: Step response using the moving average filter with custom variable sampling frequency method for two separate experiments for 30 RPM (signal 1) and 60 RPM (signal 2). Note: time is normalized to match the same speed.

4.4.3 Adjusting zero of absolute encoder

As the advancement depends on the sine of the angle of the swivel, the zero of the absolute encoder should be adjusted so it uses values as close as possible to reality and the equation stays in the linear zone of sine equations, which happens at very low angles [47].

In order to adjust the zero of the absolute encoder (where there is no advancement), an experiment was conducted where the device was turned 20 times while on the stop position. It was noticed that the stop position does not represent an advancement of 0, but an advancement backwards; towards the end of the cable. Taking into account that every turn means a rotation equivalent to the circumference of the circle, using figure 4.6 as reference, the angle of displacement can be obtained using Eq. 4.15 solving for θ_R using real life measured values as all variables can be measured using a caliper. Therefore, the difference between the average angle obtained in real life and the one shown by the robot can be used to set this zero value using both Eq. 4.15 and Eq. 4.16, where θ_R is the angle obtained by doing the procedure previously described and θ_D is the angle detected by the device.

$$\theta_R = \arctan A/D \tag{4.15}$$

$$\theta_R = \theta_D - (\theta_D - \theta_R) \tag{4.16}$$

The output of the sensor both filtered and without filtering can be seen in 4.25 for a section of the entire 20 turns as it is easier to appreciate in detail. The average of the filtered signal gave an average angle of 0.020366 radians.

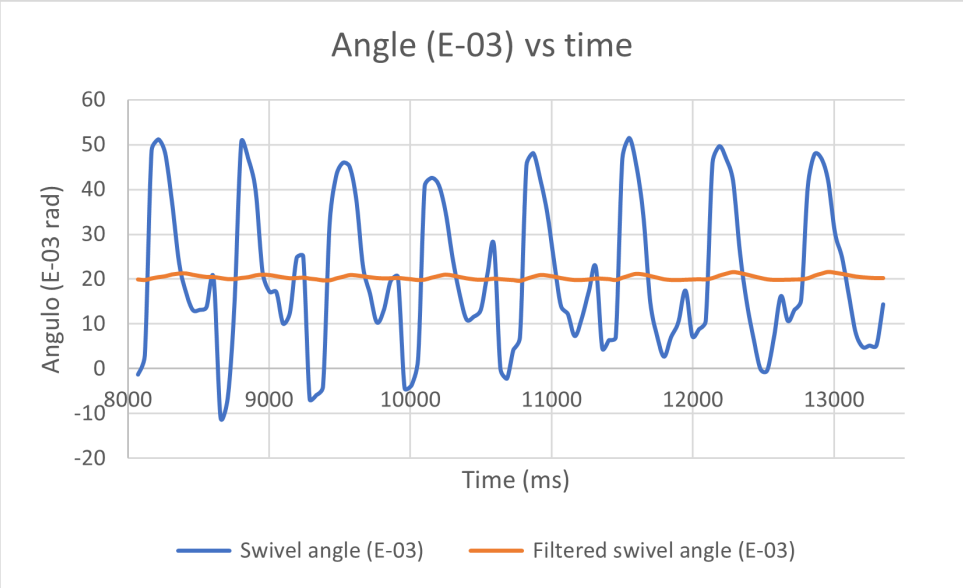

Figure 4.25: Angle obtained when turning the device 20 times in stop position

Meanwhile, the results of the measurements performed using a caliper can be seen in table 4.2. It is worth noting that in order to make sure that each turn ended in a very similar angle, a digital bubble was used which had an uncertainty of $\pm 0.5^o$, which represents a linear uncertainty of the order of $x10^{-4}$. The diameter of the cable was measured to be of (30.7 ± 0.05) mm, rendering then a circumference of (96.45 ± 0.16) mm using Eq. 4.15 an angle of (-0.00345 ± 0.00004) radians was obtained. It's worth pointing out that the uncertainty of this value is much lower than the maximum error for angle reading according to previous calculations. This way, substituting the now known values in equation 4.16, a difference of 0.02381 radians was obtained between the sensed angle and the measured angle.

Table 4.2: Measurements obtained using a caliper to set the zero of the absolute encoder sensor

Position	Real value (mm)
Starting	121.35 ± 0.05
Ending	114.7 ± 0.05
Displacement	-6.65 ± 0.07
Displacement per turn	-0.3325 ± 0.004

Once this adjustment was made, a test was performed to see the behaviour of the system when used in position "2", rendering the output from the swivel sensor seen in figure 4.26. The experiment consisted of moving the device and stopping for a while at positions 156 mm, 171 mm, 185 mm, 200 mm, 216 mm, 231 mm and 243 mm. The maximum error obtained was of 17.66 mm, which represents an error of 7.27% as seen in figure 4.27. This error is to be reduced through an adjustment of the output using the calibration curve as explained in the next subsection.

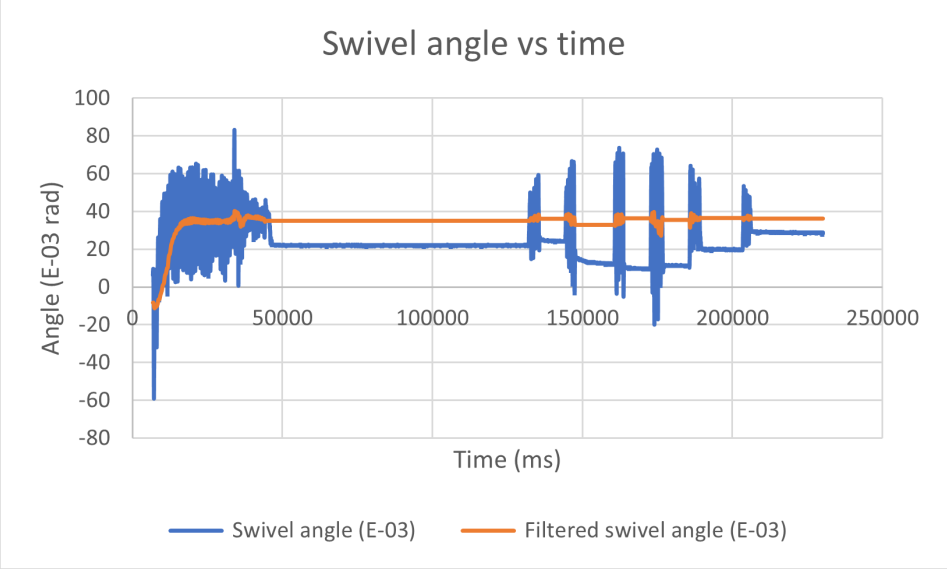

Figure 4.26: Swivel angle with the adjustment when used for typical use in position 2 stopping at positions 156 mm, 171 mm, 185 mm, 200 mm, 216 mm, 231 mm and 243 mm

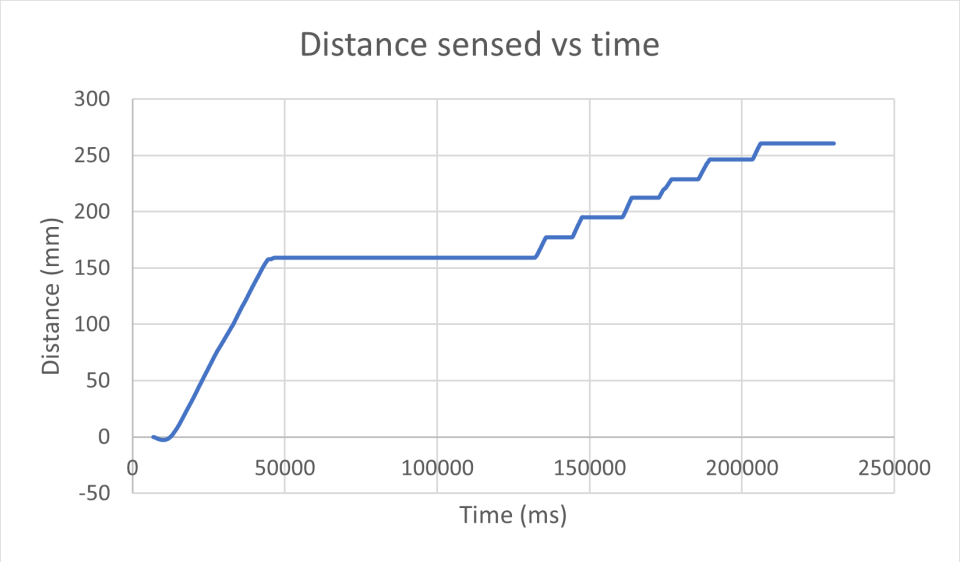

Figure 4.27: Distance output when in typical usage in position 2 stopping at positions 156 mm, 171 mm, 185 mm, 200 mm, 216 mm, 231 mm and 243 mm

4.4.4 Calibration

Using the same setup and filtering the signal from the absolute encoder as previously described, the position of the robot obtained without calibration can be seen in figure 4.28, where a linear behavior was observed when the robot was moved at a constant speed. The robot was stopped at different known positions between 150 and 240 mm, which is the range in which the robot is going to work. It can be seen that the sensed distance does not coincides with the measured distance. The exact sensed distance at which the device stops can be seen in table 4.3 compared to the distance measured with a ruler with 0.5 mm of uncertainty.

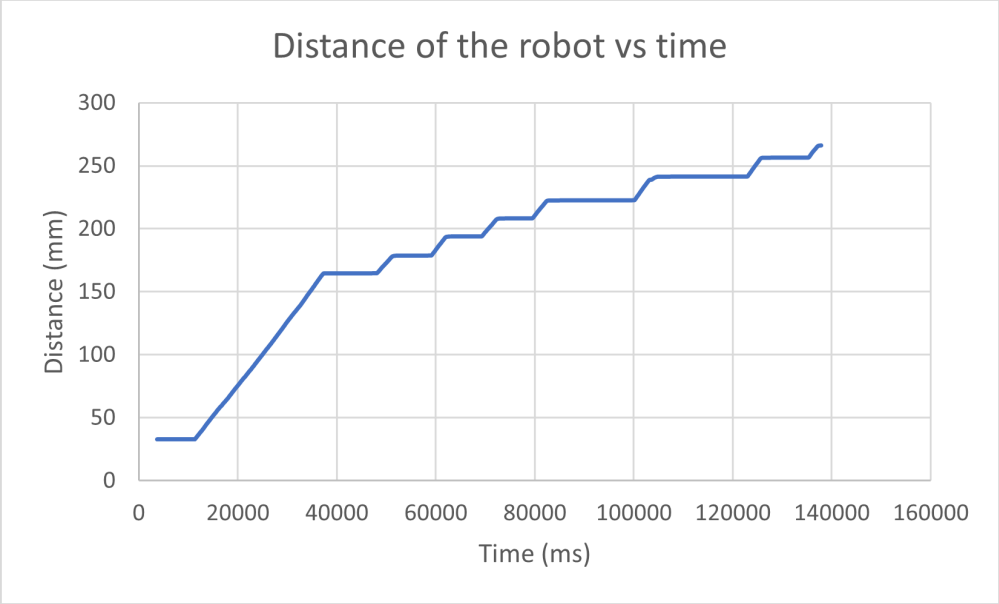

Figure 4.28: Position of the robot without calibration.

Table 4.3: Data used for initial calibration of the system

Sensed distance (mm)	Real distance (±0.5mm)	Error (±0.5)
163.49	149.0	14.49
178.77	162.0	16.77
194.03	175.0	19.03
208.34	187.0	21.34
222.01	201.0	21.01
241.63	217.0	24.63
256.55	231.0	25.55
266.39	239.0	27.39

The error explained above may come from different sources, but mainly that the average angle might deviate from the actual angle of movement due to bending of the pieces or irregularities that are very hard to model.

As explained in the theoretical framework, using as many points as possible is desirable for calibration, especially in this case where the pattern used is not certified and has a high uncertainty. Using the comparison between real and obtained values depicted in table 4.3, a calibration curve and its equation is obtained and portrayed in figure 4.29.

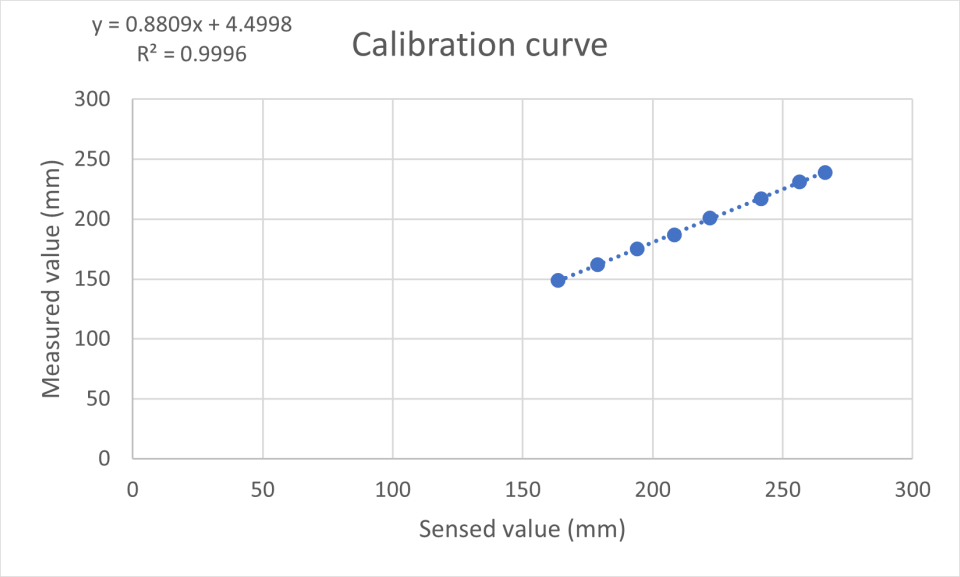

Figure 4.29: Calibration curve and equation for the data in table 4.3

As the sensed angles are always extremely low, the sine of said angle will behave in a mostly linear manner. Therefore, additive and multiplicative error correction can be performed through calibration using the equation seen in figure 4.29, which has the form seen in figure 4.17, where M is the multiplicative error correction and A is the additive error correction value, or in numbers, 0.8809 and 4.4998 respectively in this case.

$$X_R = X_D * M + A \tag{4.17}$$

This process was repeated several times until a satisfyingly low error was consistently observed throughout the validation tests, therefore the calibration values seen in appendix E might not be the same shown in this chapter.

4.5 Micro-controller programming

The micro-controller is in charge of receiving data from the sensors and outputting the corresponding signals. As it was previously discussed, the micro-controller to use is an Arduino Nano so the programming language is embedded C++. The code used on the Arduino can be seen in the Appendix E.

The main sequence used on the micro-controller is shown in figure 4.30, this will automate the whole measuring process and detection of the cable end and only requires the distance as human input.

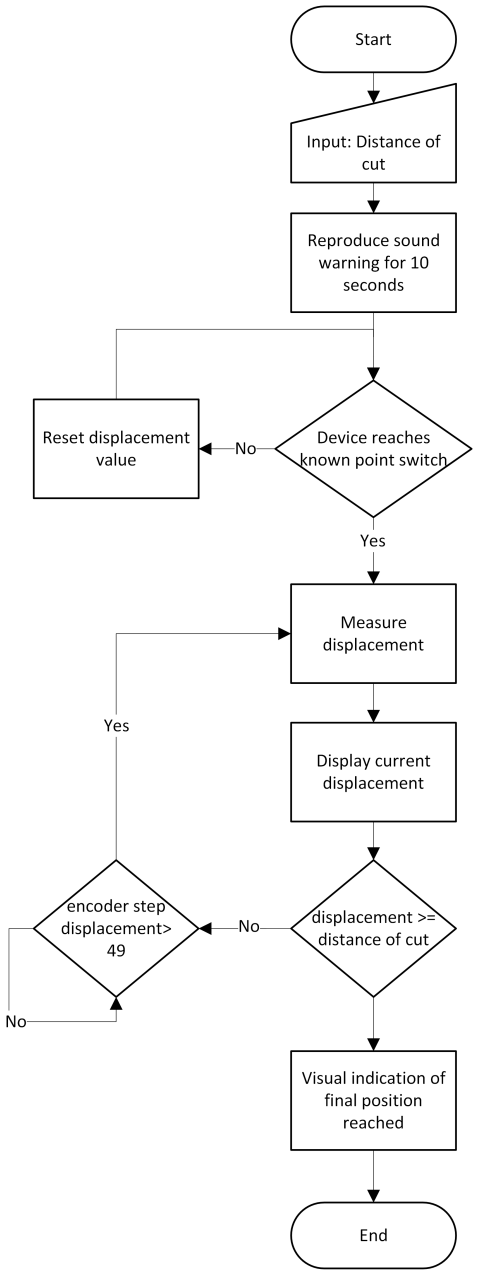

Figure 4.30: Flow chart for the main sequence to be used on the Micro-controller

Within the main sequence, there is calculus performed to obtain the actual distance travelled along the axis as seen in figure 4.32. There is also an interrupt procedure, whose inputs correspond

to the interrupt pins on the micro-controller and enables the device to not miss steps due to the execution time of the program whose sequence can be seen in

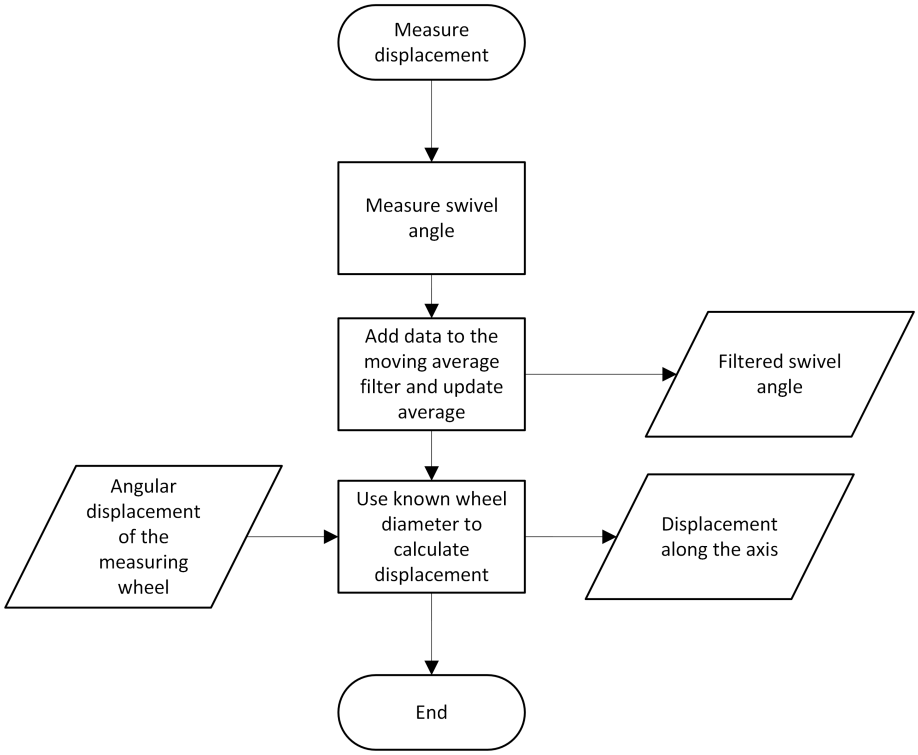

Figure 4.31: Displacement measurement procedure

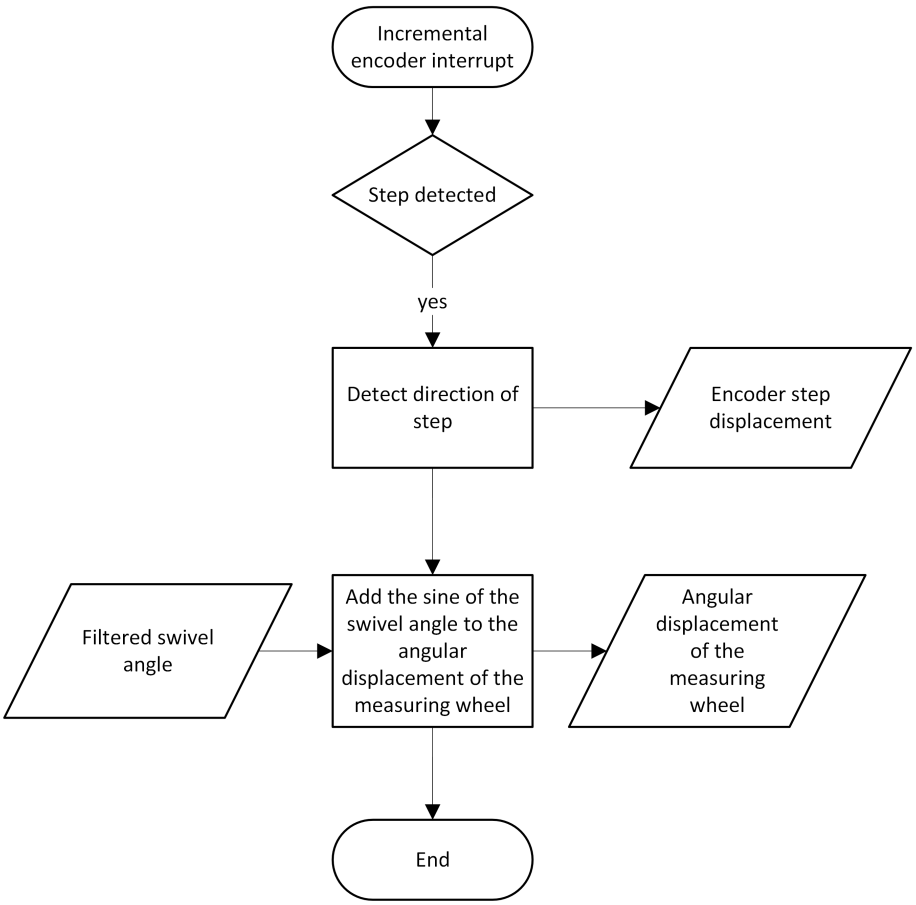

Figure 4.32: Interrupt procedure within the Arduino program

4.6 Overview

It can be seen that all main specific elements of the final design have been discussed, which by themselves are all connected, but at this point it's also necessary to perform an overview of all of what has been just talked, mainly the sum of errors which will ultimately determine the accuracy of the device.

Assuming worst case scenario for every element previously discussed, the maximum error that could come from the measuring wheel is in theory of about 0.044 mm. From the swivel sensing assuming a minimum advance rate of 3 mm/rev and without accounting for backlash as it is expected to be very low the expected error is of around 0.025 mm according to Eq. 4.4 and considering that a moving average filter with N=100 is used. The sampling rate is variable but it is modelled to be of approximately 30 ms, which at an expected advance per revolution of 3 mm/rev and 60 RPM,

yields an advance per unit of time of 3 mm/s which at said sampling period could mean an expected delay both to detect the cable (zero-setting) and to send the stop signal of around 0.09 mm (using Eq. 3.2) for each and 0.18 mm both combined. First two errors can be modeled by calculating the root squared of the sum of squares of the error and it yields an error from the sensors of $E_{sensors}$ = 0.05 mm, whereas the error because of delay can be added to this sum, yielding a total error of E_{total} = 0.23 mm, which is of less than the goal value for accuracy.

The previously calculated error corresponds only to the main systematic error variables that the designer was able to quantify in this design, and as there is no current state of the art more research is required to fully obtain and quantify all the systematic error causes. Furthermore for the swivel angle, an average value of multiple values is used which may help reduce the error but at the same time creates for varying initial conditions. On the other hand there will be also a non-systematic or random error component, which mainly comes from the system being turned by hand which greatly reduces the system's precision and this is very hard to calculate but it is expected to be reduced once the system is implemented in the robot.

Further discussion of the fulfillment of requirements using this design can be seen in chapter 6.

Chapter 5

SAFETY AND ENVIRONMENTAL CONSIDERATIONS

Safety and environmental considerations were taken into account throughout the whole design process in this project. How this was done is discussed in this chapter for the safety and the environmental aspects by separate.

5.1 Health and safety considerations

As the project was developed in the European union, the design should follow the health and safety guidelines and norms taking place in that specific region. For this reason, the Machine Directive EN60204 of the European Parliament and the Council [48] was used to ensure the fulfillment of health and safety requirements. This directive describes a machine as an assembly with at least one moving part [48] and all machines to be used in European countries should adhere to the guidelines described in it.

In this case, the designed system corresponds to a measuring device with moving parts and a control system, which are both elements subjected to directive EN60204 [48]. The fulfillment of requirements is going to be checked following the same order used in the directive.

The following items are the main safety requirements for the control system [48] and how this is followed or why it does not apply to the project design.

- **They should withstand their intended workload and environmental conditions:** The device is to be used in humid environments, nonetheless a protective tent is used in order to protect both the cable and the peeling device from rainy conditions. None of the elements used in the design is sensitive to humidity to the point of possible malfunction on typical real-life usage, so this requirement is met. Temperature working ranges are also taken into account and that's in fact one of the specifications for the system.

- **The hardware and software of a control system should be safe:** The software in this system is considered very straightforward and no complex actions have to be performed by

the operator. The hardware used is considered safe with the only concern being the gearbox, which moves in a very slow and predictable manner and has a protective carcass where the fingers would otherwise be able to get clamped between gears.

- **All possible logic errors in a control system should not escalate to a hazard situation:** As the control system is mainly in charge of making the robot move or stop along the axis, a logic error could involve a halt in the position tracking due to a cable being disconnected or a malfunctioning device, this could make the robot reach unexpected positions (aside from a significant loss in accuracy) which might create a hazard situation. For this reason, the stop signal is negated and in case of power loss or logic malfunctioning once a reset is received the system immediately outputs a stop signal.

- **All foreseeable human errors should not escalate to a hazard situation:** The only human input in the fully implemented device should be the distance of cut, which is entered using a potentiometer and pressing a button to confirm the start of the operation. In this process, the distance could be wrongly entered or the button could be pressed by accident. For this reason, an easily accessible reset button is implemented in the design and a waiting period of 5 seconds with an easily noticeable buzzing noise was added before starting the peeling sequence, which enables the user to react to his mistake and avoid unexpected movement.

- **A machine must not start unexpectedly:** As discussed earlier, this is fulfilled by adding an alarm sound for 5 seconds before the movement starts while showing a 0 on the display. This way the start of the movement can be easily foreseeable and give the user time to take action accordingly.

- **It must not be possible to change a machine's parameters without supervision if it can possess a safety risk:** In this case, the system should only have one easily modifiable parameter, which is the distance of cut. All other parameters come from calibration of the system, which cannot be performed by accident as the user has to access and modify the Arduino code. This is considered discouraging and difficult enough to avoid unwanted parameter modification.

- **Stopping of a machine must not be blocked if the power has been switched off:** The designed control system uses 9 Volt batteries to power itself, so it is expected that eventually the battery will not be able to power the system. For this reason, the stop signal is normally closed, which means a stop signal will be represented as low (0V), therefore in the case of power outage or battery fault the control system will output a "stop" position.

- **None of the moving or transportable parts must come off or fall down when a machine is switched off:** All moving components are enclosed in the assembly and fastened using screws and bolts or tight adjustments to avoid this. Screw tightness should be checked if vibrations are visible in the system when in use. The proposed design does not require to be left on to ensure the integrity of its parts.

- **Automatic or manual stopping of all moving parts must not be blocked:** A reset button is visible and accessible at all times. Nonetheless as the system will be moving, access to it could be limited. For this reason, a radio frequency control is to be used in a final implementation design that goes on the robot. This was not considered necessary for the concept prototype being developed in this project as it is to be moved by hand (the directive states that manual machines do not need an emergency stop), nonetheless it is necessary for a final product in a moving and operational and autonomous robot.

- **The protective devices used must perform as expected or transmit a stop signal:** There is a protective device around the gearbox, nonetheless the gearbox does not move at sufficient speeds or has enough torque to produce significant damage on someone. Another error could be the insertion of a human hand or finger between the cable and the measuring wheel, for this reason the sliding motion of the wheel is limited to a range of less than 10 mm, which when tested avoid human parts clamping and avoids hazardous situations.

- **The devices connected with the control system must, if deemed necessary, apply to the entire assembly or a part of it:** As this is a control that applies only to two other subsystems, this safety consideration will have to be revisited once the device is implemented in the robot where the control system of the various devices will most likely be put together, but for now it is unnecessary.

- **In case of a wireless control, the machine must stop automatically if there is no correct signal or data transmission.** The control system itself is completely in the device except for the reset signal of the final design, therefore, to make sure that the signals from the control are being received, the start button was also added to be part of the wireless control, therefore the process will not start if the wireless control is not present and is able to also send the reset signal. It is worth noting that this was not implemented on the prototype of this project as it is to be moved by hand and no wireless elements are involved.

The guide also includes requirements for the starting and stopping of machines using control devices, these are contemplated as follows [48]:

- **Visible and recognizable and, if necessary, with proper pictographs and text:** All the process that involve human interaction are correctly described using text. The distance of cut selection potentiometer has the words "DISTANCE" on top of it and the start button has the word "START" as seen in figure 6.5.

- **Installed in a way that their use is understandable, safe, quick and does not cause any mistakes:** This was taken into account during the design process. It was ensured via testing with random individuals that used it and gave their feedback on ease of use.

- **Designed so that the movement of a control device matches its function:** The movement of the device is mostly rotational, for this reason the distance of cut is selected using a rotary knob, which mimics the rotational movement of the system.

- **Placed outside the hazard area, if possible:** This would be achieved using a remote controller for both the start and emergency stop buttons in a final robotic implementation.

- **Installed so that their use does not introduce any additional risks caused by the environment:** As already explained, there are no elements of the design sensible to ambient humidity or usual temperatures which is expected to be the most important environmental consideration in normal operating conditions.

- **Designed so that a risky procedure cannot be performed, unless it is the user's intention:** Using the buzzing noise and giving the user 5 seconds to act before the device starts moving is considered to be enough to avoid risky procedures.

- **Constructed for their intended use at rated load or overload if switching an emergency stop device or disconnecting from a power supply can introduce an additional load:** No additional loads that can create a safety hazard are present in the designed system.

- **All control devices must be positioned so that their layout, movement and counter-effect movement are in accordance with the performed actions, at the same time considering the fundamentals of ergonomics:** This is also confirmed using the survey conducted for ease of use. The HMI components are also easily visible and comfortable to access.

- **If a control device is designed and constructed for executing several different commands, the selected function must be visible and, if necessary, be confirmed by an operator. For safe use, the machine must be equipped with indicators which the operator can use to read data:** As the machine in discussion will execute various commands after one single interaction, the current state of the machine is also shown using 2 LEDs. The first one indicates that the cable is detected, therefore the machine state is to cut cable and the second one indicates if the robot is in position 2 or stop for its advancement per revolution.

The directive also includes requirements for selecting control modes, nonetheless, there is only one control mode present in the designed system, therefore those are not taken into account.

Finally, the risk from moving parts must also be taken into account so that they do not cause injuries. The directive also lists the following requirements for safety guards [48]:

- **The affixed protective guards must be secured so that they can be opened or removed only by using a tool:** This was ensured for the gearbox, where the protective guard is attached with bolts and screws. As for the wheel, the sliding axis can only move clamp a finger if the protective measure is removed using a tool.

- **The protective guards that can be opened should stay connected to a machine. If possible they should be designed and constructed in such a way that they can only be modified**

intentionally: There are no protective guards that can be opened without disassembly, therefore this requirement does not apply.

- **All adjustable protective guards that provide access to areas near moving parts which are absolutely necessary for specific operations should be automatically or manually adjustable without any tools:** There are no adjustable or movable protective guards in this design, therefore this does not apply. This types of protective guards are only recommended where the operator might need frequent access to a guarded component and this is not the case of the designed system.

5.2 Environmental considerations

Initially taking a look at current regulations, the European commission has guidelines for energy consumption of a certain product as an incentive for the reduction of carbon emission (Directive 2009/125/EC of the European Parliament)[49]. In this case, the designed system is not part of any of the products which are categorized with an energy label. Nonetheless, there is already new regulation for the coming years, therefore it is going to be used to assess the environmental aspect of the design.

This new regulation corresponds to the proposal "Ecodesign for Sustainable Products Regulation" [50], which not only takes into account efficiency and power consumption, but the following points, which are also gonna be explained on how they were taking into account for the design of the device in discussion:

- **Product durability, reusability, upgradability and reparability:** A safety factor greater than 2.5 is used for all the elements subjected to significant forces. Life expectancy of the product was not calculated as it was considered unnecessary in this early stages of the concept design. Reusability, upgradability and reparability on the product design are easily obtainable as the whole design is modular and replacing parts is not hard to do with basic assembly tools.

- **Presence of substances that inhibit circularity:** No such substances are present in the product design, therefore this requirement is inmediately met.

- **Energy and resource efficiency:** All electronic components in the design use low power. The design also uses single use 9V batteries and this is not ideal from an ecological standpoint, therefore in future iterations of the product it is recommended to use a rechargeable battery.

- **Recycled content:** All of the designed components are manufactured using either aluminum or PLA. Aluminum is a material that can be obtained from recyclable sources with relative ease and PLA is a biodegradable and renewable polyester [51]. Therefore, the designed product was manufactured using ecological materials and a high recycled content.

- **Remanufacturing and recycling:** As for remanufacturing and recycling, for the same reasons depicted in the previous point, aluminum and PLA were used for the design and therefore most of the elements of the assembly can be easily recycled and use for future manufacture of different objects.

- **Carbon and environmental footprints:** Carbon and environmental footprints are kept to a minimum in the manufacture and usage of the designed system. The only causes for pollution are the energy used for manufacture on the 3D printers and the utilization of disposable batteries, which is relatively low for demonstration purporses. For mass production this steps will have to be revisited.

Chapter 6

RESULTS AND ANALYSIS

6.1 Technology comparison and winning method description

The results from the technology comparison experiments are shown in the following subsections. The unprocessed data obtained from the experiments can be seen in annex I.

6.1.1 Computer vision camera: CMOS with laser sensor

Precision values are of most interest in this experiments, as repeatability is what is being looked for. It is important to keep in mind that the maximum distance to measure will be of 240 mm with a maximum absolute error of 0.5 mm as goal value, which corresponds to a relative error of 0.21‰. Therefore a good relative precision value would fall under that relative error.

The results obtained can be seen in table 6.1. It can be seen from there that by changing the distance from the sensor to the object to the same as used in the nominal mouse application, precision was greatly improved as expected. Nonetheless, when better sealing the system to avoid light bleeding, precision got worse and there is no certain reason for this as there are many variables to take into account. There are also errors present in the experiments done as the mouse was moved manually and the parts of the sensor were attached using double sided tape, meaning parts could have moved inside the test bench.

Also, precision values did not see a significant increment when using the system on the white XLPE layer, suggesting that the material is too regular and provides too little diffuse reflection and too much specular reflection.

Table 6.1: Results for the experimenting with CMOS laser mouse sensors

Test #	Sensor	Real ($\Delta Y \pm 0.025$) (mm)	ΔY Avg. (Pixels)	Precision (Pixels)	Relative Precision (%)
1	Genius GM-04003A	55.000	197.8	168	84.93
2	Microsoft Basic	46.000	663.4	19	2.86
3	Microsoft Basic	46.000	577.2	48	8.32
4	Microsoft Basic	46.000	453	17	3.75

The measurements in test 2 were the most accurate and for this reason the movement sensed was more deeply analyzed as seen in figure 6.1. It is worth clarifying that every sample happens every time the mouse detects movement, so jumps in the y axis values suggest changes in the sensibility according to the point of the cable in which the device is. This is just an hypothesis and it could also be attributed to involuntary hand movements when performing the test.

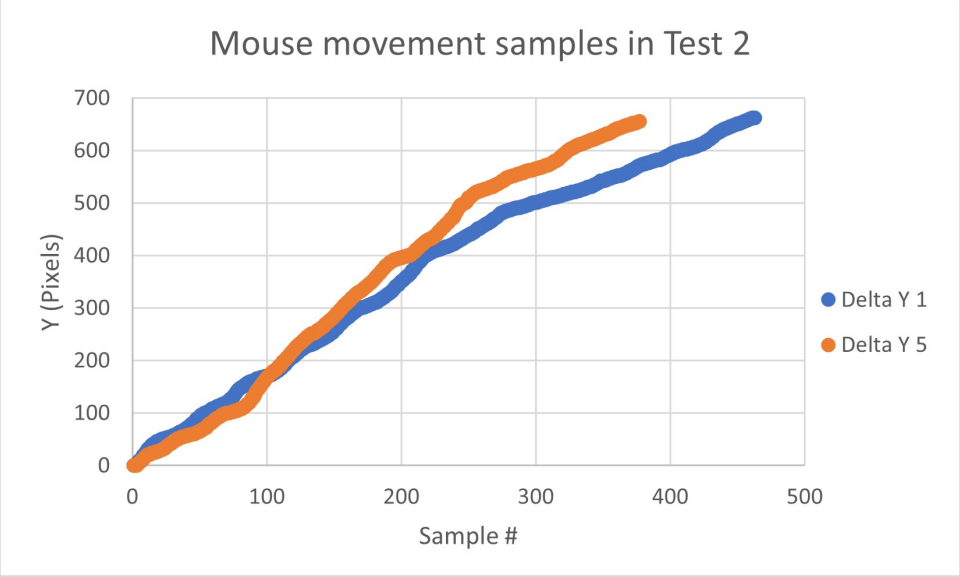

Figure 6.1: Mouse movement samples for test 2

6.1.2 Rotary potentiometer

The results obtained for the tests performed can be seen in table 6.2. Precision was greatly over 0.5 mm, which is the goal precision. It can be noticed that precision descended from test 1 to test 2 and the main hypothesis for this is that the axis had too much play in the second test-bench used, enabling it to slip and lose friction. This was also observed in the first test but to a lesser extent. There was also slippage between the wheel and the cable in both tests. Error is attributed mainly to the slippage in those two contact areas, nonetheless the uncertainty present in the potentiometer also creates loss in precision and finally the ADC converter has a limited range, using 1024 values which is a relatively low number when compared to some encoders available.

Table 6.2: Accuracy and maximum absolute error obtained for the tests performed with the rotary potentiometer

Test #	Real distance ± 0.5 (mm)	Average (mm)	Standard deviation	Accuracy (mm)	Precision (mm)
Test 1	55.0	55.49	1.05832415	0.49	2.55
Test 2	55.0	46.4608	20.9117795	8.5392	53.98

6.1.3 Encoder

Test 1: By doing the experiment 5 times, the results obtained can be seen in table 6.3. It can be seen that precision is very good using this method, as it has the same value as resolution. This indicates that minimum or no slippage may be present, as error most likely had to do with human involuntary movements when measuring.

Test 2: Also doing this experiment 5 times, it can be seen in 6.3 that there was a significant accuracy and precision loss; the main causes for this have been identified. The main issue is that the tension in the cable is not constant, subjecting the system to an unknown and variable play distance that is not measured before starting moving and when stopping, ultimately reducing the repeatability of the experiment. There is also human induced error, as the start and end points were observed without any stopping mechanism.

Table 6.3: Results obtained for the experiments with the encoder

Real distance ± 0.5 (mm)	Average (mm)	Precision (mm)	Accuracy (mm)
180.0	179.772	0.12	0.228
180.0	179.53	0.81	0.524

6.1.4 Presence/absence detection technologies

The different detecting technologies showed varying results, these are broken down in the following paragraphs.

Magnetometer: The magnetometer was able to detect the cable peeling machine, but not the cable. This is probably due to the cable being made out of aluminum, which is not ferromagnetic [52].

Photoelectric: The photoelectric sensor was able to trigger a signal only when the laser was pointed at it without issues because of ambient light.

Inductive sensor: Both the cable core and the cable peeler were successfully detected using the inductive sensor. Nonetheless, the maximum detection distance was of $(4 \pm 0.025)mm$ for the cable peeler and $(2.7 \pm 0.025)mm$ for the cable core.

6.1.5 Summary

Out of all the measuring technologies, the only one that gave acceptable results for position tracking was the encoder. It is considered that if an already-available technology is used (which is strongly preferred), it should be the 2000 step incremental encoder. In the case of the wheel, it is only needed that the fit between the axis and the wheel is tight enough to avoid slippage (or glued) and also to take into account that the linear resolution will vary depending on the mechanism that converts displacement to rotation used. As for the measuring reel that also utilizes the same rotary encoder, adding a torsional spring should enable the system to maintain tension and get precision values as good as with the wheel.

From the presence/absence technologies, all of them could be used depending on the concept selected. Therefore it is not possible to select a best one in this stage, but it is possible to ease the selection of one in the next design steps when found convenient using the observations gathered from each of them.

6.2 Accuracy of the measuring system

In order to measure the accuracy of the measuring system and make sure that the indicator "Average absolute error is below 1 mm when using the designed measuring technology from 150 to 240 mm of displacement from the cable end to the device" is being fulfilled, an experiment was conducted where using the designed measuring technology and the data gathering set-up, the error was obtained for every 3 turns of the system from 150 to 240 mm repeating this until the amount of samples was of 100, the results of this extensive experiment can be seen in appendix J.

It can be seen that the accuracy is of 0.679 mm or 0.2829% from its maximum range (240 mm), which is below the 1 mm value that was set as indicator, showcasing that success was reached for its corresponding objective. As seen in figure 6.2, the error does not seem to be directly linked to any side of the measuring range when it's above 1.5 mm, meaning it is probably of non-systematic nature and occurs because of random factors.

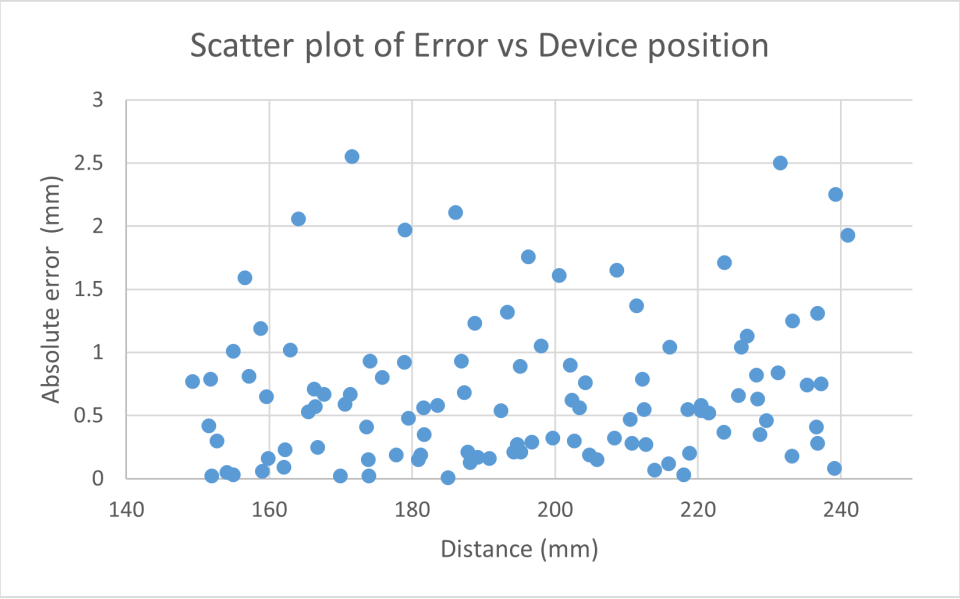

Figure 6.2: Scatter plot of error vs distance

Some of the factors that are thought may be behind this non-systematic error found through experience and experimentation on the device:

1. Different clamping force: A different clamping force may create a deviation in the angle.

2. Different placement on the cable: The device might be initially placed in a crooked position and that may induce a different behaviour.

3. Errors while visually reading the distance value on the ruler: As the experiment was repeated so many times, fatigue might provoke wrong readings.

4. External irregularities in the cable: the cable end sometimes presented irregularities that could trigger a slightly earlier or later detection of itself.

5. Difference in external forces when turning it by hand: There could be forward or backward force components on the system when pushing which might modify the behaviour of the system and reduce its accuracy.

Another thing that is important mentioning is that the error obtained is lower than the one that an operator would get by doing the process by hand as explained in the initial data acquisition.

6.3 Mechanical structure and prototyping

After constructing the mechanical structure in Solid Works, the results obtained for the structural simulations are the following:

6.3.1 Creation of the prototype

As seen in the drawings for the final solution in appendix K, most of the designed parts for this project were 3D printed using the Ultimaker S5 3D printer available in laboratory 3 at the RAM installations using a 0.4 mm nozzle, which allows for layer resolution of 0.02 mm and XYZ resolution of 0.0069, 0.0069 and 0.0025 mm respectively [53], which makes it great for applications that involve high precision (i.e low module gears and bearing fits). In cases where close fits are expected, the lowest resolution setting was used (0.1 mm), this meant low printing speeds but a very high-quality result.

It is worth pointing out that as a recommendation from the technicians in the laboratory, an unbranded special spray for 3D printing was used to enhance the printing quality as in some cases warping in the lower parts of the pieces was observed if said product was not used. Some pieces

also required special configuration when slicing them for 3-D printing, these details are on the drawings for each part on appendix K

As described in subsection 4.3.4 for the computer simulations, the material used in all the 3D printed parts that were subjected to stress was Tough PLA. This material was chosen because it offers the convenience of PLA with the added toughness and durability needed for assembly, specially for tight fits in roller bearings, were a bench press tool and sometimes a hammer with a cloth was used to install them, depending on the accessibility of installation.

As calculating the resistance of materials for assembly processes is outside of the scope of this project, the creation of prototypes also involved the re-manufacture and re-design of certain parts due to them breaking when pressing bearings or when introducing an axis to already assembled bearings as seen in figure 6.3. In this process some bearings were also broken which lead to the design decision of using tougher and bigger bearings as seen in the final design of the gearbox.

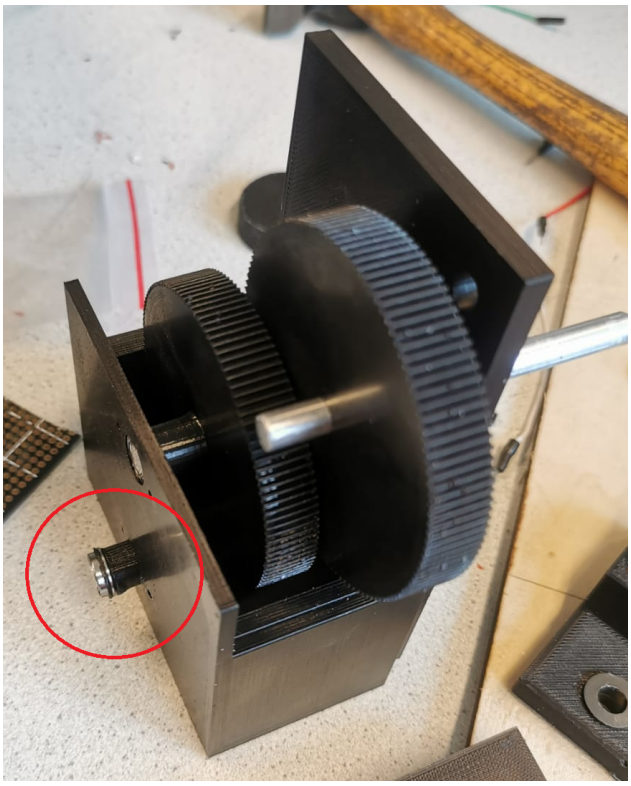

Figure 6.3: Broken gearbox (broken part seen inside the red circle)

Additionally, the wheel axis had to be specially re-designed because it was sliding to the sides when enough force was applied, this involved the machining of an aluminum rod using a lathe

present within the building installations as seen in figure 6.4. Also some axis have threads made using thread dyes on the edges to secure them with nuts.

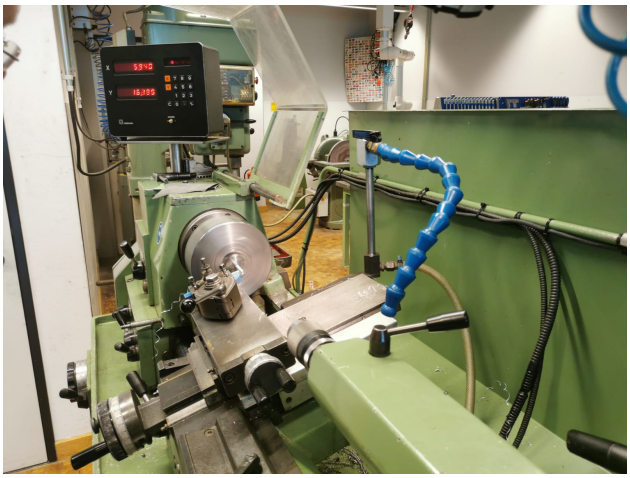

Figure 6.4: Lathe used to manufacture the custom axis

The final result of this assembly can be seen in figure 6.5 once all the electronic components are added. It is worth noting that all moving parts behave as expected, no significant resistance because of interference was found in the gears. Therefore it is considered that this design can be successfully manufactured within RAM premises following the drawings in appendix K.

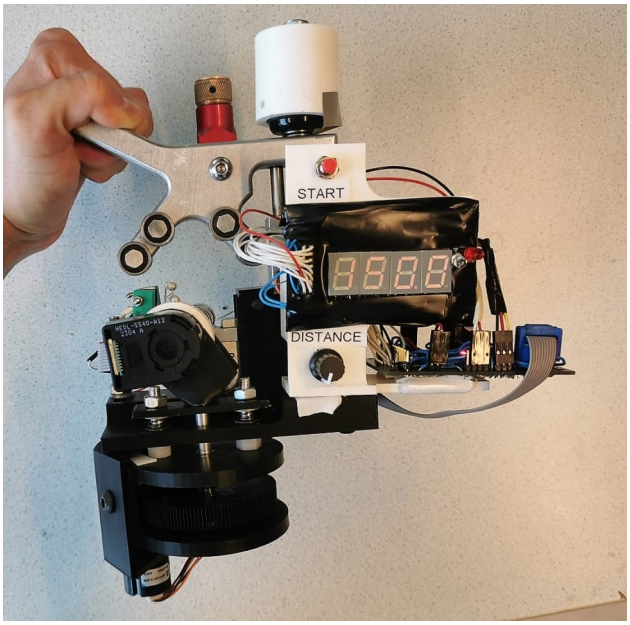

Figure 6.5: Resulting assembly of the system's prototype

A lateral view of the device placed in the cable can be seen in figure 6.6 as well as a rear view

in figure 6.7 for better visualization of the ending result of the prototype. In future iterations of this project it is recommended that the cables are cut shorter to enable for less or no cable management work and a final more clean look. Hanging cables in this case do not represent a problem as all the signals sent using long cables are digital and interference is unlikely.

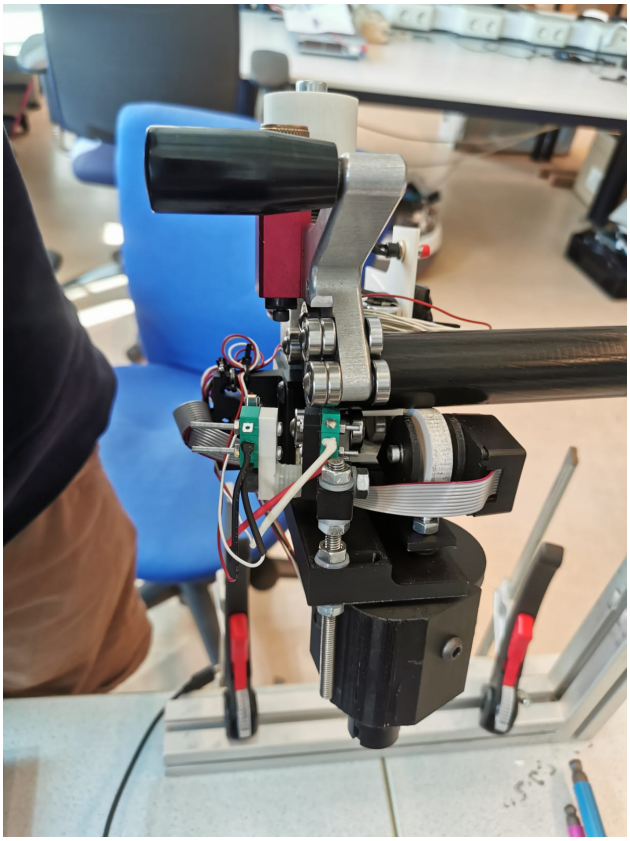

Figure 6.6: Lateral view of final prototype when placed on cable

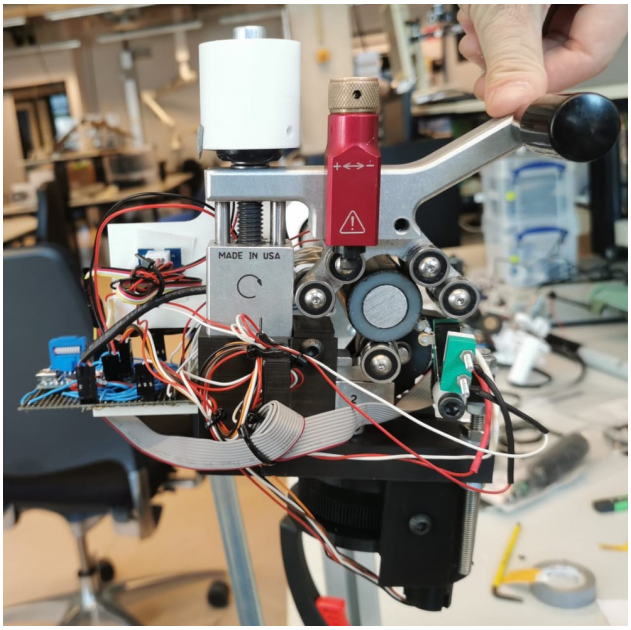

Figure 6.7: Rear view of final prototype when placed on cable

6.3.2 Mechanical stability simulations

The results from this analysis can be seen in Solidworks archives in appendix K.

Von Mises analysis

When performing a von Mises stress analysis, the results obtained can be seen in figure 6.8. It can be seen that the stress is very low throughout the piece with the exception of the cable detector threaded rod, but as this piece is made from a steel alloy this doesn't suppose an integrity risk as it can be seen in the rest of the analysis performed.

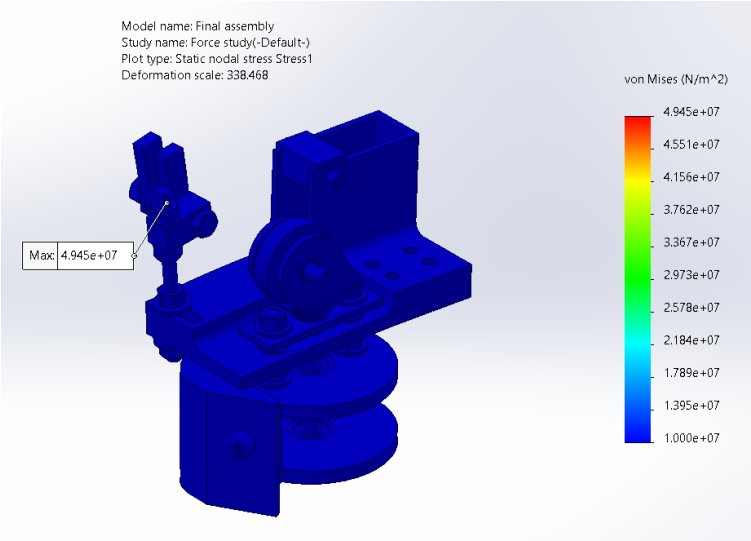

Figure 6.8: Von Mises stress analysis on the final assembly

Displacement

According to the simulated results, the displacement of the parts subjected to stress can be seen in figure 6.9 and figure 6.10. It can also be seen that the maximum displacement occurs in the Tough PLA presence-absence sensor holders, which withstand the pressure from the zero detecting sensor, nonetheless its maximum value is of 42.25 μm, which is negligible and would not suppose any significant accuracy losses.

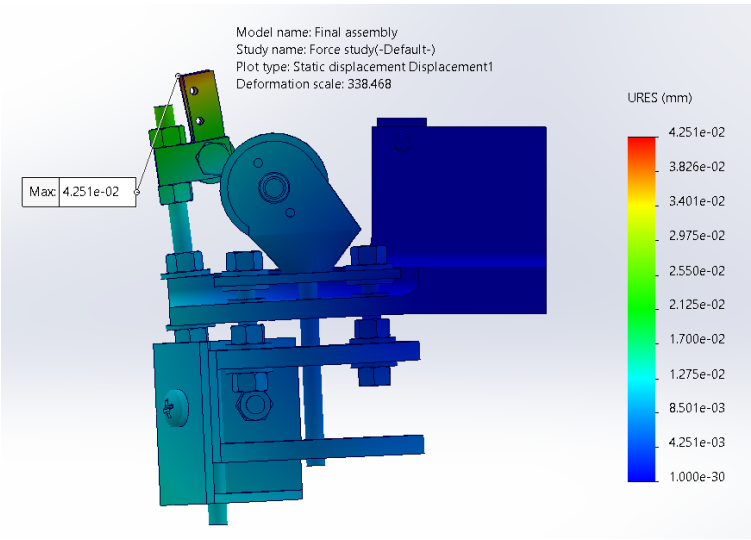

Figure 6.9: Frontal view of displacement simulation

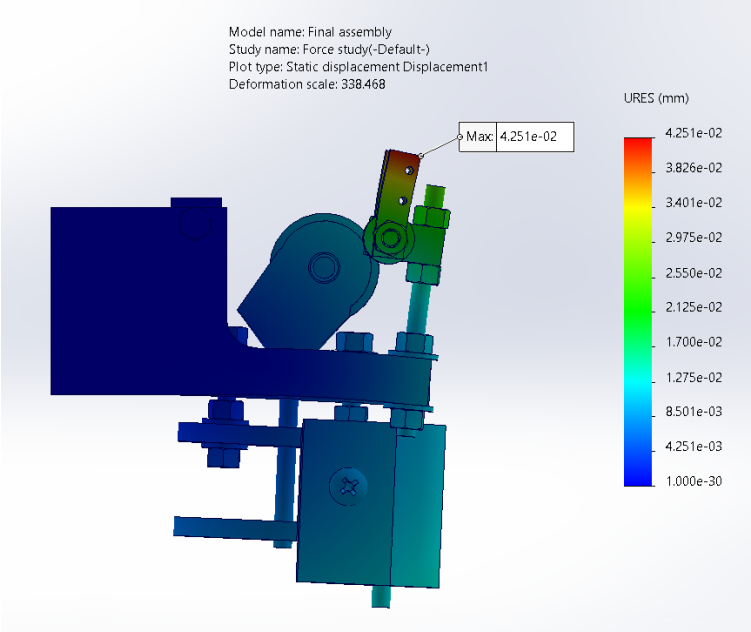

Figure 6.10: Rear view of displacement simulation

It is worth mentioning that the axis deformation may cause problems in the gears and bearings and create unwanted vibrations that might ultimately cause loss of accuracy, nonetheless, this is generally a problem only on systems were high rotational speeds are reached [20] and for this application, speeds are not supposed to reach more than 60 RPM and displacements are so low that this does not suppose a problem.

Factor of safety

Finally, as one of the indicators for the success of this project is a minimum FOS of 2.5 and as it is an important request from the client to be able to present the prototype without risking the system breaking in the middle of a presentation with potential investors, the FOS analysis results can be seen in figures 6.11, 6.12, 6.13 and 6.14. Both analysis show a factor of safety much larger than 2.5. As real-life mechanical testing is outside of the scope of this project the most conservative result is going to be used as the factor of safety of the system, which is of 11.

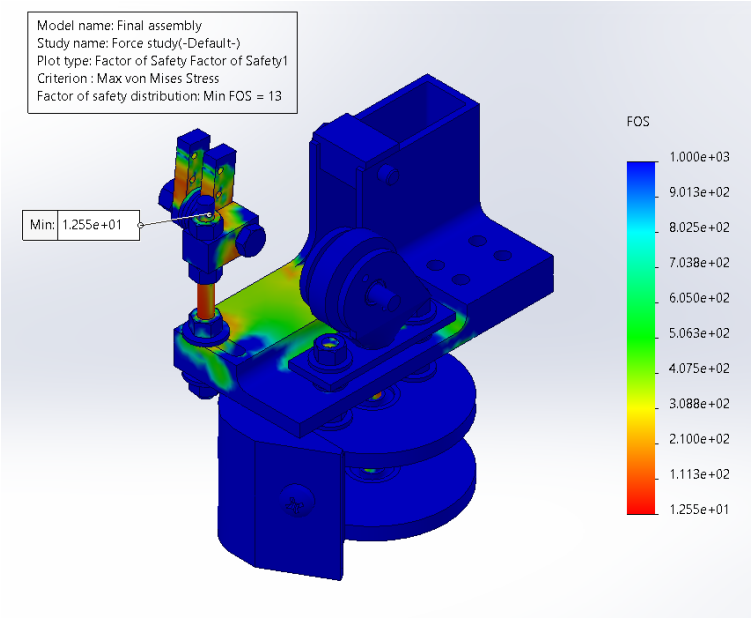

Figure 6.11: Result for the factor of safety utilizing von Mises criterion isometric view

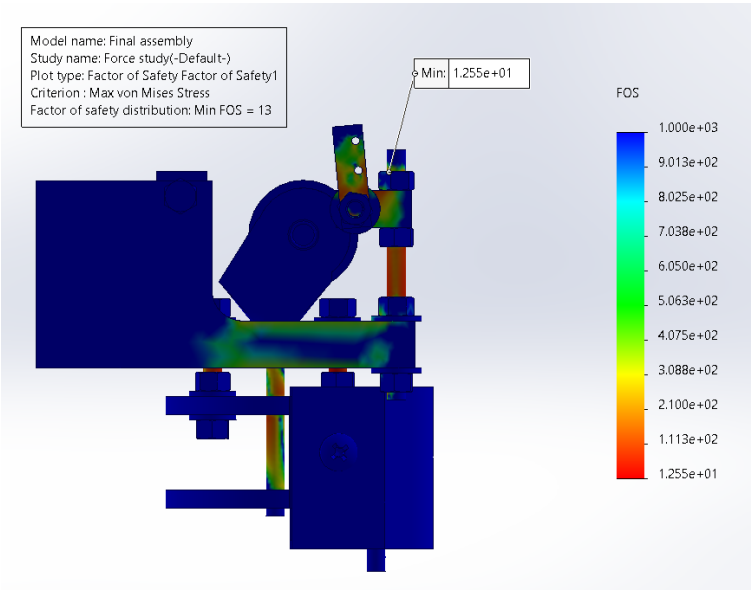

Figure 6.12: Result for the factor of safety utilizing von Mises criterion frontal view

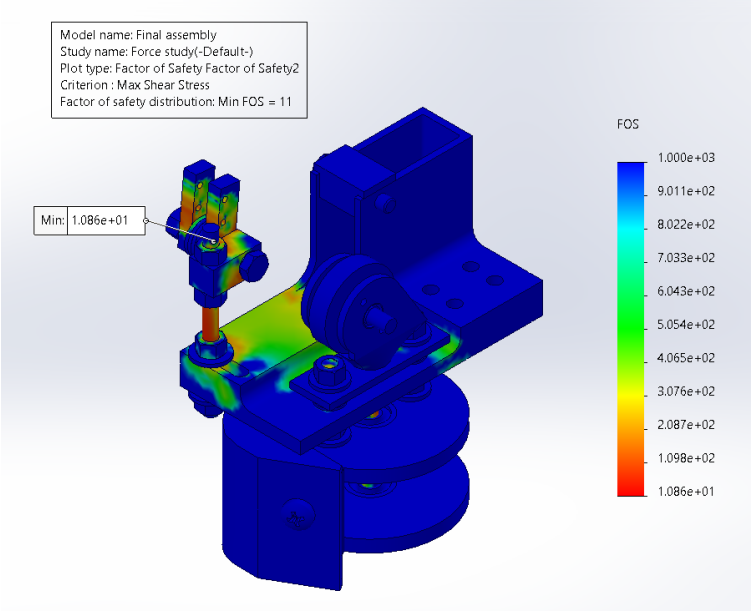

Figure 6.13: Result for the factor of safety utilizing max shear stress criterion

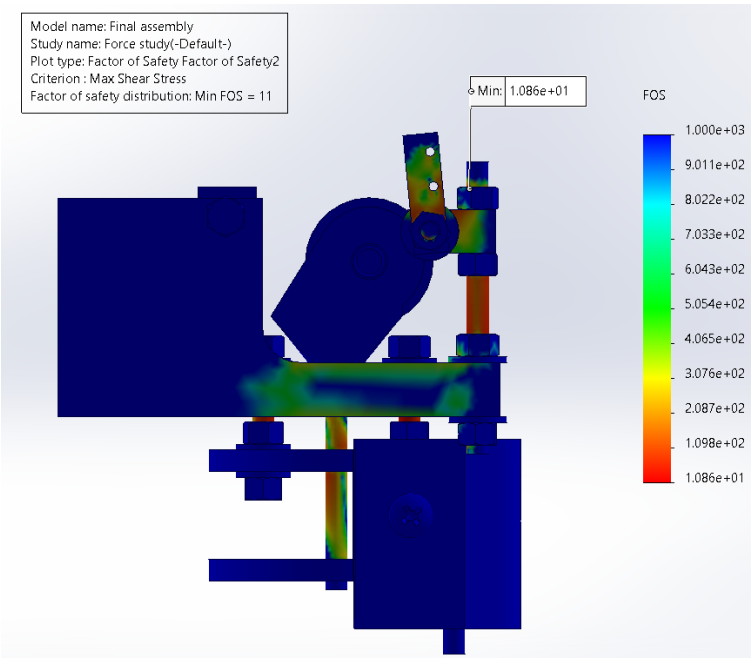

Figure 6.14: Result for the factor of safety utilizing max shear stress criterion

Having a high FOS value means that the the assembly will not only be able to withstand typical usage, but also incorrect use which is helpful in the context of a concept design where changes might be made to it in the future. It is also useful to have this high FOS as 3D printing quality deficit may occur in future implementations.

This FOS value also allows for a less accurate selection of springs that create greater forces and to implement the electronic elements without fearing that the FOS value will drop to a value of less than 2.5.

This analysis also enables to identify the parts of the assembly that are more likely to eventually reach the yielding point. It can be seen that the most vulnerable parts are some axis and screws, therefore if the device is used for a long period of time and erratic behaviour is observed, it would be a good practice to visually inspect this pieces first.

6.3.3 Integration with the rest of the robotic system

As it was mentioned throughout the document, the design for the rest of the robotic system is still in development. In spite of this, communication was constant between designers of the different subsystems to try to avoid future problems when integrating all the concepts into one robotic system. The only currently finished design is the one for the computer vision chip inspection subsystem, which was part of a master thesis performed [54], the tool height control subsystem is already working as expected but modifications might still be performed on it, as for the drive-train testing is still being performed. It is worth mentioning that the part of the drive-train in charge of physically modifying the advance per revolution has yet to be designed.

The latest design for the rest of the subsystems of the robotic system can be seen in figure 6.15, where the micro-controllers and other electronics have been removed as they can be later rearranged and/or combined. Both the tool height control and the computer vision chip monitoring systems are located in the higher part of the assembly. The drive-train however takes a lot of space in the form of two motors seen in figure 6.15 on the back of the assembly. The use of two motors (instead of one) was a recent addition to better distribute the forces along the cable and minimize damage possibilities and a rearrangement of components to locate the second motor on the other upper wheel instead of the lower wheel, completely removing the wheel or the use of 3 smaller motors are options still considered.

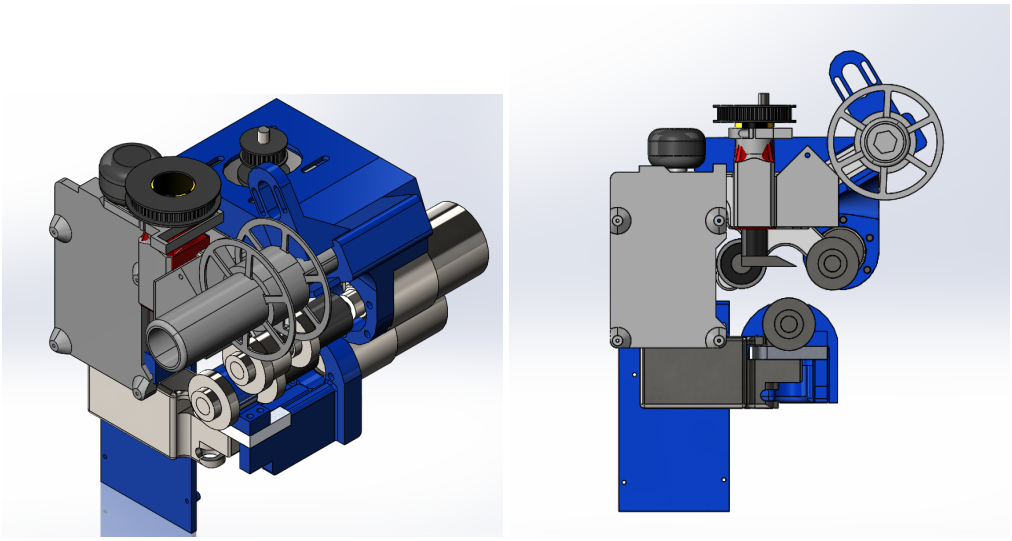

(a) Isometric view (b) Frontal view

Figure 6.15: Latest design iteration for the rest of the subsystems of the robotic system

An analysis looking for interference between the designed systems was performed, rendering the results seen in figure 6.16. With the exception for electronic component holders, which as mentioned earlier are going to be modified in the final integration of the system, it can be seen that the only interference that affects the correct functioning of the robot occurs between the DC motor on the lowest wheel and the measuring wheel. This is because the decision to add an extra motor there was made recently once the final design proposal was already finished and validated.

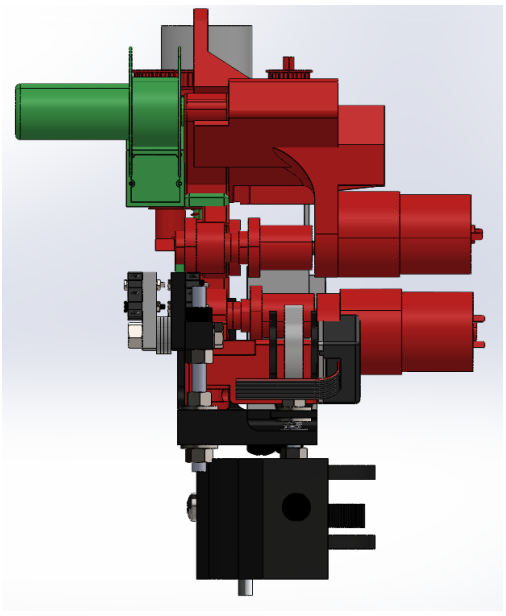

(a) Lateral view

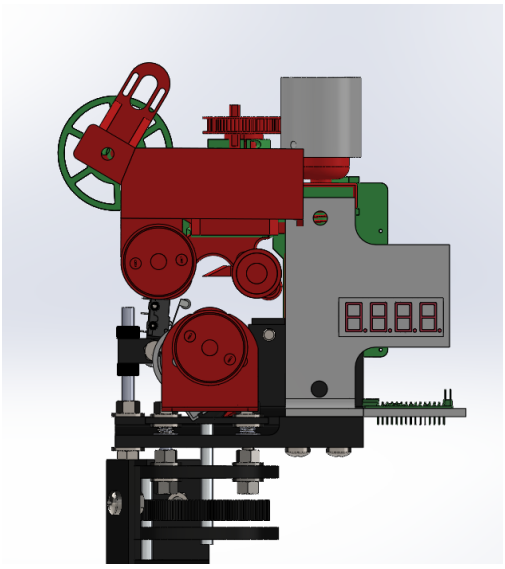

(b) Frontal view

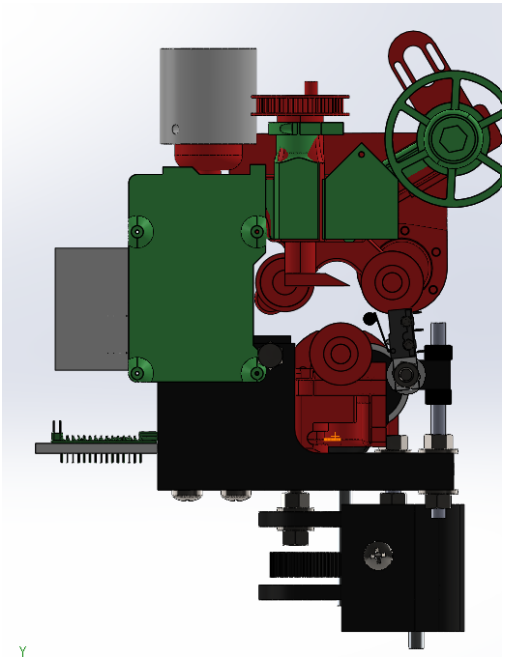

(c) Rear view

Figure 6.16: Interference between subsystems when implementing this project's design in the latest design iteration of the robotic system. In green the mechanical structure for the chip monitoring system and in red for the drive-train and depth of cut control

In order to solve this interference three different solutions are proposed, namely:

1. **Removing the newly proposed motor:** This newly added motor was added as a precautionary measure to avoid damage on the cable, nonetheless empirical evidence has still to be gathered

to determine if this has a meaningful impact, therefore it is recommended that first testing is performed using only one motor to move the device as originally intended. It can be seen in figure 6.17 that this immediately solves the issue as the proposed design was based on using only one motor.

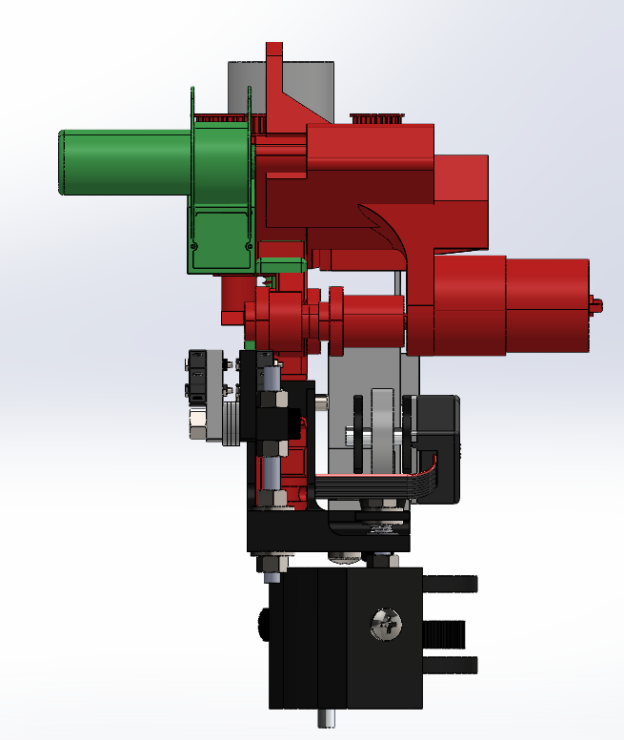

Figure 6.17: Interference analysis when removing the newly proposed motor

2. **Moving the motor to the other wheel:** Moving the motor to the other wheel is another possibility as this would require minimal modifications in the overall design and would also completely avoid interference. This can also be seen in figure 6.17 as this modification would represent a symmetrical reflection of the motor in a plane in the middle of the two upper wheels, therefore not representing an interference to the correct functioning of the mechanical structure.

3. **Moving the measuring wheel away from the interference:** This would require modifications in the design proposed in this project as seen in figure 6.18, but this does not represent a risk to the proper functioning of the device as a mechanical analysis was effectuated and a minimum factor of safety of 9.5 and a maximum displacement of 63.7 μm was obtained for

the mechanical structure following the same steps for simulation used for the design proposal, where the results can be seen in figure 6.19.

Moving the measuring wheel farther along the cable also means that it is going to be more susceptible to the cable's curvature (which was previously negligible). This curvature is expected to be of a minimum radius of 4 meters, which means that the cable can move up and down 2.08 mm from the measuring wheel's perspective (as seen in figure 6.18). This can make the measuring wheel slip, but it can be fixed by not pre-loading the springs so the movement of the anti-slippage system can be of 3 mm and changing the spring constant to 562.2 N according to Eq. 4.11 so that it maintains the minimum required normal force. This also means that the force on the springs can be 2 times higher at times so the maximum force was used for the simulation shown in figure 6.19. The system will most likely have to be calibrated again and as this is a novelty concept, the behaviour should be studied to see if there are more implications attributed to this change, but that is outside of the scope of this project.

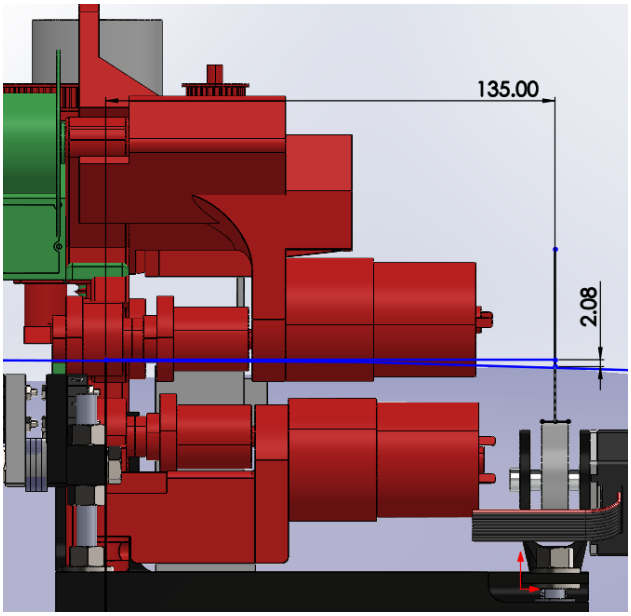

Figure 6.18: Result of moving the measuring wheel to the right to avoid interference. The maximum displacement of the cable at the wheel due to curvature is marked with annotations.

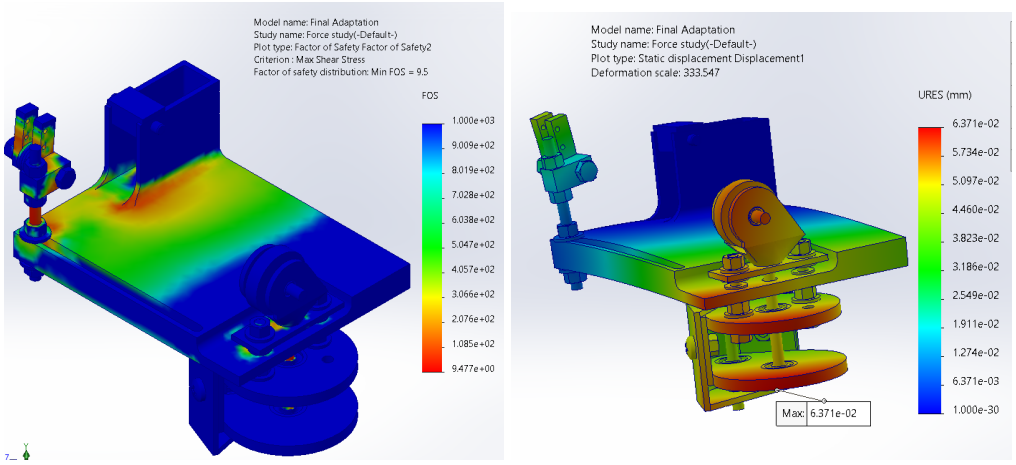

(a) FOS analysis (b) Displacement analysis

Figure 6.19: Mechanical analysis of displacing the measuring wheel to the right

6.4 Software routine capable of controlling the feed position

Throughout the validation phase of this project, the software routine was used and it worked flawlessly. As requested by the client, the required output signals of this project were the indication that the cable has been end has reached the cutting tool and that the final position has been reached in order to change the feed per revolution to stop.

The subsystems of the robot that will receive signals from the designed device will act according to the truth table in 6.4, which uses only two bits as specified in early stages.

Table 6.4: Truth table for the control of the subsystems within the robotic system

~STOP	~Cable detected	Drive-train action	Cutting tool control system
0	0	FPR in stop	Cut
0	1	FPR in stop	Do not cut
1	0	FPR in "2"	Cut
1	1	FPR in "2"	Do not cut

In order to indicate this, the outputs are represented using LED lights. This corresponds to the HMI seen in figure 6.5, where using the dial, the desired distance can be modified while reading the 7 segment LED display and once the red button is pressed, the system makes a loud alarm noise for safety reasons explained in chapter 5, afterwards the measuring can be started. In order to use the full potential of this HMI, the current position is also constantly displayed on the LED 7 segment display. This entire process worked without any perceivable software issues or bugs.

The designed on-off control system effectively uses a software routine that only receives the distance of cut as input, the user press enter and the measuring is then performed in an autonomous manner as the user only has to turn the device. This measuring system could also be implemented in the intended robotic system and therefore enable the entire process after placing the robot completely autonomous, where the drive-train subsystem would receive a start signal when enter button is pressed (and should wait 5 seconds to start the motors) and then receive a stop signal once the device needs to continue rotating but in a still position.

Still more research has to be done to determine the time it takes for the device to change from position “2” to position “stop” and effectively stop, but at the moment this is not possible as that part has yet to be designed by the client and therefore is outside of the scope of this project.

6.4.1 Results of signal processing

Using the variable sampling frequency and the filters explained earlier in the design proposal, the combined result to obtain the DC component can be seen in 6.20. Notice that if the device is stopped, bias is minimum. The resultant DC value of the signal (obtained using the moving average filter) contains around 0.94 E-03 rad of amplitude oscillations along the signal, as seen in the FFT in figure 6.21. Even though the amplitude of these oscillations is greater than the accepted error for the angle according to previous calculations, as this signal is symmetrical along the true DC value of the signal and the angle is very low (meaning a linear behaviour), the accumulative error should be negligible leaving only the error from the last cycle, which is extremely low.

Another thing worth noticing is that as seen in 6.21, the frequency of this peak in oscillations is of almost 1, meaning that the device successfully gathers data as if it was turning at an almost constant speed of about 60 RPM as intended. Nonetheless it was observed when performing testing (as seen in appendix C) that for higher speeds there is an erratic behaviour and the turning speed is no longer constant at 1 Hz. This shouldn’t be a problem as the robot will be turning at around 60 RPM.

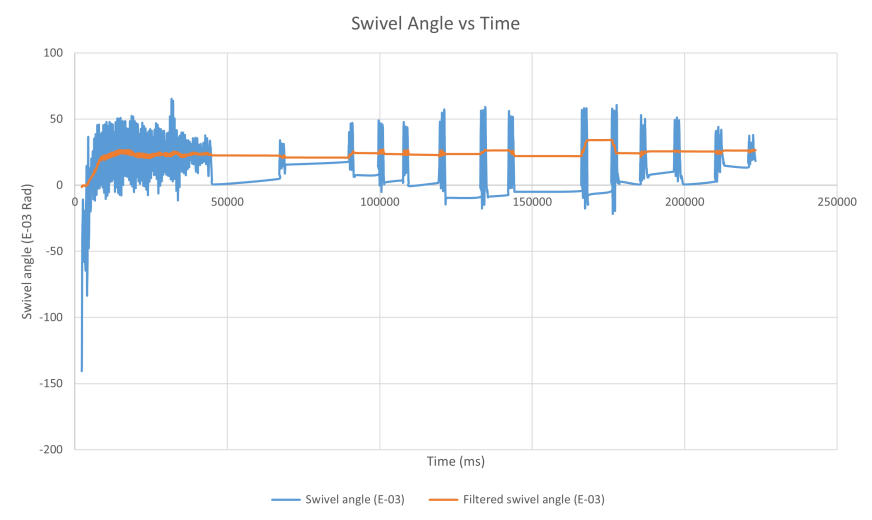

Figure 6.20: Results of filtering the signal with a 100-sample moving average filter and using a variable sampling period

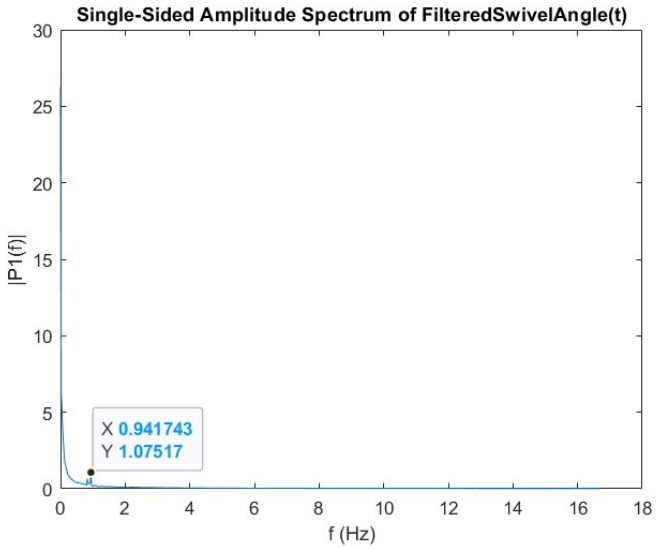

Figure 6.21: Filtered swivel angle in the power domain using a 100-sample moving average filter and a variable sampling period

Through the use of the average value of the signal, an increase in accuracy was observed. This is estimated to be because various periods of the signal are taken into account, therefore the resolution of the swivel angle is lower than the resolution of the sensor itself. This is thought to enable the use of a 1:5 relation for the gearbox instead of 1:25. More research is advised to study the behaviour of the signal to improve accuracy.

6.5 Validation

As specified in the objectives, one of the deliverables corresponds to a validation document. This document is the result of testing and simulations performed to the final version of the device designed in this project. Initially, to get to a final version that is as optimized as possible and to figure out possible external variables that influence on the system's precision, testing was performed. The results of these tests can be seen in appendix C. Once the optimization was done, the final testing was finished and the results of this can be seen in appendix A. Finally, to make sure that the client is able to use the device properly, a manual of use (appendix B) was also made and a final spec-sheet is shown in the validation document. In the following subsections the results obtained for both the testing and for the validation document are discussed separately.

6.5.1 Optimization testing

As seen in the appendix C, three different test were performed on the system and these had the following implications in the final design:

1. Clamping force heavily influences the behaviour of the system and it is directly related to the repeatability of the measurement process.

2. The variable sampling frequency seems to not work properly when turning the device at very high frequencies, probably due to the high amount of interrupts which might influence the sampling rate of the swivel angle sensing.

3. A rounded wheel will not work with the system as any tangential force to the wheel moved it to an unusable position.

Testing was deemed necessary to obtain such accurate results and optimize the design to the current level. Mainly to determine the influence that clamping force has on the system, as before testing it was thought to barely modify the system's behaviour but in reality using a torque screwdriver greatly increased accuracy.

6.5.2 Validation document

According to the tests and simulations performed for validation seen in the validation document on appendix A, all specifications discussed with the client throughout the design process were met when comparing with the original specification sheet (Table 3.8).

Some validation results show that the device even surpasses goal values discussed with the client, and when he was presented with the working device he was clarified been very much satisfied with the result.

Chapter 7

ECONOMICAL ANALYSIS

In this chapter an economical analysis is performed in order to justify the implementation of this product as an eventual solution for some of Alliander's cable installation problems.

7.1 Cost Analysis

It can be seen according to the table of costs portrayed in table 7.1, that the total cost of the design proposal is of €17,396.72, nonetheless the software was already available at no extra cost for the university and the labor costs are an estimation as in reality the designer was not compensated, therefore the real cost was of €177.72, a very small sum considering the level of accuracy that the robot achieves and its complexity. Note that the estimated salary comes from a starting salary as Mechatronics Engineer in The Netherlands [55].

Table 7.1: Cost of production and development of the product

Type	Name	Amount	Price unit	Total price	Provider
	RS PRO Deep Groove Ball Bearing - Sealed End Type, 6mm I.D, 19mm O.D	4	€ 2.49	€ 9.96	RS Online
	Seeed Studio Grove-Buzzer Module	1	€ 2.09	€ 2.09	Farnell
	Igus GFM-0608-04, Bearing with 8mm Outside Diameter	4	€ 1.52	€ 6.08	RS Online
	Broadcom Absolute Mechanical Rotary Encoder with a 6 mm Plain Shaft	1	€ 32.48	€ 32.48	RS Online

Electronic Components	HEDL-5540#A12	1	€ 57.54	€ 57.54	Farnell
	WLK-4MINI Switch	2	€ 0.94	€ 1.88	Stores U.T.
	Arduino Nano	1	€ 3.64	€ 3.64	Stores U.T.
	LED 7 segment 13mm Common Anode Red	4	€ 0.74	€ 2.96	Stores U.T.
	Switch momentary make contact	1	€ 0.51	€ 0.51	Stores U.T.
	Potmeter 5KΩ Lineair metal	1	€ 0.38	€ 0.38	Stores U.T.
	Resistor 330Ω 5% 0.25Watt	2	€ 0.05	€ 0.10	Stores U.T.
	Resistor 1kΩ 5% .25Watt	8	€ 0.06	€ 0.48	Stores U.T.
	1W LED	2	€ 0.06	€ 0.12	Stores U.T.
	NMB Radial Ball Bearing - Shielded End Type, 6mm I.D, 10mm O.D	3	€ 6.39	€ 19.17	RS Online
	M6 Steel Hex nut	17	€ 0.04	€ 0.60	RS Online
	Stainless steel threaded rod M6 1 meter	0.08	€ 5.80	€ 0.46	RS Online
	M6 steel washer	10	€ 0.02	€ 0.20	RS Online
	M6 nylon washer	4	€ 0.10	€ 0.40	RS Online
	M6x30 Steel hex head screw	1	€ 0.21	€ 0.21	RS Online
	Slot Pan Brass Machine Screws DIN 85, M6x12mm	2	€ 0.67	€ 1.33	RS Online

Mechanical Components	M6x25 Steel hex head screw	4	€ 0.17	€ 0.68	RS Online
	6 mm Aluminum rod 61 cm	0.35	€ 10.22	€ 3.62	RS Online
	Potmeter knob push fit	1	€ 0.73	€ 0.73	Stores U.T.
	Ultimaker 2.85mm Black Tough PLA 3D Printer Filament, 750g	0.63	€ 48.34	€ 30.68	RS Online
	10 mm Aluminum rod 1 m	0.03	€ 43.04	€ 1.42	RS Online
Software	Solidworks annual license	0.33	€2797	€932.33	N/A
	Matlab annual license	0.33	€860	€286.67	Mathworks
Labor	Hour of work	640	€ 25.00	€ 16,000.00	N/A
Total				€ 17,396.72	

7.2 Revenue Analysis

Calculating the revenue can be done in different ways as this subsystem could be used by itself to increase precision and efficiency in the measuring of the distance of cut or as part of the robotic system.

According to the interview performed to Alliander Employees as part of the determination of needs procedure, an estimate of 2.5% of all insulation defects are due to measurements, which represents a rough estimate of 250 thousand euros in damage from all cables, from which 158 thousand euros can be attributed to the 240 mm^2 XLPE cable directly. As it is expected from Alliander to double the amount of medium voltage cable connectors by 2050 [6] it can be estimated that this number may be doubled if solutions are not implemented, making it around 500 thousand euros by that year or 316 thousand euros directly attributed to the cable in question. It is estimated that by implementing the device designed in this project, the accuracy of distance of cut is enough to avoid cable installation issues and eliminate all of this losses, effectively winning the company

said amounts as revenue by just adding this system to the currently used device.

As also discussed in the identification of needs step of the methodology, the measuring of the distance process takes around 1 minute per cable, and considering that the process is performed around 12 times a day according to employees, which represents a total time of 3120 minutes or 52 hours annually. The designed device on the other hand takes around 5 seconds per use, which represent 4.33 hours of work annually plus calibration which takes around 257 seconds and if performed daily (which is more than necessary) represents 18.56 hours, for a total of 22.89 hours annually. Therefore an estimate of 29.11 hours of work are saved using this device, which at an hourly salary of €16.9 (estimated from national average [56]) signifies a total annual saving of €491.959.

Finally once this device is implemented in the robotic system, it will enable the robot to perform the peeling of the insulating layer process in a totally autonomous manner, which would not be possible without it as it is required to control the movement of the robot and also to detect the presence of the cable. This way, knowing that annually an estimated €1.250 million euros are lost (including both fixing costs and cost of lost minutes of electricity) because of incorrect peeling of the semiconductor during the cable installation procedure, from which 80% are XLPE cables and 79% from those are 240 mm^2 size, which means that improving the success rate of the current process from 99.9% to 100% represents a saving of €790 thousand euros [4].

Therefore the revenue can be divided in two categories, the first one is the revenue if the designed system is used by itself and not with the robotic system, which would create an annual revenue of around €158,491.96 as seen in table 7.2. On the other hand once the system is slightly modified to fit with the rest of the robotic system the annual revenue is expected to reach €790,491.96 as seen in table 7.3.

Table 7.2: Expected first year revenue of implementing the designed device as an addition to the current technique

Description	Revenue
Damage reduction	€ 158,000.00
Employee time saved	€ 491.96
Total	€ 158,491.96

Table 7.3: Expected first year revenue of implementing the designed device in the cable peeling robotic system

Description	Revenue
Damage reduction	€ 790,000.00
Employee time saved	€ 491.96
Total	€ 790.491.96

7.3 Financial Viability

As for financial viability, two different scenarios are proposed to illustrate the high viability of implementation of this project. These are: Using the designed system as an addition to the current technique and using it in the cable peeling robotic system that is currently under development.

To analyze the profitability of this investment, a return on investment metric (ROI) is used. ROI helps understanding how much profit or loss an investment will earn. It is presented as a percentage and calculated using Eq. 7.1 [57].

$$ROI = \frac{NetProfit}{CostOfInvestment} * 100 \tag{7.1}$$

Therefore, if the device is used as an addition to the current technique, the return of investment can be calculated as ROI = (€ 158,491.96 - € 17,396.72)/€ 17,396.72 that is ROI = 811% which is a very good number in terms of ROI and given the context, meaning the inversion is completely justified. On the other hand, the ROI if the system is implemented in the robot cannot yet be calculated because it is necessary to know the cost of investment associated to the rest of the robot, so that cost is going to be left as a variable, yielding ROI = (€ 790,491.96 - € 17,396.72 - C_{Rest})/(€ 17,396.72 + C_{Rest}) = (€ 790,491.96)/(€ 17,396.72+C_{Rest})- 1.

It is worth noting that the ROI will be lowered if the device breaks because of too many cycles, as life expectancy was not calculated. In this case, the ROI would be reduced by 1% per extra device in the first scenario (used as an implementation on the current device) and even less in the second scenario, which does not represent a significant risk to the investment's viability.

7.4 Other benefits

As this project is a first iteration of a highly innovative device, it is going to be left at the University of Twente to be used in future research. This means that the value of this device and this document is beyond monetary as it will provide enough intellectual material to continue upgrading it over the course of time.

For the University of Twente this represents a great deal as this will create more opportunities for graduation assignments for both Bachelor's and Master's students, ultimately increasing the research output of the university and the laboratory. This is because as described in previous sections, the real cost of this project is relatively low, therefore the required budget is highly accessible and because a highly iterative methodology was used throughout the design, it is possible to make changes from any point of the design process and upgrade it accordingly.

Finally, the university often organizes tours in the RAM laboratory, showcasing some of the inventions and discoveries made within the group. The author of this project already conducted some presentations in the "Open House Day" at the University of Twente for the general public where the designed device was presented and explained to people from all backgrounds and ages, undoubtedly rising awareness over different problems being solved at RAM which ultimately works as publicity, probably increasing investment from companies and student recruitment rates. The designed device is likely to be used in future tours and presentations adding on to this benefit for some time.

Chapter 8

CONCLUSIONS AND RECOMMENDATIONS

8.1 Conclusions

Through a comparison of all the available and easily obtainable technologies at the University of Twente premises, the rotary encoder was found as the best for position tracking of a device that displaces and rotates around the cable as its main limitation for this application is that slippage may occur, while it was found that a CMOS sensor with laser as light emitter is not accurate enough due to the light properties of the cable materials, a rotary potentiometer was limited by the resolution of the potentiometer, by the ADC resolution of the controller, potential axis slippage and its relatively high tolerance. As for detection of the cable there was not a clear winner as all the available technologies could be used in different ways, so ultimately a presence-absence switch was chosen because of its ease of use and as it is accurate enough to detect the starting point of the measuring without affecting the overall accuracy of the system by a significant margin.

Using the winning technologies from the technology comparison and selecting from the totality of created concepts the one that could use said technologies, a measuring system was designed and a prototype was built which enabled for data gathering and observation of the system's behaviour. The prototype of the designed system is capable of tracking the device position along the cable with an accuracy of 0.679 mm or 0.28% of its max range using a novelty position tracking system, which involves the use of a caster-wheel where the rotation of the wheel and the swivel angle are sensed to obtain the displacement in the along-the-cable direction using trigonometry.

An on-off control system was used to control the feed position between two different positions as this enables for easier later modification and integration in a fully automated robot. In order to do this, the signals from the sensors had to endure a special type of processing that used a variable sampling frequency allowed for variable speeds when rotating the device around the cable manually and also served to obtain the DC value of the signal to get the real advance per revolution and perform calculus for the position of the robot and finally send a stop signal when the desired distance was reached. This sequence requires only the distance selection input to automatically

measure the position of the device once correctly placed and calibrated, and that eliminates most human intervention which is the main cause for error.

A mechanical structure that integrates with minimal modifications in 3 different ways with the latest iterations of the robotic system was created and analyzed. Said structure involved a mechanical gear to increase the sensibility of angle sensing and a slippage accuracy loss avoidance system, designed with a factor of safety of 11 according to computer simulations, enabling the system to withstand not only typical usage but also incorrect use and manufacturing problems that may lead to a decrease in the resistance of the material. This will enable the client to present the project several times without the risk of a part suddenly breaking. As part of this mechanical structure, a special adaptor that enables the system to be clamped with relatively constant clamping force was designed as it was determined that a constant clamping force greatly increases the accuracy of the system.

Finally, through extensive testing on the final prototype of the design proposed in this project and knowing that this product is of innovative nature and there is no current state of the art, the creation of experiments to make a validation document of the entire system enabled not only to ensure that the client's specifications were met adequately but also characterized the system and identified main loss of accuracy causes for future optimization of the device. As the final prototype was tested with all of its components assembled, this enabled also to test for correct mechatronic integration, where all of the elements work together to make a working solution for real-life applications.

8.2 Recommendations

Throughout the design of the cable peeling device tracking device and advance per revolution control, the following recommendations for future research were found:

First of all, the system was never tested while also cutting the cable as this would have required the waste of unavailable amounts cable, so calibration and testing will have to also be performed with the cutting tool on in future implementation.

Second, as clamping force was found to be so relevant to determine the system's behaviour and calibrate it, a fully automated device should also automate the clamping process and try to achieve a constant torque in future implementations.

Third, this system doesn't necessarily has to be implemented in a fully automated cable splicing system but can also be used as a visual aid for the technicians when cable cutting in order to increment the distance of cut accuracy and reduce the lost time from measuring.

Fourth, once the system is implemented in the fully automated robotic system, considering a different approach than on-off control and use the position data to control the motors as well as the feed lever might improve accuracy results.

Finally, calibration patterns recognized by a national or international entity should be used to calibrate the system and reduce the systematic calibration error, this was not done in this project because of lack of resources, but a better calibration may decrease the error to a more acceptable value.

BIBLIOGRAPHY

[1] Alliander. *Organisation*. https://www.alliander.com/en/organisation/. Accessed: February 17, 2023. n.d.

[2] SER. *Energieakkoord voor duurzame groei*. Dutch. https://open.overheid.nl/documenten/ronl-archief-2c12d99a-e816-4e93-a199-f9e9feef318c/pdf. Accessed: February 17, 2023.

[3] United Nations. *What is Climate Change?* https://www.un.org/en/climatechange/what-is-climate-change. Accessed: February 17, 2023.

[4] Elderhorst T. *Robotics for Autonomous Cable Splicing*. Available upon request. Year of publication not provided.

[5] Dutch News. *Electricity supply issues will hit housing development, builders say*. 2022. URL: https://www.dutchnews.nl/news/2022/09/electricity-supply-issues-will-hit-housing-development-builders-say/.

[6] Liander. *Investeringsplan 2022*. https://www.liander.nl/over-liander/investeringsplan2022. Accessed: February 17, 2023. 2022.

[7] 3M. *Power Cable Splicing and Terminating Guide*. Guideline. 3M, 2018.

[8] Alliander. "Bewerken XLPE kabel". In: Video recording. Available upon request. Year of publication not provided.

[9] BV Twensche Kabelfabriek. *Twenpower Medium-Voltage XLPE Cables*. https://www.tkf.nl/files/content/twenpower-engels-2015.09.09.115800.pdf. Sept. 2015.

[10] Power and Cables. *Ripley US02-7000 Semicon Shaver Stripping Tools*. https://www.powerandcables.com/product/product-category/ripley-us02-7000-semicon-shaver-stripping-tools/. May 2023.

[11] T. Elderhorst. "How to use the US02-7000 tool". In: *Cable splicing workshop*. Robotics and Mechatronics (RAM). University of Twente, Feb. 2023.

[12] J. Fraden. *Handbook of Modern Sensors*. 5th. New York, NY: Springer, 2010. ISBN: 978-3-319-19303-8. DOI: 10.1007/978-3-319-19303-8.

[13] R. Walpole, R. Myers, S. Myers, et al. *Probability & Statistics for Engineers & Scientists*. 9th. Pearson, 2017.

[14] T. Ulrich and D. Eppinger. *Product Design and Development*. McGraw-Hill Education, 2015. ISBN: 0078029066.

[15] ULC Technologies. *Electric Cable End Preparation Machine*. https://ulctechnologies.com/technologies/electric-cable-end-preparation-machine/. Accessed on 17 February 2023.

[16] E. Rigger, T. Vosgien, K. Shea, et al. "A top-down method for the derivation of metrics for the assessment of design automation potential". In: *Journal of Engineering Design* (2022).

[17] World Bank. *Climate Knowledge Portal - Netherlands Climate Data Historical*. https://climateknowledgeportal.worldbank.org/country/netherlands/climate-data-historical. Accessed: May 31, 2023. 2023.

[18] E. Callegati, G. Zanelli, B. Bezzi, et al. "Smart and adaptive interfaces for INCLUSIVE work environment". In: ().

[19] Canadian Centre for Occupational Health and Safety. *Pushing and Pulling Objects: Ergonomics*. n.d. URL: https://www.ccohs.ca/oshanswers/ergonomics/push1.html (visited on 03/09/2023).

[20] E.Oberg, F. Jones, H. Horton, et al. *Machinery's Handbook*. 31st ed. Industrial Press, Inc., 2020. ISBN: 9780831138015. DOI: 10.1016/C2017-0-04218-4.

[21] X. XuandM. Liao and P. van Beek. "Methods and systems for vision-based motion estimation". US Patent US20160063330. 2022. URL: https://patentscope.wipo.int/search/en/detail.jsf?docId=US159933279&_cid=P21-LDMZMH-90108-2.

[22] E. Avallone, T. Baumeister, and A. Sadegh. *Marks' Standard Handbook for Mechanical Engineers*. 12th ed. McGraw-Hill Education, 1996. ISBN: 0070049971.

[23] E. Ramsden. *Hall Effect Sensors: Theory and Application*. Newnes, 2006. ISBN: 978-0750677295.

[24] Y. Zhang, W. Liu, H. Zhang, et al. "Design and analysis of a Differential Waveguide Structure to Improve Magnetostrictive Linear Position Sensors". In: *Sensors* 11.5 (2011).

[25] K. Sawa, S. Kakino, T. Shigemori, et al. “Degradation process of a sliding system with Au-plated slip-ring and AGPD brush for power supply”. In: Oct. 2005, pp. 312–317. ISBN: 0-7803-9113-6. DOI: 10.1109/HOLM.2005.1518262.

[26] nd R. Dorf R. Bishop. *Modern Control Systems*. 13th. Pearson Education, 2015. ISBN: 1-292-42237-8.

[27] Stephen J. *Human Factors Engineering and Ergonomics: A Systems Approach*. 2nd ed. CRC Press, 2014. ISBN: 9781466554241. URL: https://www.crcpress.com/Human-Factors-Engineering-and-Ergonomics-A-Systems-Approach-Second/Guastello/p/book/9781466554241.

[28] G. Mok. “The design of a planar precision stage using cost effective optical mouse sensors”. Supervisor: J.W. Spronck; Professor: J.L. Herder. Master Thesis. Delft, Netherlands: Delft University of Technology, 2015. URL: https://repository.tudelft.nl/islandora/object/uuid:a3c3dd56-5e32-4b5b-9a20-f7dcf606dcd9/datastream/OBJ/download.

[29] A. Baudry, S. Guegan, and M. Babel. “Taking caster wheel behavior into account in the kinematics of powered wheelchairs”. In: *Modelling, Measurement and Control C* 79 (Dec. 2018), pp. 168–172. DOI: 10.18280/mmc_c.790403.

[30] Bulldog Castors. *5-Step Guide to Castor Wheel Installation*. https://www.bulldogcastors.co.uk/blog/5-step-guide-castor-wheel-installation/. Accessed: June 15, 2023.

[31] TME (Transfer Multisort Elektronik). *WLK-4MINI Microschakelaars snap-action*. TME.eu. Oct. 2021. URL: https://www.tme.eu/nl/details/wlk-4mini/microschakelaars-snap-action/ (visited on 05/04/2023).

[32] *Farnell Netherlands*. https://nl.farnell.com/. Accessed: June 15, 2023.

[33] Farnell. *Farnell Catalog Datasheet: Product HEDL-550x/554x, HEDL-560x/564x, HEDL-9000/9100, HEDL-9040/9140/ 92xx*. Online. Accessed: April 18, 2023. 2023. URL: https://www.farnell.com/datasheets/1884439.pdf.

[34] Avago Technologies. *AEAT-6010/6012 Magnetic Encoder*. Accessed: June 15, 2023. RS Components. Year not specified. URL: https://docs.rs-online.com/5574/0900766b80e8dd0c.pdf.

[35] *Arduino Nano*. https://store.arduino.cc/products/arduino-nano. Accessed: June 15, 2023.

[36] RS Components. *Omron H3CR-A8E AC100-240/DC100-125 Timer, 8-Pin, DPDT, 24-48VAC/12-48VDC*. RS Online. Oct. 2018. URL: https://nl.rs-online.com/web/p/remote-control-systems/1926546 (visited on 05/04/2023).

[37] European Parliament and Council. *Directive 87/372/EEC of 25 June 1987 on the frequency bands to be reserved for the coordinated introduction of public pan-European cellular digital land-based mobile communications in the Community*. Directive L 185. Official Journal of the European Communities, 1987, pp. 72–75. URL: https://eur-lex.europa.eu/legal-content/EN/TXT/?uri=celex%3A31987L0372.

[38] RFSolutions. *FOB-OEM*. RS Online. N/D. URL: https://docs.rs-online.com/3d55/A700000006686296.pdf (visited on 05/04/2023).

[39] *iglidur® G – The All-Round Performer*. RS Online. Available: https://docs.rs-online.com/8fb5/0900766b80cdff66.pdf [Accessed: 14 Jun, 2023].

[40] H. Zemansky, H. Young, and R. Freedman. *Sears and Zemansky's University Physics: With Modern Physics*. 15th. New York, NY: Pearson, 2023.

[41] *Ultimaker Tough PLA Technical data sheet*. Ultimaker. [Online; accessed May 8, 2023]. May 2022. URL: https://makerbot.my.salesforce.com/sfc/p/#j0000000HOnW/a/5b000004UgTE/z40nDBo3Clypj7u9xI7MbeVe.CNpDM_Mq0nhvbpyne8.

[42] R. Ferreira, I. Amatte, T. Assis, et al. "Experimental characterization and micrography of 3D printed PLA and PLA reinforced with short carbon fibers". In: *Composites Part B: Engineering* 124 (May 2017). DOI: 10.1016/j.compositesb.2017.05.013.

[43] A.Oppenheim and G. Verghese. *Signals, Systems & Inference*. 2nd. Upper Saddle River, NJ: Pearson, 2015. ISBN: 978-0-13-394328-3.

[44] L. Chuan-Zheng. *Signals and the Frequency Domain*. https://web.stanford.edu/class/archive/engr/engr40m.1178/slides/signals.pdf. Lecture notes for course ENGR 40M, Stanford University. Accessed on June 5, 2023. 2017.

[45] National Instruments. *What is DC Level?* https://www.ni.com/docs/en-US/bundle/labview/page/lvanlsconcepts/what_is_dc_level.html. Accessed on June 5, 2023.

[46] Smith and Steven W. *The Scientist and Engineer's Guide to Digital Signal Processing*. California Technical Publishing, 1997.

[47] R. Larson. *Algebra and Trigonometry*. 8th. Boston, MA: Cengage Learning, 2010. ISBN: 9780538733526.

[48] *Directive 2006/42/EC of the European Parliament and of the Council of 17 May 2006 on Machinery, and amending Directive 95/16/EC*. Official Journal of the European Union. EN 60204-1:2006+A1:2009, Safety of machinery - Electrical equipment of machines - Part 1: General requirements. 2006. URL: https://eur-lex.europa.eu/legal-content/EN/TXT/?uri=CELEX:02006L0042-20101229.

[49] European Parliament and of the Council. *DIRECTIVE 2009/125/EC OF THE EUROPEAN PARLIAMENT AND OF THE COUNCIL*. https://eur-lex.europa.eu/legal-content/EN/TXT/PDF/?uri=CELEX:32009L0125&from=EN. 2009.

[50] European Parliament and of the Council. *Ecodesign and Energy Labelling Working Plan 2022-2024*. https://eur-lex.europa.eu/legal-content/EN/TXT/?uri=CELEX%3A52022XC0504(01)&qid=1651649049970. 2022.

[51] D. Anderson, Q. Li, and Q. Yang. "Physical and Mechanical Properties of PLA, and Their Functions in Widespread Applications—A Comprehensive Review". In: *Polymers* 10.11 (2018), p. 1256.

[52] M. Anderson. *Types of Magnetic Metals: List of Magnetic Metals*. https://www.meadmetals.com/blog/types-of-magnetic-metals-list. 2022.

[53] Ultimaker. *Ultimaker S5 Technical Specifications*. https://ultimaker.com/3d-printers/s-series/ultimaker-s5/. Accessed: May 25, 2023.

[54] R. van den Berg. "Using Computer Vision for Monitoring the Peeling Process of Semiconducting Insulation Shield of Medium Voltage Cables". MA thesis. University of Twente, May 2023.

[55] *Glassdoor: Mechatronics Engineer Salaries in Netherlands*. https://www.glassdoor.com/Salaries/netherlands-mechatronics-engineer-salary-SRCH_IL.0,11_IN178_KO12,33.htm. Accessed: June 15, 2023.

[56] *GrabJobs Netherlands Salary Guide: Electrical Technician*. Accessed: June 15, 2023. URL: %5Curl%7Bhttps://grabjobs.co/netherlands/salary-guide/electrical-technician#:%5Csim:text=The%5C%20average%5C%20salary%5C%20for%5C%20an,2%5C%2C700%5C%20per%5C%20month%5C%20in%5C%20Netherlands%7D.

[57] B. Curry. "What Is ROI (Return on Investment)?" In: *Forbes* (June 2023). Accessed: June 15, 2023. URL: https://www.forbes.com/advisor/investing/roi-return-on-investment/.

Appendix A

VALIDATION DOCUMENT

A.0.1 Validation by simulation

In order to test the FOS of the device, a Solidworks force analysis was performed, and the results can be seen in figures for both von Mises and max shear criteria. Using the most conservative value as result, the minimum factor of safety for the device according to simulation is of 11.

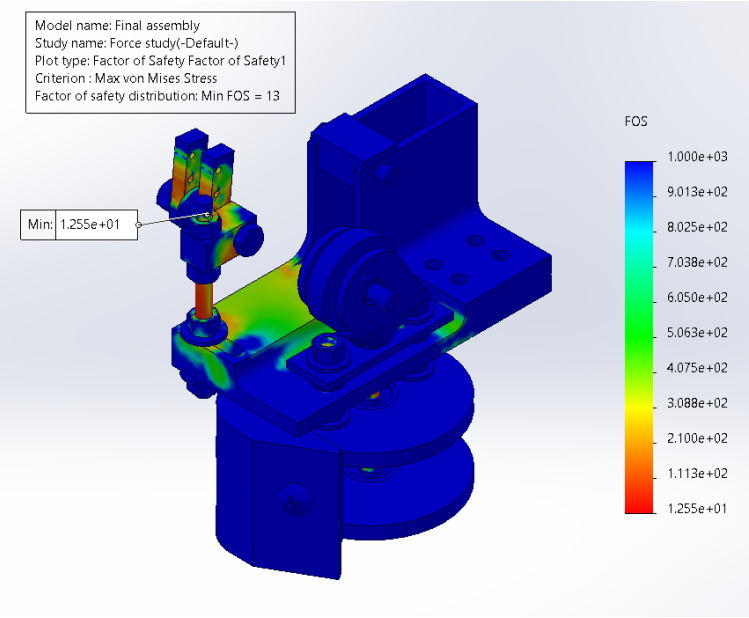

Figure A.1: Result for the factor of safety utilizing von Mises criterion isometric view

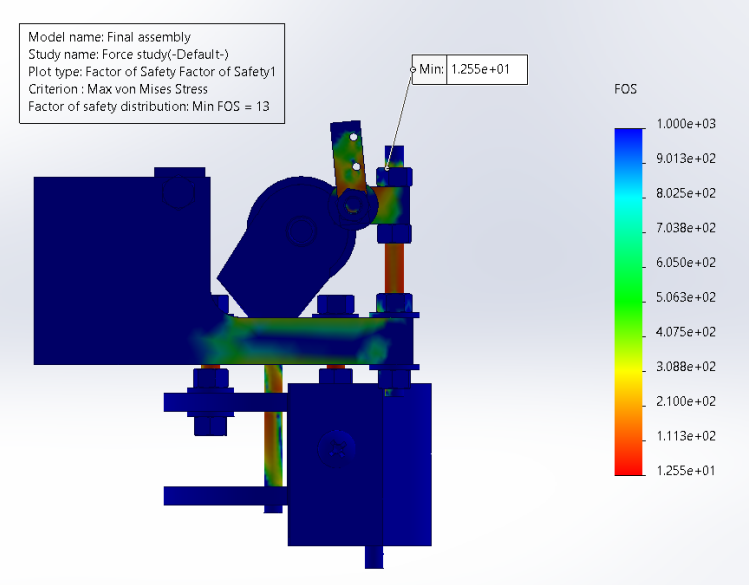

Figure A.2: Result for the factor of safety utilizing von Mises criterion frontal view

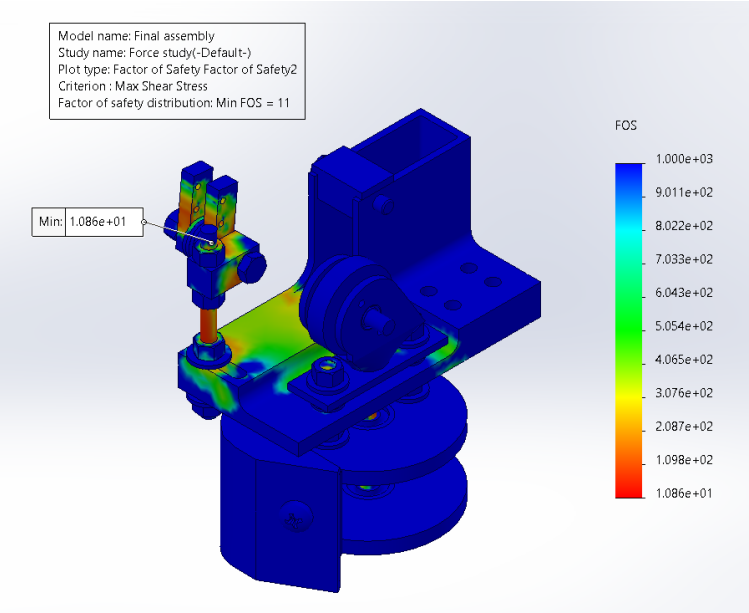

Figure A.3: Result for the factor of safety utilizing max shear stress criterion

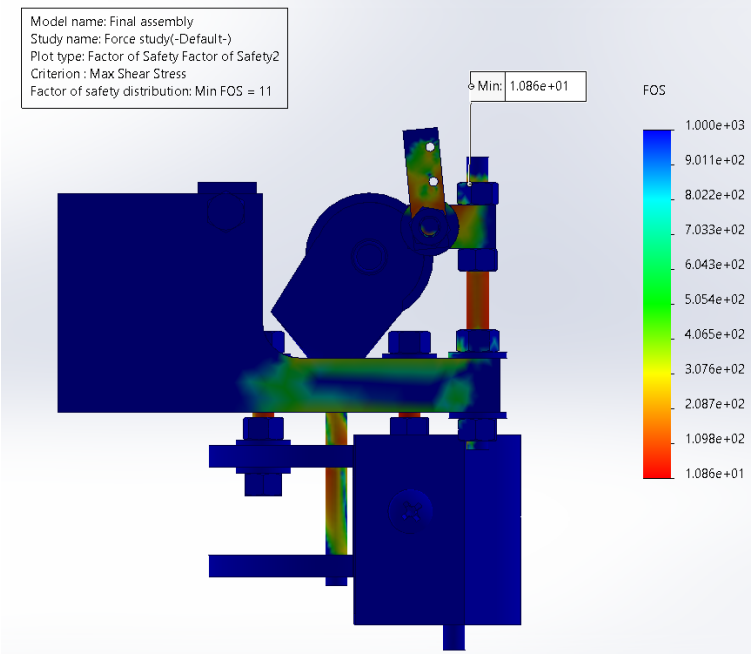

Figure A.4: Result for the factor of safety utilizing max shear stress criterion

A.0.2 Validation by prototype testing

In this subsection of the validation document all the real-life tests performed for validation are discussed. It is worth mentioning that tests that involved the use of the cable were done without peeling the cable. **Validation test 1: Using the final prototype measure 5 times the force required to start the rotation of the device on its initial position attaching a string with a bottle whose weight is known using a scale with 1 gram of uncertainty to the handle and adding a small force component with a newtonmeter of range 0-10N and uncertainty of 0.2N.** The set-up for this experiment can be seen in figure A.5 and the results of this validation can be seen in A.1. The average force is of (7.1 ±0.2) N using the combination of uncertainty of tools and the precision of the average as uncertainty. This value is way below the 148 N set as marginal and goal value, therefore this validation was successful.

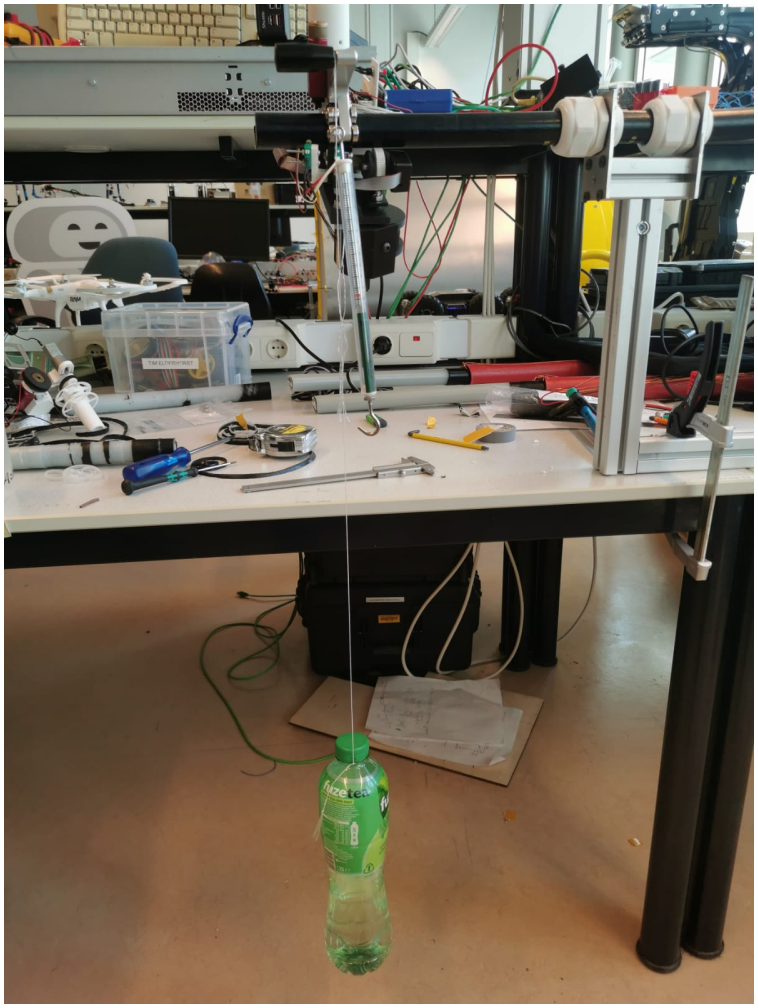

Figure A.5: Set-up for validation test 1

Table A.1: Force required to start the rotation of the system validation

Experiment #	Newtonmeter force (± 0.2N)	Bottle weight (± 1 g)	Force (±0.2N)
1	1.6	532	
2	1.8	532	
3	1.8	531	
4	2.2	530	
5	2.0	534	
Average	1.9	532	7.1

Validation test 2: The designer performs the calibration procedure explained in appendixB at 60 RPM and records the time it takes to do using a chronometer. The result of this test was of four minutes and 17 seconds, and as there are not many variables involved in this process, one

experiment was considered enough. It's worth noting that this time falls below the 900 seconds (or 15 minutes) set as marginal value considerately.

Validation test 3: The completely assembled final prototype is weighted 5 times and then the original cutting tool without the project additions is also weighted. The difference of the average is used to obtain the weight of the designed device. The table with results can be seen in table A.2. Notice that the total weight of the designed device is of (680.0 ± 1.4) g, which is below the 1 kg requirement for weight. The goal value was not reached, nonetheless it is still considered very much acceptable by the client.

Table A.2: Validation of the weight of the designed device

Experiment	Weight without device (± 1 g)	Weight with device (± 1 g)	Weight of only the designed device (± 1.4 g)
1	664	1345	
2	664	1345	
3	663	1343	
4	665	1345	
5	665	1343	
Average	664	1344	680.0

Validation test 4: Using the functional prototype of the system on the cable peeling tool without the cutting tool, the system is placed in its initial position and advance per revolution position 2, it is set at a given distance 5 mm longer every experiment and rotated at a hand-felt constant speed until the designed device outputs the stop signal. The difference between the selected distance of cut and the measured distance with a ruler is used as error. Between experiments no calibration is allowed as a way of determining the amount of cycles before calibration and the cable is inspected on the look for damage. The results obtained for this validation test can be seen in A.3. It can be observed that no cable damage was present after 19 experiments, therefore the device is capable of maintaining cable integrity adequately. As for the error, it never reaches 3 mm of maximum error, which is the marginal value for this parameter and the average of this error is of 0.52 mm, which is below the 1 mm marginal value for this other parameter. After 19 experiments the error never reaches an error of more than 3 mm, it is considered that the marginal value of the cycles between calibration is met. The goal value might also be met but there is need for further testing to confirm this.

Table A.3: Validation of accuracy, cycles between calibration and avoidance of cable damage

Experiment	Sensed value	Measured value (± 0.5 mm)	Error (± 0.7 mm)	Cable damage visible?
1	150	150.0	0.0	No
2	155	155.0	0.0	No
3	160	160.0	0.0	No
4	165	165.0	0.0	No
5	170	170.0	0.0	No
6	175	175.0	0.0	No
7	180	180.0	0.0	No
8	185	186.0	1.0	No
9	190	191.0	1.0	No
10	195	195.0	0.0	No
11	200	200.0	0.0	No
12	215	216.0	1.0	No
13	205	206.0	1.0	No
14	210	212.0	2.0	No
15	220	221.0	1.0	No
16	225	225.0	0.0	No
17	230	231.0	1.0	No
18	235	236.0	1.0	No
19	240	241.0	1.0	No

In order to know if the amount of samples taken is adequate, knowing that 0.0526 of samples have an error of more than 1 mm and it is not desired for that number to be more than 50% ($e = (0.5 - 0.0526)/0.0526 = 8.5057$), it is possible to refer to Eq. 2.1. A quick observation can be made as values on the numerator of the equation are much lower than the error on the denominator, therefore n is less than 1 and just taking 1 sample would be enough for this specific case. Therefore this validation has more than enough samples than it needs.

Validation test 5: A survey aiming to grasp an understanding on the level of easiness of use of the device was performed. The questions asked as well as the results were the following seen in A.4. Before making the questions a basic explanation on how to use the device was made.

Survey title: Satisfaction with HMI of product survey.

Description: The objective of this survey is to find out the experience the user will have when using the HMI in the cable peeler tracking tool. Based on "Smart and adaptive interfaces for INCLUSIVE work environment" by Prof. Cesare Fantuzzi for the European Union's Horizon 2020 research and innovation programme under grant agreement N723377.

Scale goes as follows (5 point likert scale): 0 = Not at all 4 = Completely

Note: In parenthesis the questions from the original survey from which this is based of.

Table A.4: Results of survey for level of easiness

ID	**Academic level**	**Age**	**How safe does this device look and feel? (4.4.1)**	**How clear and visible would you qualify this interface? (4.4.2)**	**How easy is it to modify values? (4.4.3)**	**How easy is it to identify what is about to happen? (4.4.3)**	**Average**
1	Master student	26	3.00	2.00	4.00	3.00	3
2	BSc.	22	2.00	4.00	4.00	4.00	3.5
3	BSc. Student	25	4.00	3.00	4.00	4.00	3.75
4	MSc.	24	4.00	3.00	4.00	4.00	3.75
5	MSc.	25	4.00	4.00	4.00	4.00	4
Average			3.40	3.40	4.00	3.80	3.65

An average of 3.65 as easiness of use was obtained, and given the sample size, using 2.1 to calculate the margin of error, knowing that 1 of the results yielded a 3 which is under the accepted value according to the specification sheet, this corresponds to a proportion of 80%. Therefore it is possible to be 95% confident that the results are within 35% of the initially obtained proportion. This level of error is very high but due to the low amount of available participants it is not possible to get more samples and increase the accuracy of this test. Nonetheless even if the proportion drops to 45% it is likely that the average would still be above 3.

Validation test 6: Using the zero detection system, the device is rotated very slowly until the zero is detected. Once it is detected the device is stopped and the distance from the actual zero to the cable end is measured using a ruler of 0.25 mm of uncertainty. This process is done 10 times and the average value is noted. The results for this validation test can be seen in table A.5. It can be seen that the goal value is met even on the high side of the uncertainty with an average of (0.1 ± 0.15) mm, using average absolute deviation as uncertainty.

Table A.5: Results for zero detection accuracy validation

Experiment #	Measured distance (±0.25 mm)
1	0.0
2	0.0
3	0.0
4	0.5
5	0.0
6	0.0
7	0.0
8	0.5
9	0.0
10	0.0
Average	0.1

A.1 Final specification sheet

Finally, using the results from the tests performed for validation a final specification sheet is constructed, showing the actual numerical values that were obtained for the specifications set throughout the process. This can be seen in A.6.

Table A.6: Final specification sheet

#	Metric	Units	Value	Note
1	Total delay produced by the measuring cycle	s	~ 0	1
2	Force required to start moving the device when in feed position "2"	N	7.1	
3	Working temperatures	Celsius	[-25,58]	2
4	Total calibration time	s	257	
5	Number of cycles before a calibration curve adjustment is needed	Cycles	19	3
6	Weight	kg	0.68	
7	Minimum visible already-cut cable from 150 to 240 mm distance of cut	%	79	4
8	Minimum distance of cut from which the most recently cut cable can be seen during the process	mm	31.57	4

9	Maximum absolute error for position tracking the robot	mm	2.0	
10	Average absolute error for position tracking the robot	mm	0.52	
11	Average absolute error for zero detection	mm	0.1	
12	Sub-processes where human interaction is required	List	Distance selection	
13	Output bits	bits	2	
14	Resolution of the distance selector	mm	1.0	
15	Range of measurements that can be selected	mm	[150,240]	
16	Sampling period	s	0.03	5
17	Level of easiness to modify the distance measurement	subj. survey Lickert scale	3.65	
18	Safety factor for the mechanical structure	non-dimensional	11	
19	The cable's XLPE layer is unharmed during the process	Binary	Yes	

A.1.1 Notes on the final specification sheet

Note 1

The real total delay produced by the measuring cycle is of 5 seconds because there is a waiting period where a sound is reproduced for security reasons. Apart from this waiting period, the measuring occurs without any further delay on the process.

Note 2

Assuming the system is calibrated at ambient temperature (to account to changes in the system's behaviour due to metal expansion or similar phenomena), this can be verified checking the working temperatures for the main electronic components used for measuring as follows:

- Arduino Nano: -40 to 85 ^{o}C [35].
- HEDL-5540#A12: -40 to 100 ^{o}C [33].
- AEAT-6010/6012: -40 to 125 ^{o}C [34].
- Presence-absence switch WLK-4MINI: -25 to 65 ^{o}C [31].

Another element that was checked for temperature range of use were the Iglidur linear bearings, as temperature may effectively add friction to said components and limit the efficacy of the anti-slippage system, but its working range was found to be from -40 to 130 ^{o}C [39]. Temperature resistance of Tough PLA (main structural material of the design) makes it usable on temperatures of less than 58 ^{o}C.

This way using all the information described under this note, the working temperatures defined by the components present in the design are from -25 to 58 ^{o}C.

Note 3

Actual number of cycles could be higher but that would require more time-consuming testing which at the moment is not available.

Note 4

Minimum visible already-cut cable from 150 to 240 mm was calculating using the Solidworks model of the device. Using figure A.6 as reference, it can be seen the area of the already-cut cable that is blocked by the designed device. There's a point when rotating the device around the cable where the entire segment of the cable is blocked as seen in figure A.7. This distance is also used for the minimum distance from which the cable is visible.

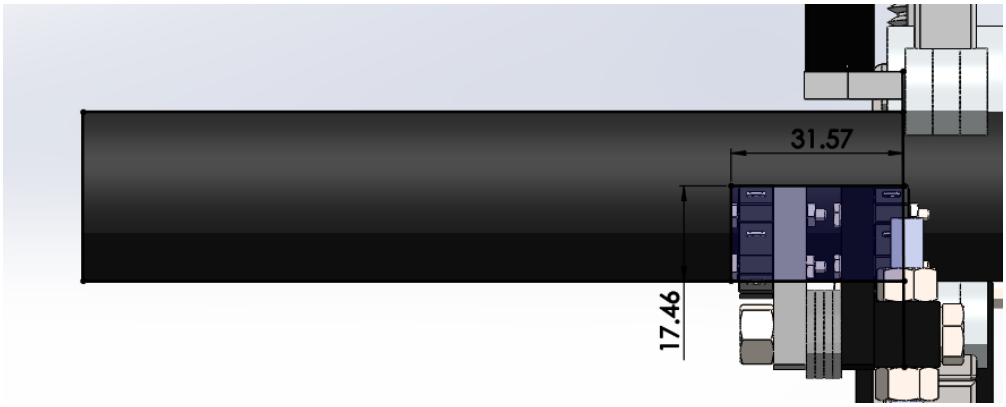

Figure A.6: Already-cut cable visibility obstruction dimensions

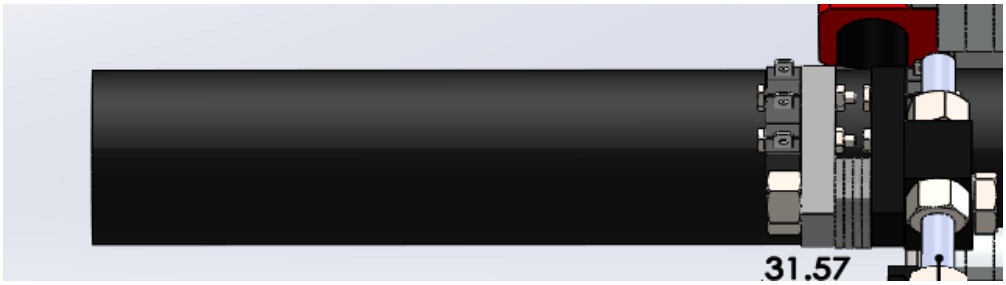

Figure A.7: Already-cut cable maximum visibility obstruction

Therefore the worst case scenario for cable visibility would be when the less cable has been cut (150 mm of already cut cable) and the most amount of cable is obstructed. This way 150 mm being the distance of cut cable and 31.57 mm being the distance of cable visually obstructed, this corresponds to a 79% minimum visibility of cable after 150 mm.

Note 5

Sampling period is variable, nonetheless at a nominal speed of 60 RPM, the sampling period is of around 0.03 s and the delay for 0 detection is virtually non-existant. According to Eq. 3.2, using the average error 0.52 mm and knowing that the nominal speed is of T_{1mm} = 0.33 s, the fulfillment of the in-equation can be verified as $0.03 \leq 0.1584$ which is true, therefore the requirement for the specification is met.

Appendix B

MANUAL OF USE

B.1 Set-up

In order to set-up the device with the US-7000 cable peeling tool, only three steps are required once the device components are fully assembled.

Step 1: Place and press firmly the position tracking device on the US-7000 device as seen in figure B.1.

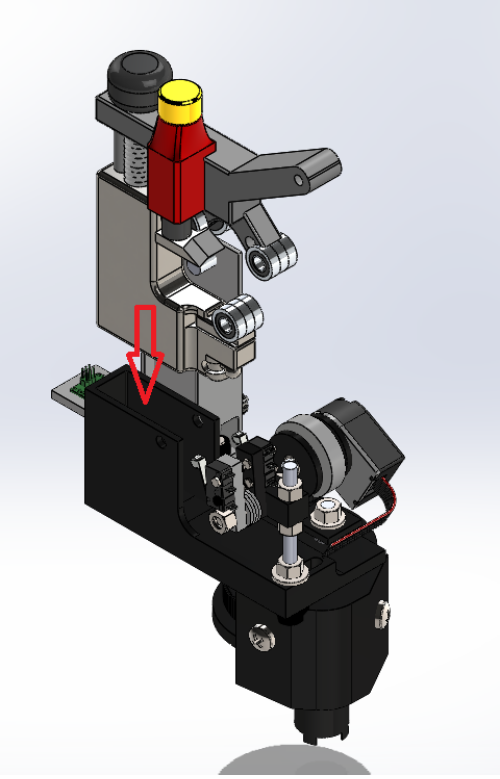

Figure B.1: First step to set up the designed device on the peeling tool

Step 2: Place the base fixture on top of the US-7000 tool so that the holes on the base carcass and the base fixture align and screw the M6x30 screw through said holes as seen in figure B.2.

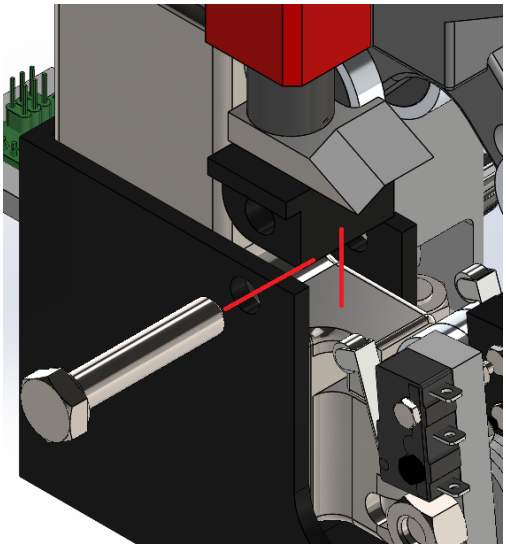

Figure B.2: Second step to set up the designed device on the peeling tool

Step 3: Finally, place the torque screwdriver adaptor on top of the clamping knob of the US-7000 as seen in figure B.3and turn it until one of the holes of the adaptor aligns with the hole in the knob. Once the holes are aligned, place a 2 mm metallic pin or any pointy and long metallic object until the knob and the adaptor turn without any perceivable slippage. Tape can be used to secure the inserted object.

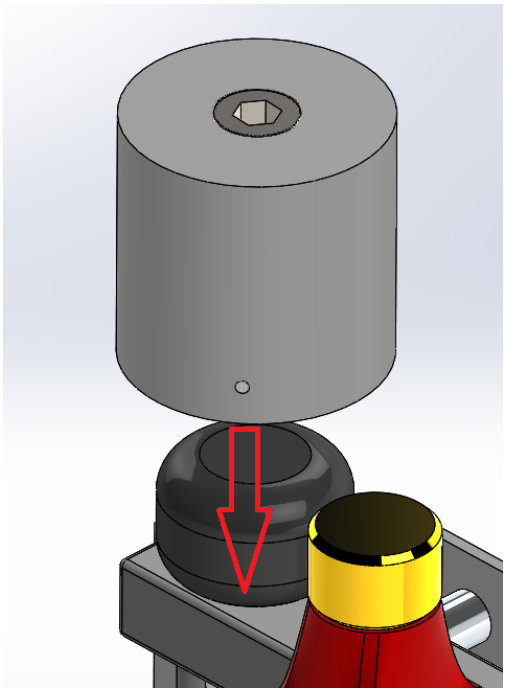

Figure B.3: Third step to set up the designed device on the peeling tool

Once this steps are completed the device is ready to use. Make sure that the battery is well connected to the electronic circuit and with a voltage of more than 7 V. To place the device on the cable, a torque screwdriver has to be used and set to 0.2 Nm as seen in figure B.4. Place the device so the first presence absence sensor slightly touches the star of the cable but it's not activated.

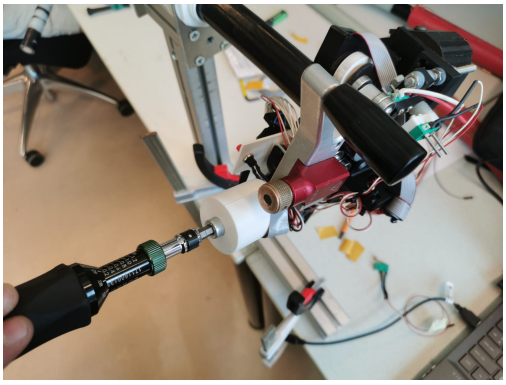

Figure B.4: Clamping the device to the cable

B.2 Calibration

Once the previously stated steps have been followed and the designed device is placed on the cable adequately using the torque screwdriver, to perform calibration the following procedure must be performed:

Step 1: Using a spare piece of a as straight-as-possible 240 mm^2 XLPE cable with at least 300 mm of available space to account for the space taken by the measuring wheel. Measure with a 0.5 mm of uncertainty ruler a distance of 150 mm from the cable end and carefully mark it with a white pen making sure it is drawn as accurately as possible checking multiple times, then do the same at a distance of 240 mm.

Step 2: Turn the device until it cuts through the the 150 mm marking, stop and measure the real value with the ruler and read the sensed value and mark both down on an Office Excel or similar software sheet.

Step 3: Turn the device 3 times and save the sensed and real values in an Excel sheet and repeat this step until it reaches the 240 mm marking.

Step 4: Construct a calibration curve using the real distance as Y value and the sensed distance as X value. A linear function will appear, obtain the equation for said function using Excel graph

tools.

Step 5: Disconnect the battery from the electronic circuit and connect the Arduino Nano to a computer with Arduino IDE. Modify the code seen in E and change the m as the multiplicative error and b as the additive, where it is clearly marked as follows:

```
////////////////////////////////////////
//Calibration Eq.///////////////////////
////////////////////////////////////////
distance = distance*m+b;
////////////////////////////////////////
```

Once all the previous steps have been completed, compile the code into the Arduinuo. The device is now calibrated.

B.3 Use of the device

Once the device is calibrated and placed on the cable, in order to activate the measuring procedure the following steps have to be followed:

Step 1: Press the reset button.

Step 2: Select a distance moving the knob and observing the screen. Units are in mm.

Step 3: Press the start button.

The device is now ready to be used as intended.

Appendix C

OPTIMIZATION TESTS

C.1 Effect of different turning speeds on the system

The following test was performed to obtain at which speeds the system behaves the better and take action according to that:

Put the cable peeling device in position 2 with the data-gathering set-up and use as intended. Perform an FFT analysis on the swivel angle without filtering to obtain the amplitude of vibrations for 3 different rotational speeds using an auditory guide (metronome). Results for this can be seen in table C.1.

Table C.1: Testing performed to observe the effect of turning speeds on the system's behaviour

Average speed (RPM)	DC component (E-03 rad)	Amplitude of main frequency (E-03 rad)	FFT
30	21.9365	20.1068	Figure C.1
60	26.2384	19.4776	Figure C.2
100	21.711	6.49917	Figure C.3

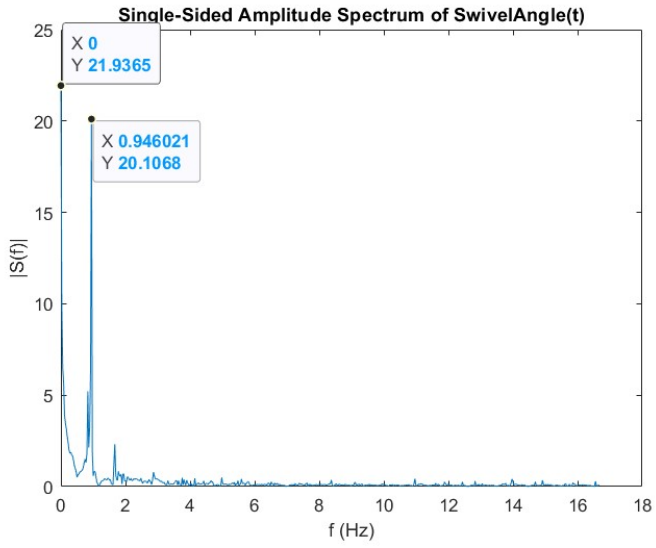

Figure C.1: Power spectrum of the swivel signal for around 30 RPM of turning speed

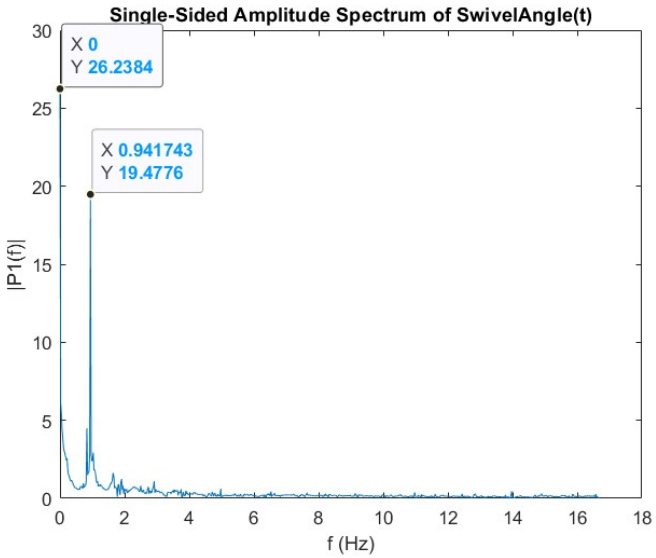

Figure C.2: Power spectrum of the swivel signal for around 60 RPM of turning speed

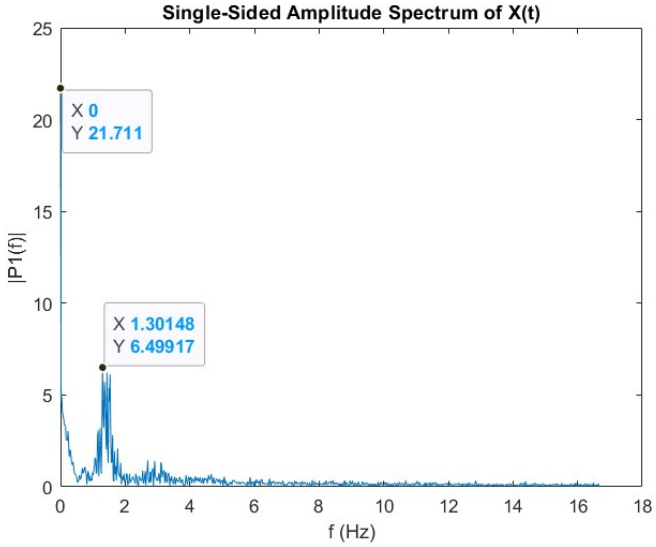

Figure C.3: Power spectrum of the swivel signal for around 100 RPM of turning speed

The results of this testing meant a few things which might be useful for future development of this project, namely:

- Lower speed of rotation mean stronger vibrations on the swivel of the caster wheel, which is undesirable and might reduce accuracy.
- After analyzing the amplitude spectrum of the swivel angle, it was observed that higher speeds seem to make the frequency of vibrations be higher, even though this was thought

accounted for with the variable sampling rate, this might be due to the increment in frequency of interrupt procedures, which might also ultimately disturb the sampling of the swivel angle.

This past points do not represent a needed change in the system's design because the abnormal behaviour was mostly seen at above 100 RPM, which is considerably above the 60 RPM at which the system is expected to be used. Also, other variables might be affecting the results of this tests, as using a constant clamping force was not yet possible at the time of realization, so this could be reducing the accuracy of the system.

C.2 Effect of different clamping forces

The following test was performed to observe the effect of changing the clamping force of the system:

Put the cable peeling device in position 2 with the data-gathering set-up and use as intended. Analyze the amplitude of the main frequency vibrations and the DC component for 3 different hand-felt clamping forces with an FFT analysis for the swivel angle without filtering. The results of this tests can be seen on figure C.2.

Table C.2: Results of testing performed to observe the effect of clamping force on the system's behaviour

Clamping force	DC Component (E-03 RAD)	Amplitude of main frequency (E-03 RAD)	FFT
Light	21.49	6.49	Figure C.4
Medium	27.84	9.28	Figure C.5
High	35.74	13.05	Figure C.6

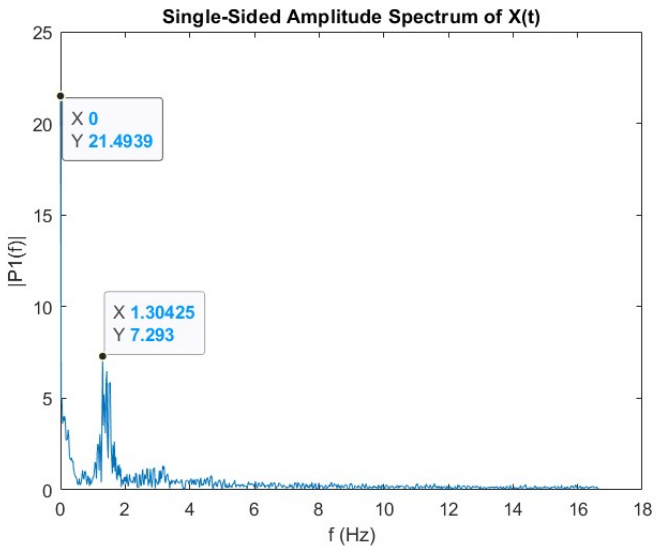

Figure C.4: Power spectrum of the swivel signal for a low clamping force

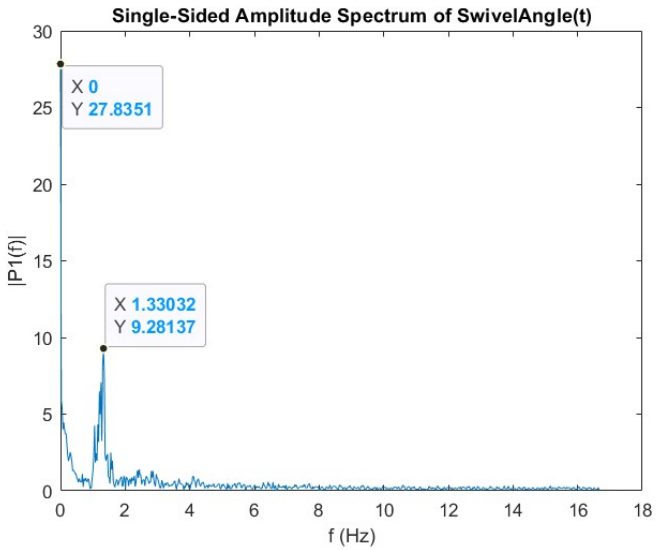

Figure C.5: Power spectrum of the swivel signal for a medium clamping force

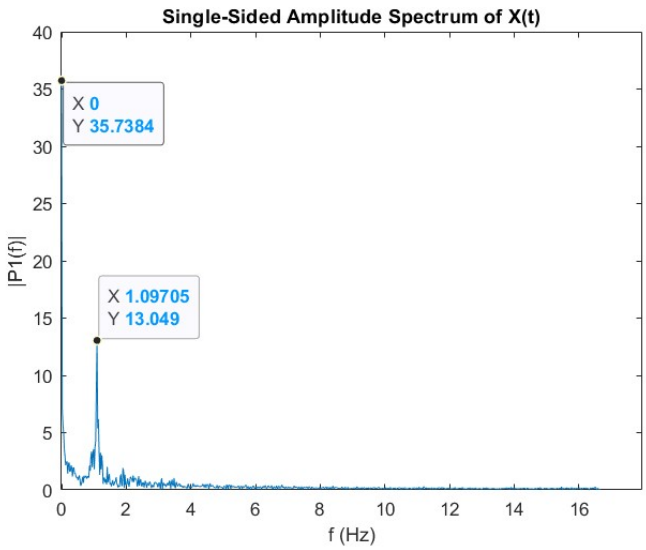

Figure C.6: Power spectrum of the swivel signal for a high clamping force

The past results had a serious implication in the design of the system: The clamping force means a significant change in the entire system's behaviour. Therefore, this test helped to encounter one of the main sources for lack of repeatability in the system. Once it was ensured that the clamping force was almost constant, the system accuracy and precision greatly increased.

Apart from this, some other observations can be made for future improvement of the device, namely:

- Higher clamping forces increment the DC value of the signal, which means the system detects a higher advance per revolution. Nonetheless it has yet to be studied if this coincides with the actual advance per revolution. Testing suggests this is not the case as with high clamping force the angle is 1.66 times the low clamping force swivel angle and the advancement per revolution was definitely lower than this value. More testing has to be performed with more accurate clamping values and less external variables to determine for sure this influence.

- Higher clamping forces seem to also have an influence in the amplitude of main frequency, but this has yet to be ensured using a system with a linear time invariant behaviour.

C.3 Effect of different wheel shape

Most commercially available caster wheel use a rounded shape approach, but as this is a novelty product used for accurate measuring, the question of whether or not the use of said wheel might improve or decrease the accuracy of the system. The test performed is the following:

Using two different measuring wheel shapes, the behaviour of the caster wheel was visually inspected.

Table C.3: Results of testing performed to observe the effect of the wheel shape on the system

Wheel type	Observations
Rounded Edges	The tangential force to the rounded edges tends to move the axis in a lateral direction, forcing the whole swivel of the caster wheel to move into the direction of the movement and therefore rendering this rounded design unusable.
Cylindrical	There is still some lateral forces that seem to create an offset resulting angle and that might be seen as an offset in the swivel angle signal, nonetheless this might be fixable through calibration. Therefore this wheel-type has to be used.

Using this results, the final design has a cylindrical wheel without any rounded shapes.

Appendix D

TESTBENCH 3-D MODELS

All the archives with the models used for the 3-D printed test-benches can be found in the following hyperlink:

Testbench 3-D Models

Appendix E

ARDUINO MICRO-CONTROLLER CODE FOR FINAL DESIGN

Code implemented in Arduino Nano in final design can be seen in the following github URL: **Arduino Micro-controller code**

Appendix F

ARDUINO CODE FOR DATA GATHERING USING SD CARD

Code implemented in Arduino UNO for data gathering using SD card can be seen in the following URL: **Arduino code for data gathering**

Appendix G

ELECTRONIC CIRCUIT USED FOR DATA GATHERING

The electronic circuit shown in figure G.1 was used to obtain the data for the analysis of the sytem and accuracy validation using an Arduino UNO.

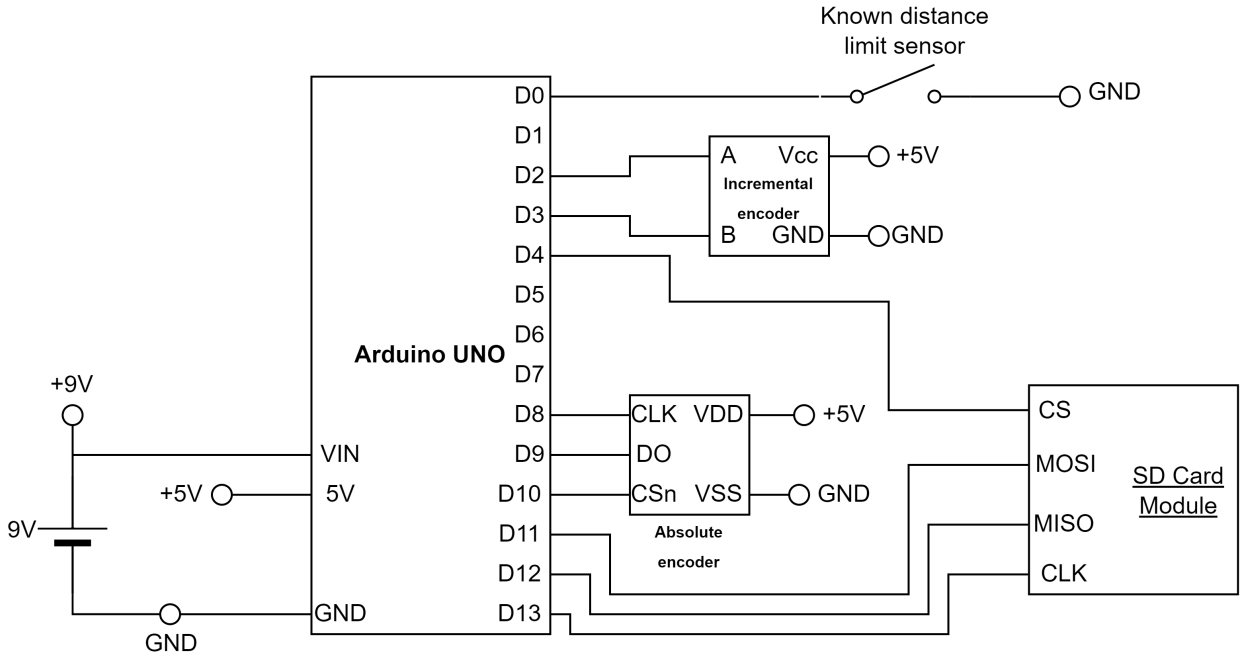

Figure G.1: Electronic circuit used for data gathering

Appendix H

CODE USED FOR TESTING THE TECHNOLOGIES

H.1 Code used for the CMOS sensor

The code used to track the movement of the cursor when moving the mouse for testing of said type of sensors can be seen in the following URL: **Code for mouse as CMOS sensor**

H.2 Code for rotary potentiometer angle detection

The code used to track the angle of a potentiometer used for testing of a rotary potentiometer can be seen in the following URL: **Rotary Potentiometer angle detection code**

H.3 Code for measuring magnetism using the hall effect proximity sensor

The code used to test the hall effect proximity sensor can be seen in the following URL: **Code for measuring Magnetism using the hall effect proximity sensor**

Appendix I

TECHNOLOGY TESTING DATA

Table I.1: Data from testing for computer vision camera: CMOS with laser sensor

Test #	Sensor	Real ΔY (mm)	ΔY 1 (Pixels)	ΔY 2 (Pixels)	ΔY 3 (Pixels)	ΔY 4 (Pixels)	ΔY 5 (Pixels)	ΔY Avg. (Pixels)	Precision (Pixels)	Relative Precision (%)
1	Genius GM-04003A	90.000 ± 0.025	244	294	158	126	167	197.8	168	84.934
2	Microsoft Basic	121.000 ± 0.025	662	675	668	656	656	663.4	19	2.865
3	Microsoft Basic	121.000 ± 0.025	566	549	584	590	597	577.2	48	8.310

Table I.2: Data from testing the rotary potentiometer

Test #	Real distance (±0.5 mm)	First measure	Second measure	Third measure	Fourth measure	Fifth measure	Average (mm)	Standard deviation	Resolution (mm)	Accuracy (mm)	Precision (mm)	Notes
1	55.0	56.66	55.16	55.07	56.45	54.11	55.49	1.06	0.21	0.49	2.55	Loss of precision due to friction
2	56.0	54.62	42.04	33.624	78	24.02	46.46	20.91	0.21	8.53	53.98	Too much torque required: Axis slipping

Table I.3: Data from testing the rotary encoder

Test #	Real distance (± 0.5 mm)	Measurement 1 (mm)	Measurement 2 (mm)	Measurement 3 (mm)	Measurement 4 (mm)	Measurement 5 (mm)	Average (mm)	Precision (mm)	Accuracy (mm)
1	180.0	179.82	179.82	179.82	179.7	179.7	179.772	0.12	0.228
2	180.0	179.53	179.8	179.53	178.99	179.53	179.476	0.81	0.524

Appendix J

SENSING PORTION OF THE SYSTEM ACCURACY STUDY

Results of the experimenting with the measuring device to obtain the average error of the system as accuracy can be seen in table J.1 for 107 samples, giving an average error of 0.679 mm, a maximum error of 2.55 with 77.57% of the error values below 1 mm.

This proportion of samples below 1 mm can be used to determine if the amount of samples taken is enough or if further experimentation should be done. Using Eq. 2.1 shown in the theoretical framework, knowing that if more than 50% ($e = (0.7757 - 0.5)/0.7757 =$) of samples have an error above 1 mm the device is likely to not fulfill the indicator of accuracy in position tracking, using Table A.3 from [13] for $alpha = 0.025$ for a confidence of 95%, yields z = -1.9., and finally substituting in Eq. 2.1, $n = \frac{(-1.9)^2 0.7757 * (1-0.7757)}{0.3554^2} = 5$, the number of samples necessary is of 5, which is way below the actual number of samples taken, rendering this validation adequate.

It is important to clarify that this experiment was performed without calibration in between measurements, but the first 2 experiments were used to calibrate (not shown as they do not represent the accuracy of the system).

Table J.1: Results for obtaining the accuracy of the measuring system

Experiment #	Sensed distance (mm)	Real distance (± 0.5mm)	Error (mm)
3	156.59	155.0	1.59
3	164.06	162.0	2.06
3	171.55	169.0	2.55
3	178.97	177.0	1.97
3	186.11	184.0	2.11
3	193.32	192.0	1.32
3	200.61	199.0	1.61
3	208.65	207.0	1.65
3	216.04	215.0	1.04
3	223.71	222.0	1.71

3	231.5	229.0	2.5
3	239.25	237.0	2.25
4	151.98	152.0	0.02
4	159.06	159.0	0.06
4	166.43	167.0	0.57
4	173.85	174.0	0.15
4	180.85	181.0	0.15
4	187.79	188.0	0.21
4	194.73	195.0	0.27
4	202.38	203.0	0.62
4	210.47	210.0	0.47
4	218.03	218.0	0.03
4	225.66	225.0	0.66
4	233.18	233.0	0.18
5	151.58	152.0	0.42
5	158.81	160.0	1.19
5	166.29	167.0	0.71
5	174.07	175.0	0.93
5	181.65	182.0	0.35
5	188.77	190.0	1.23
5	196.24	198.0	1.76
5	204.24	205.0	0.76
5	212.45	213.0	0.55
5	220.43	221.0	0.57
5	228.37	229.0	0.63
5	236.59	237.0	0.41
6	154.97	155.0	0.03
6	162.23	162.0	0.23
6	169.98	170.0	0.02
6	177.81	178.0	0.19

6	184.99	185.0	0.01
6	192.46	193.0	0.54
6	199.68	200.0	0.32
6	208.32	208.0	0.32
6	215.88	216.0	0.12
6	223.63	224.0	0.37
6	231.16	232.0	0.84
6	239.08	239.0	0.08
7	152.7	153.0	0.3
7	159.84	160.0	0.16
7	166.75	167.0	0.25
7	173.98	174.0	0.02
7	181.19	181.0	0.19
7	188.13	188.0	0.13
7	195.21	195.0	0.21
7	202.7	203.0	0.3
7	211.37	210.0	1.37
7	218.55	218.0	0.55
7	226.04	225.0	1.04
7	233.25	232.0	1.25
7	240.93	239.0	1.93
8	154.99	156.0	1.01
8	162.98	164.0	1.02
8	171.33	172.0	0.67
8	179.52	180.0	0.48
8	187.32	188.0	0.68
8	195.11	196.0	0.89
8	203.44	204.0	0.56
8	212.21	213.0	0.79
8	220.46	221.0	0.54

8	228.65	229.0	0.35
8	236.72	237.0	0.28
9	149.23	150.0	0.77
9	157.19	158.0	0.81
9	165.47	166.0	0.53
9	173.59	174.0	0.41
9	181.56	181.0	0.56
9	189.17	189.0	0.17
9	196.71	197.0	0.29
9	204.81	205.0	0.19
9	212.73	213.0	0.27
9	220.42	221.0	0.58
9	228.18	229.0	0.82
9	236.69	238.0	1.31
10	151.79	151.0	0.79
10	159.65	159.0	0.65
10	167.67	167.0	0.67
10	175.8	175.0	0.8
10	183.58	183.0	0.58
10	190.84	191.0	0.16
10	198.05	197.0	1.05
10	205.85	206.0	0.15
10	213.93	214.0	0.07
10	221.48	222.0	0.52
10	229.54	230.0	0.46
10	237.25	238.0	0.75
11	154.05	154.0	0.05
11	162.09	162.0	0.09
11	170.59	170.0	0.59
11	178.92	178.0	0.92

11	186.93	186.0	0.93
11	194.21	194.0	0.21
11	202.1	203.0	0.9
11	210.72	211.0	0.28
11	218.8	219.0	0.2
11	226.87	228.0	1.13
11	235.26	236.0	0.74

Appendix K

DRAWINGS FOR THE FINAL SOLUTION MANUFACTURING

A single file to 3D print all the manufactured pieces in one print with their specific configuration can be found in the following hyperlink: **3DPrintingCuraArchive**

The Solidwork models, assemblies and simulations can be found in the following hyperlink: **Solidwork archives**

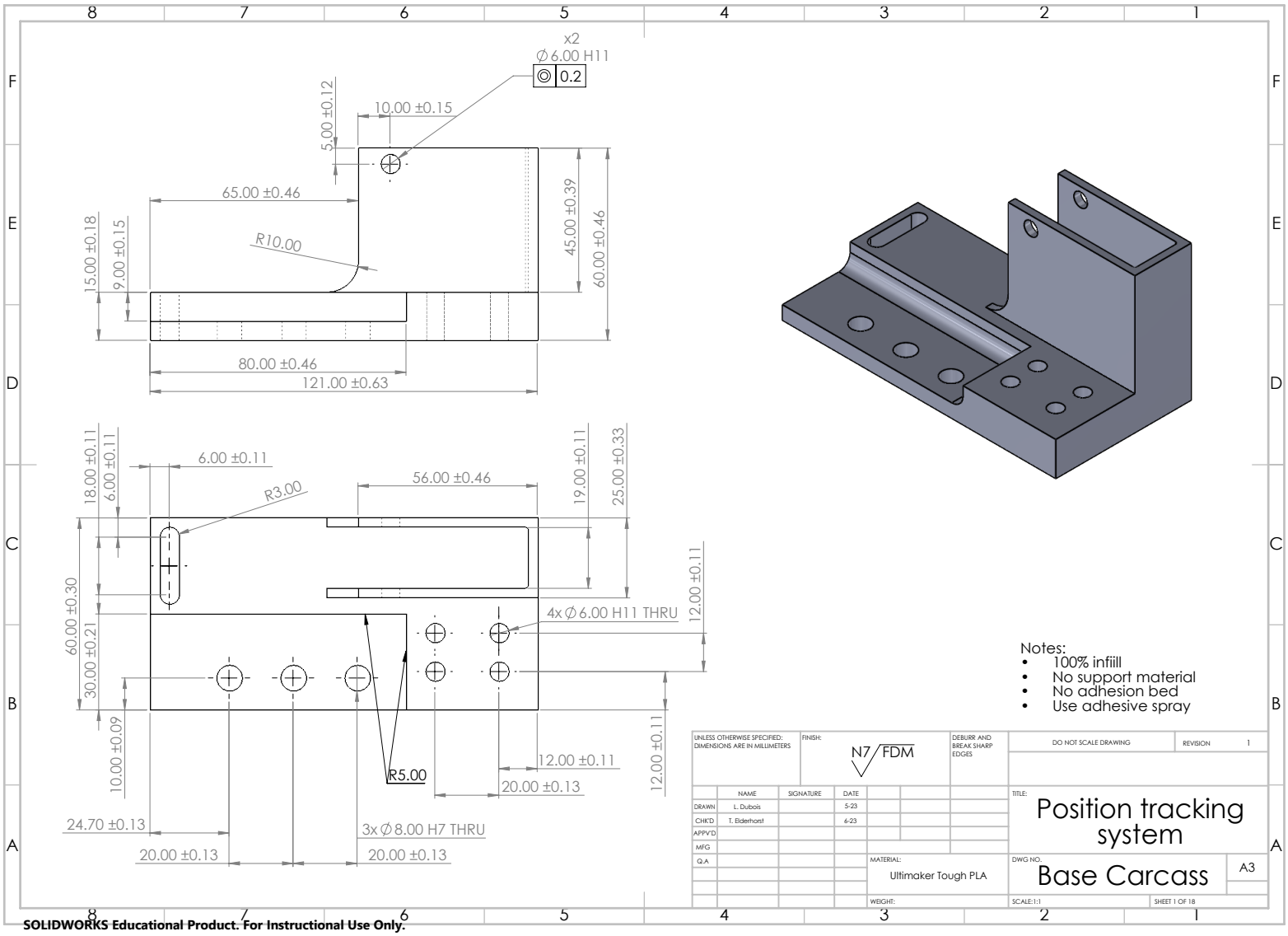

Notes:
- 100% infiill
- No support material
- No adhesion bed
- Use adhesive spray

UNLESS OTHERWISE SPECIFIED: DIMENSIONS ARE IN MILLIMETERS	FINISH: N7 FDM	DEBURR AND BREAK SHARP EDGES	DO NOT SCALE DRAWING	REVISION 1		
	NAME	SIGNATURE	DATE	TITLE: Position tracking system		
DRAWN	L. Dubois		5-23			
CHK'D	T. Biderhorst		6-23			
APPV'D						
MFG						
Q.A				MATERIAL: Ultimaker Tough PLA	DWG NO. Base Carcass	A3
				WEIGHT:	SCALE:1:1	SHEET 1 OF 18

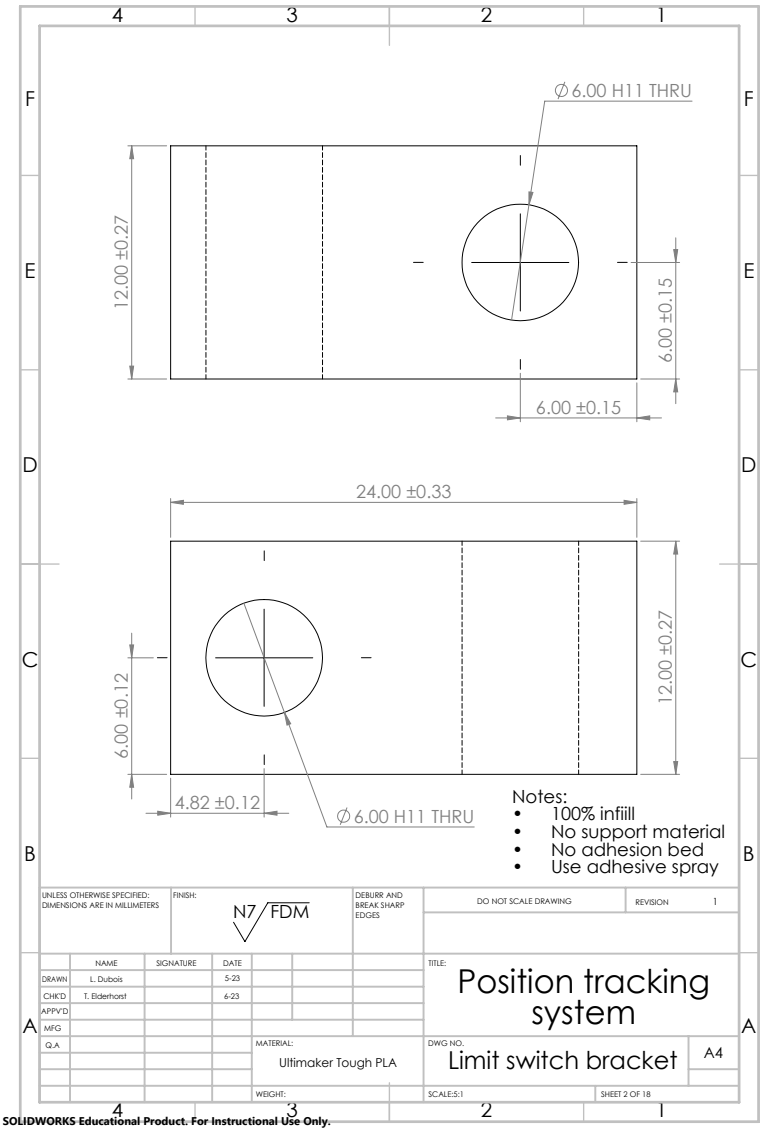

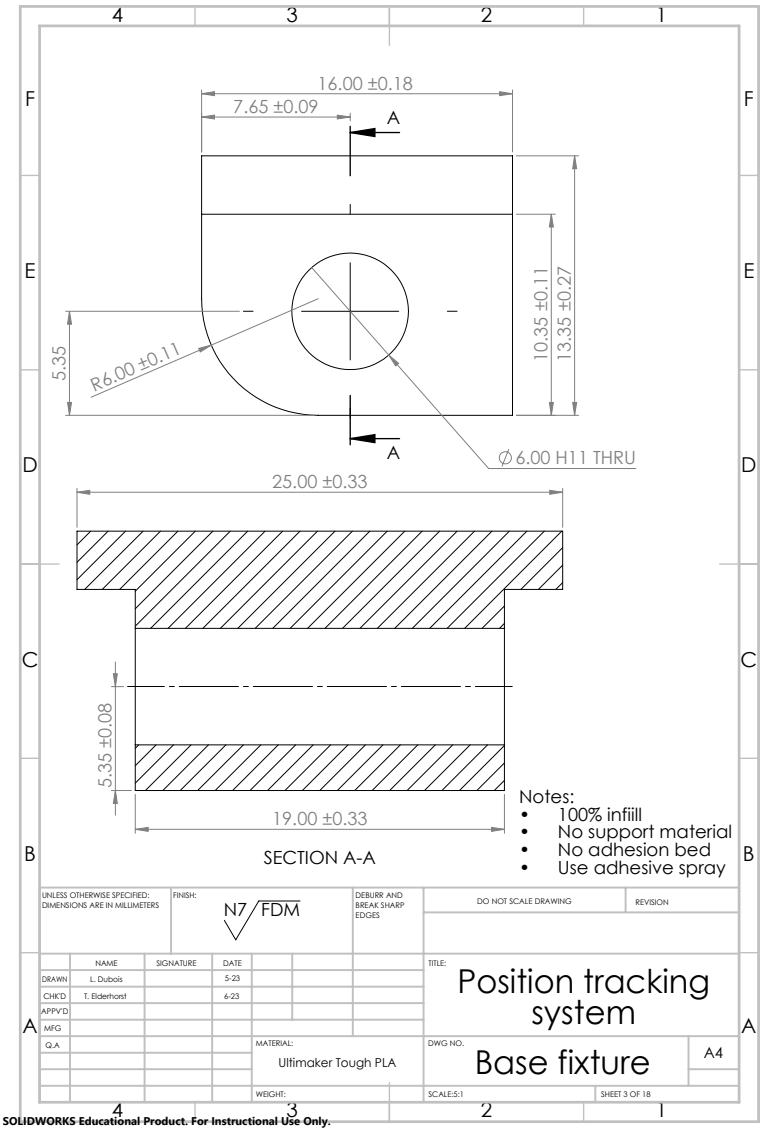

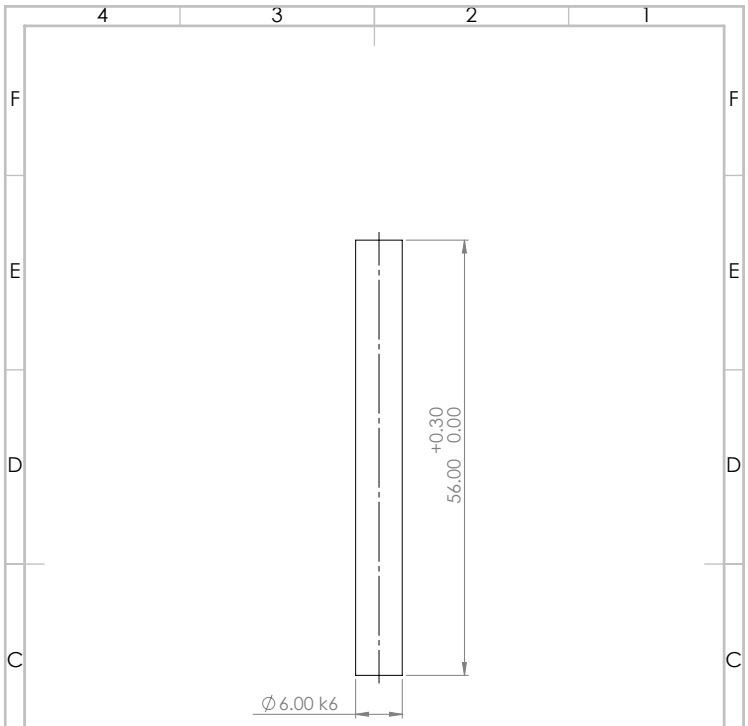

UNLESS OTHERWISE SPECIFIED: DIMENSIONS ARE IN MILLIMETERS SURFACE FINISH: TOLERANCES: LINEAR: ANGULAR:		FINISH: N7 Turning		DEBURR AND BREAK SHARP EDGES		DO NOT SCALE DRAWING		REVISION 1
	NAME	SIGNATURE	DATE			TITLE: Position tracking system		
DRAWN	L. Dubois		5-23					
CHK'D	T. Elderhorst		6-23					
APPV'D								
MFG								
Q.A				MATERIAL: Aluminum		DWG NO. Absolute encoder axis		A4
				WEIGHT:		SCALE:2:1	SHEET 4 OF 18	

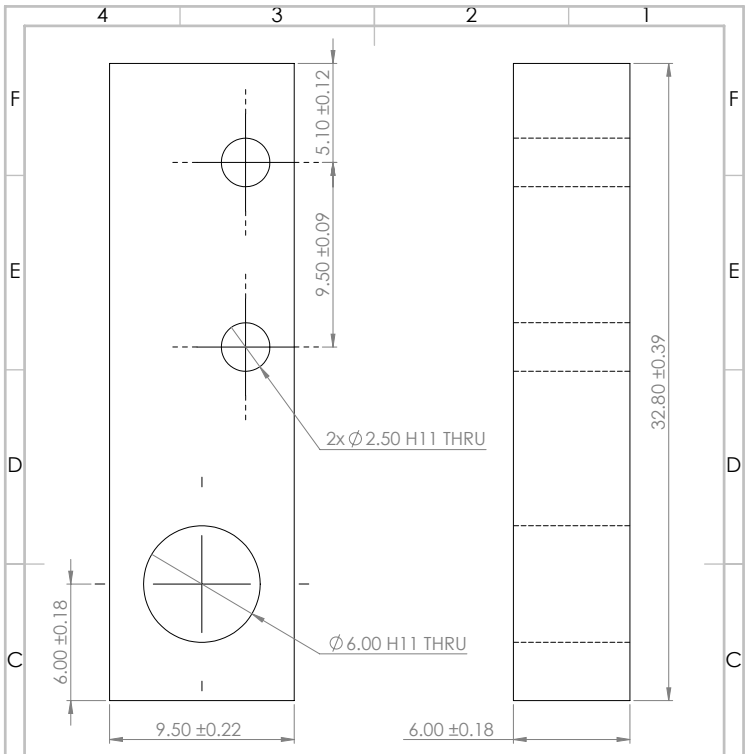

Notes:
- 100% infiill
- No support material
- No adhesion bed
- Use adhesive spray

UNLESS OTHERWISE SPECIFIED: DIMENSIONS ARE IN MILLIMETERS	FINISH: N7 FDM	DEBURR AND BREAK SHARP EDGES	DO NOT SCALE DRAWING	REVISION 1			
	NAME	SIGNATURE	DATE	TITLE: Position tracking system			
DRAWN	L. Dubois		5-23				
CHK'D	T. Elderhorst		6-23				
APPV'D							
MFG							
Q.A				MATERIAL: Ultimaker Tough PLA	DWG NO. Switch holder		A4
				WEIGHT:	SCALE:5:1	SHEET 5 OF 18	

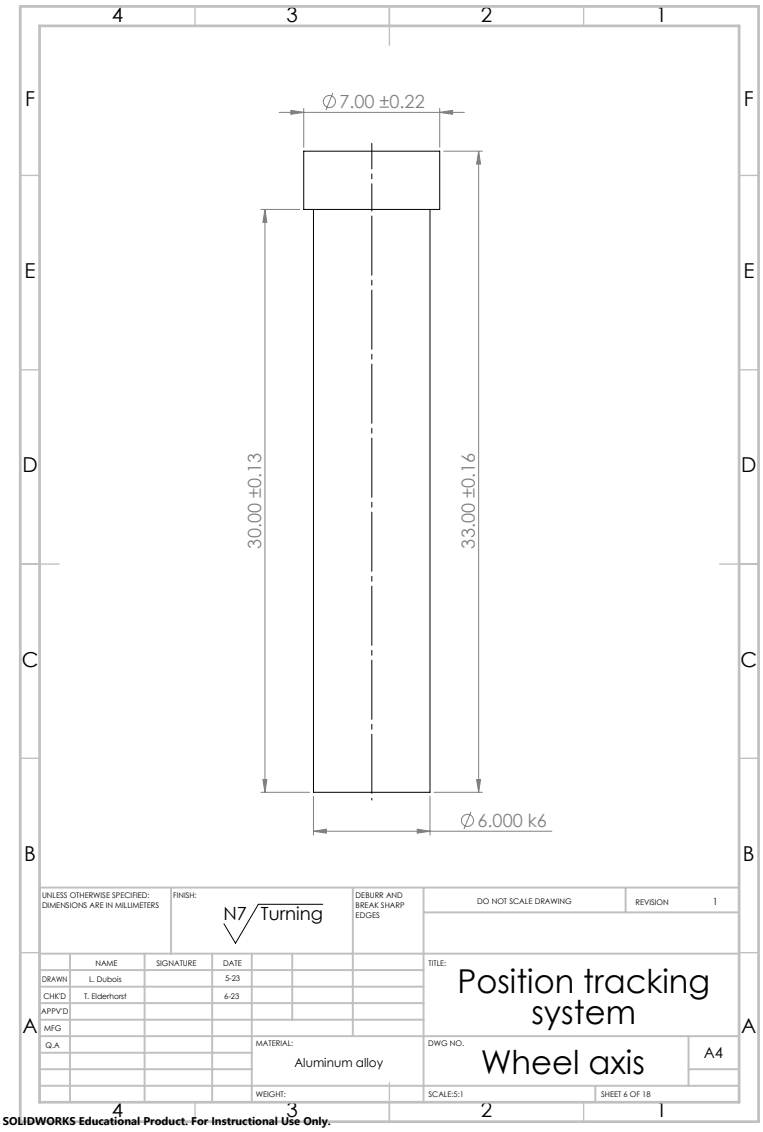

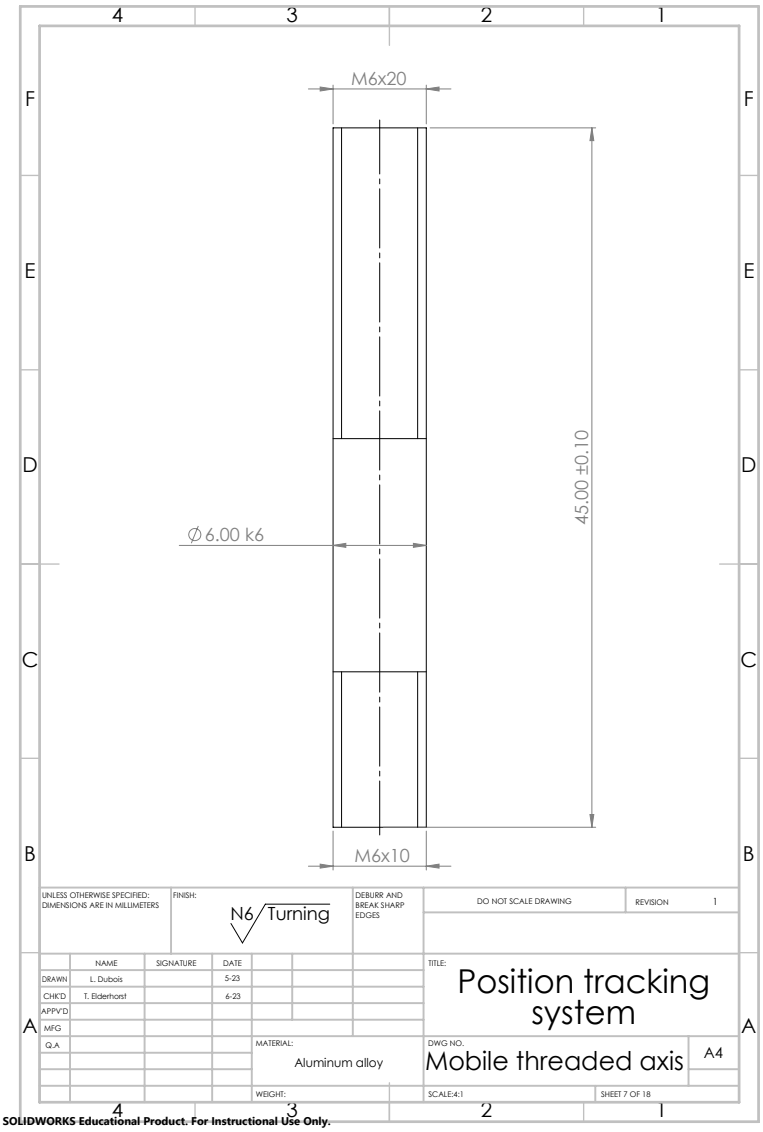

UNLESS OTHERWISE SPECIFIED: DIMENSIONS ARE IN MILLIMETERS	FINISH: N6 Turning			DEBURR AND BREAK SHARP EDGES	DO NOT SCALE DRAWING		REVISION	1
	NAME	SIGNATURE	DATE		TITLE: Position tracking system			
DRAWN	L. Dubois		5-23					
CHK'D	T. Elderhorst		6-23					
APPV'D								
MFG								
Q.A					MATERIAL: Aluminum alloy	DWG NO. Mobile threaded axis		A4
					WEIGHT:	SCALE:4:1	SHEET 7 OF 18	

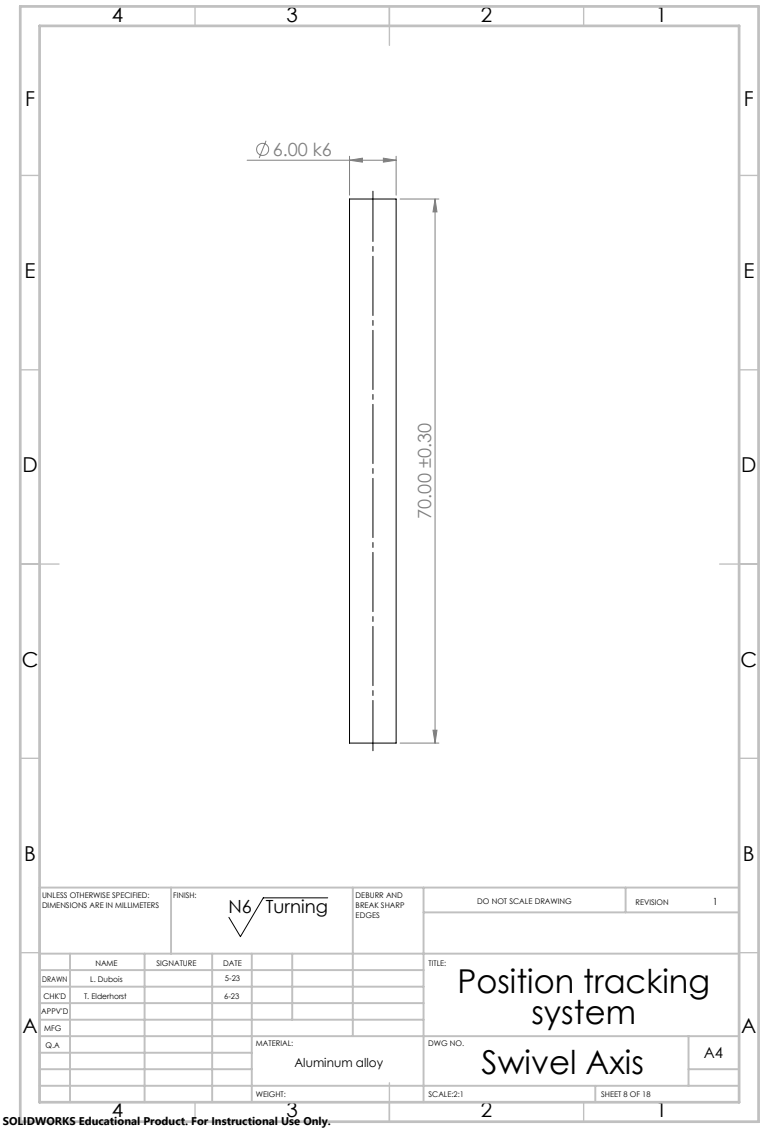

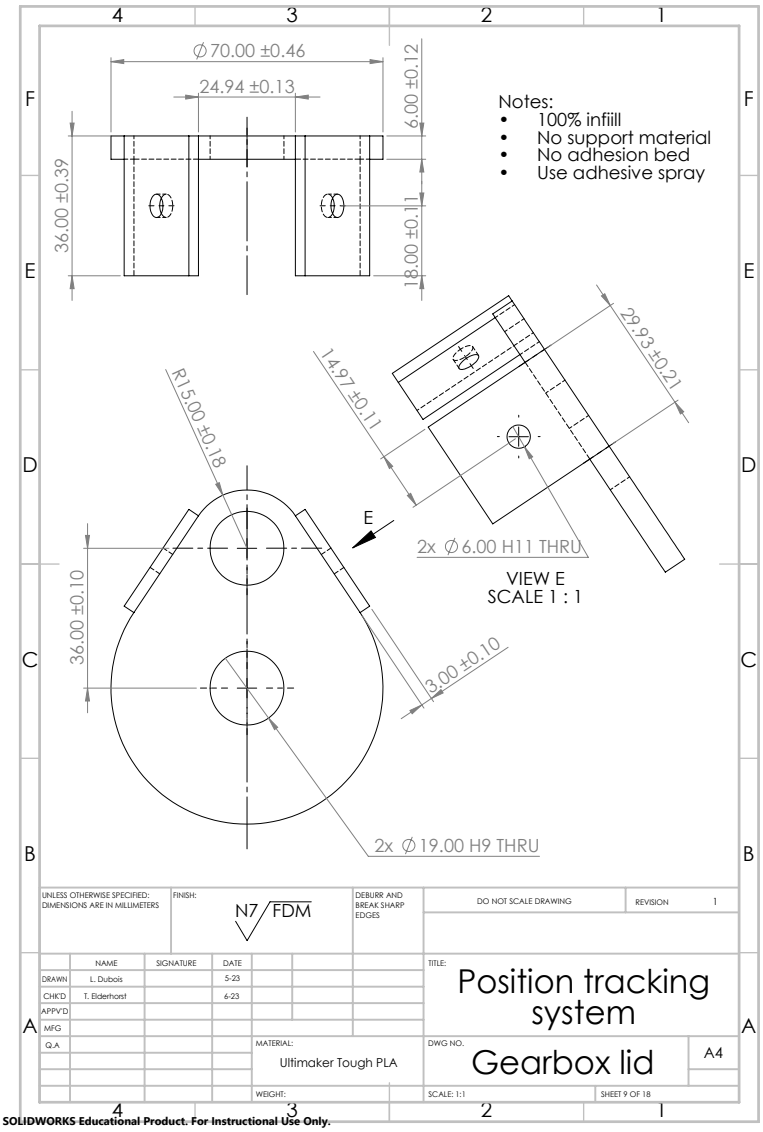

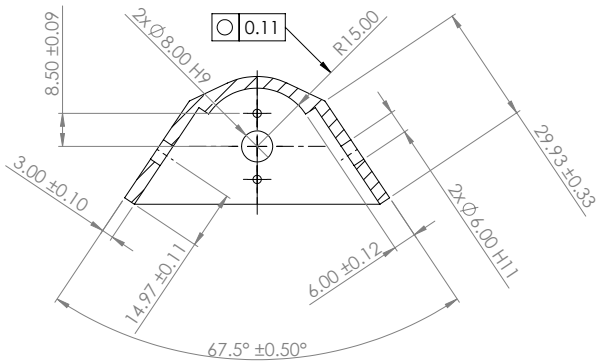

SECTION D-D

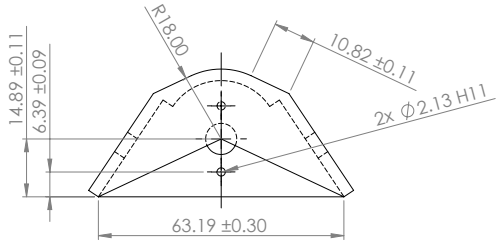

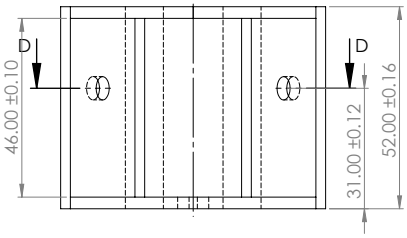

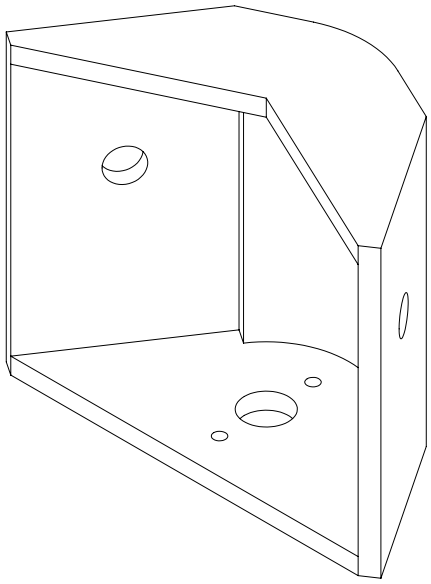

Scale 2:1

Notes:
- 100% infiill
- Use material
- No adhesion bed
- Use adhesive spray

UNLESS OTHERWISE SPECIFIED: DIMENSIONS ARE IN MILLIMETERS	FINISH: N7 FDM	DEBURR AND BREAK SHARP EDGES	DO NOT SCALE DRAWING	REVISION 1			
	NAME	SIGNATURE	DATE				TITLE: Position tracking system
DRAWN	L. Dubois		6-23				
CHK'D	T. Elderhorst		6-23				
APPV'D							
MFG							
Q.A				MATERIAL: Ultimaker Tough PLA			DWG NO. Gear cover A3
				WEIGHT:			SCALE:1:1 SHEET 10 OF 18

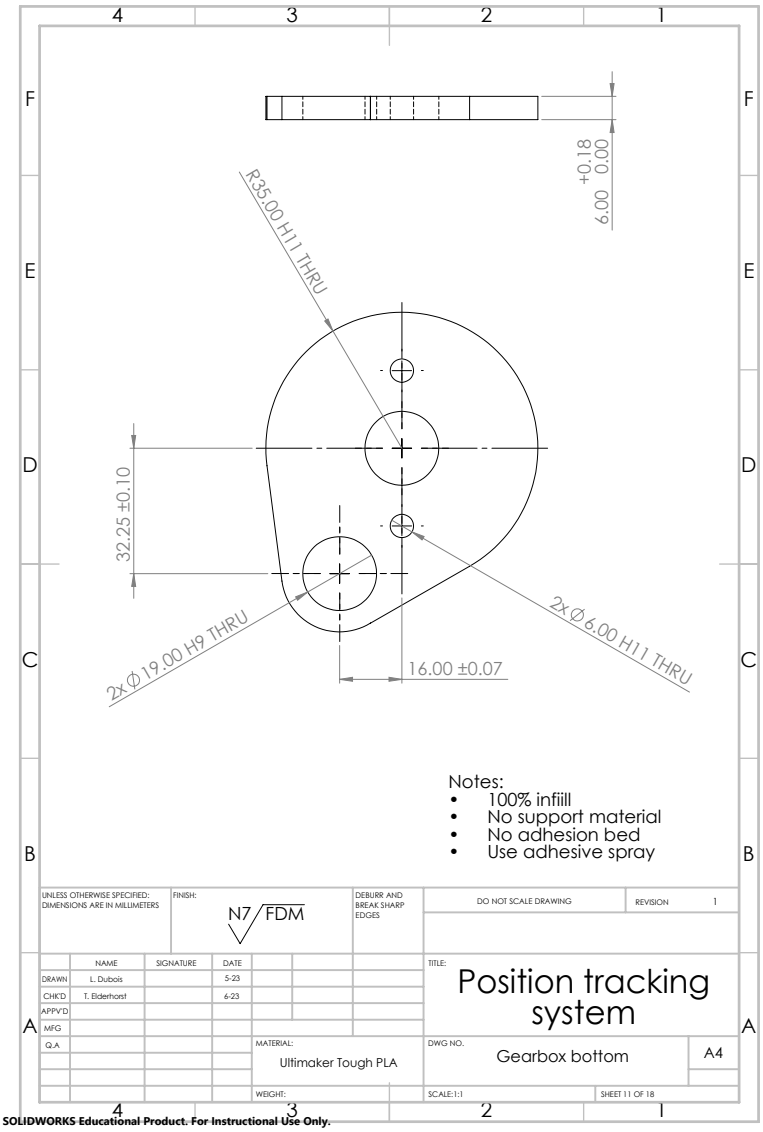

Notes:
- 100% infiill
- No support material
- No adhesion bed
- Use adhesive spray

UNLESS OTHERWISE SPECIFIED: DIMENSIONS ARE IN MILLIMETERS	FINISH: N7 FDM		DEBURR AND BREAK SHARP EDGES	DO NOT SCALE DRAWING	REVISION 1	
	NAME	SIGNATURE	DATE	TITLE: Position tracking system		
DRAWN	L. Dubois		5-23			
CHK'D	T. Elderhorst		6-23			
APPV'D						
MFG						
Q.A				MATERIAL: Ultimaker Tough PLA	DWG NO. Gearbox bottom	A4
				WEIGHT:	SCALE:1:1	SHEET 11 OF 18

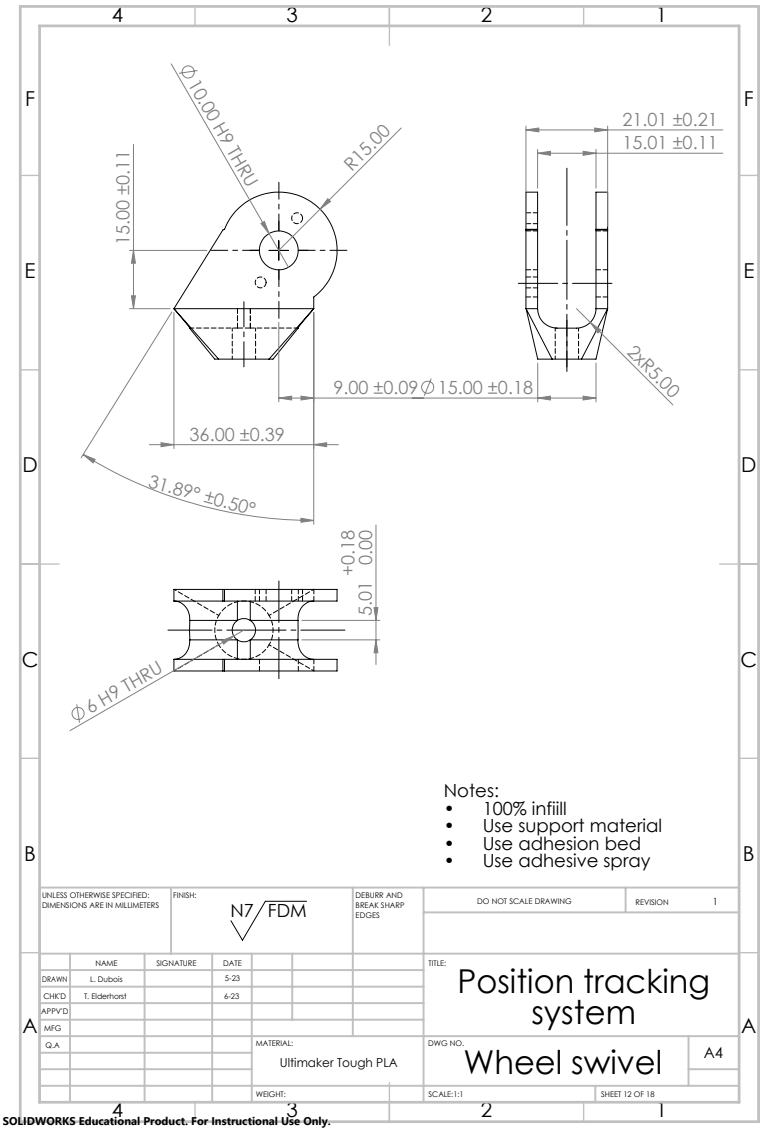

Notes:
- 100% infiill
- Use support material
- Use adhesion bed
- Use adhesive spray

UNLESS OTHERWISE SPECIFIED: DIMENSIONS ARE IN MILLIMETERS		FINISH: N7 FDM		DEBURR AND BREAK SHARP EDGES		DO NOT SCALE DRAWING	REVISION	1
	NAME	SIGNATURE	DATE			TITLE: Position tracking system		
DRAWN	L. Dubois		5-23					
CHK'D	T. Elderhorst		6-23					
APPV'D								
MFG								
Q.A				MATERIAL: Ultimaker Tough PLA		DWG NO. Wheel swivel		A4
				WEIGHT:		SCALE:1:1	SHEET 12 OF 18	

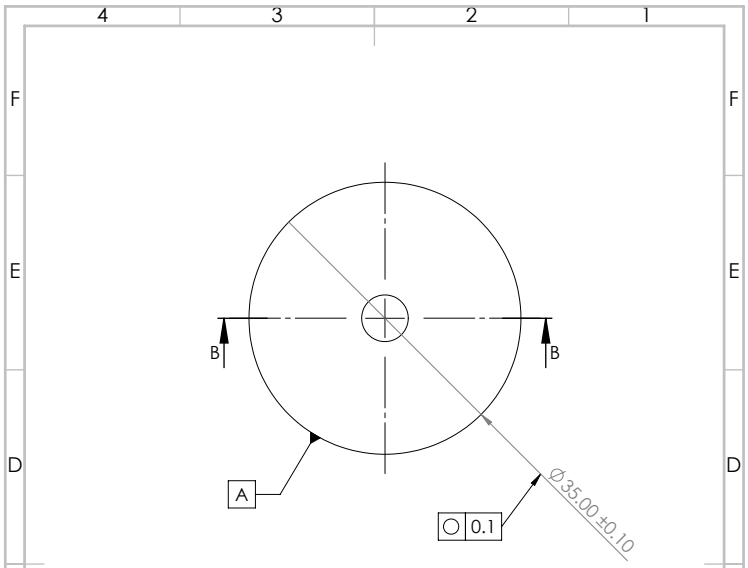

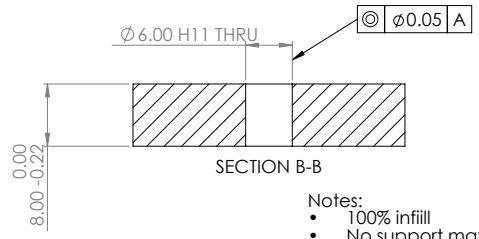

Notes:
- 100% infiill
- No support material
- No adhesion bed
- Use adhesive spray

UNLESS OTHERWISE SPECIFIED: DIMENSIONS ARE IN MILLIMETERS	FINISH: N7 FDM	DEBURR AND BREAK SHARP EDGES	DO NOT SCALE DRAWING	REVISION 1		
	NAME	SIGNATURE	DATE	TITLE: Position tracking system		
DRAWN	L. Dubois		5-23			
CHK'D	T. Elderhorst		6-23			
APPV'D						
MFG						
Q.A				MATERIAL: Ultimaker Tough PLA	DWG NO. Wheel	A4
				WEIGHT:	SCALE:2:1	SHEET 13 OF 18

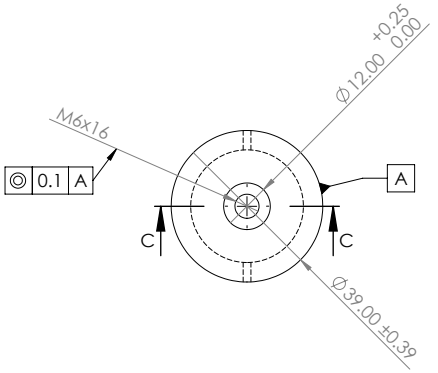

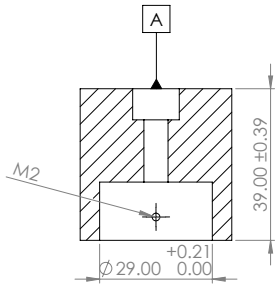

SECTION C-C

Notes:
- 100% infiill
- Use support material
- No adhesion bed
- Use adhesive spray

UNLESS OTHERWISE SPECIFIED: DIMENSIONS ARE IN MILLIMETERS	FINISH: N7 FDM		DEBURR AND BREAK SHARP EDGES	DO NOT SCALE DRAWING	REVISION 1	
	NAME	SIGNATURE	DATE	TITLE: Position tracking system		
DRAWN	L. Dubois		6-23			
CHK'D	T. Elderhorst		6-23			
APPV'D						
MFG						
Q.A				MATERIAL: Ultimaker Tough PLA	DWG NO. Torque wrench adaptor	A4
				WEIGHT:	SCALE:1:1	SHEET 14 OF 18

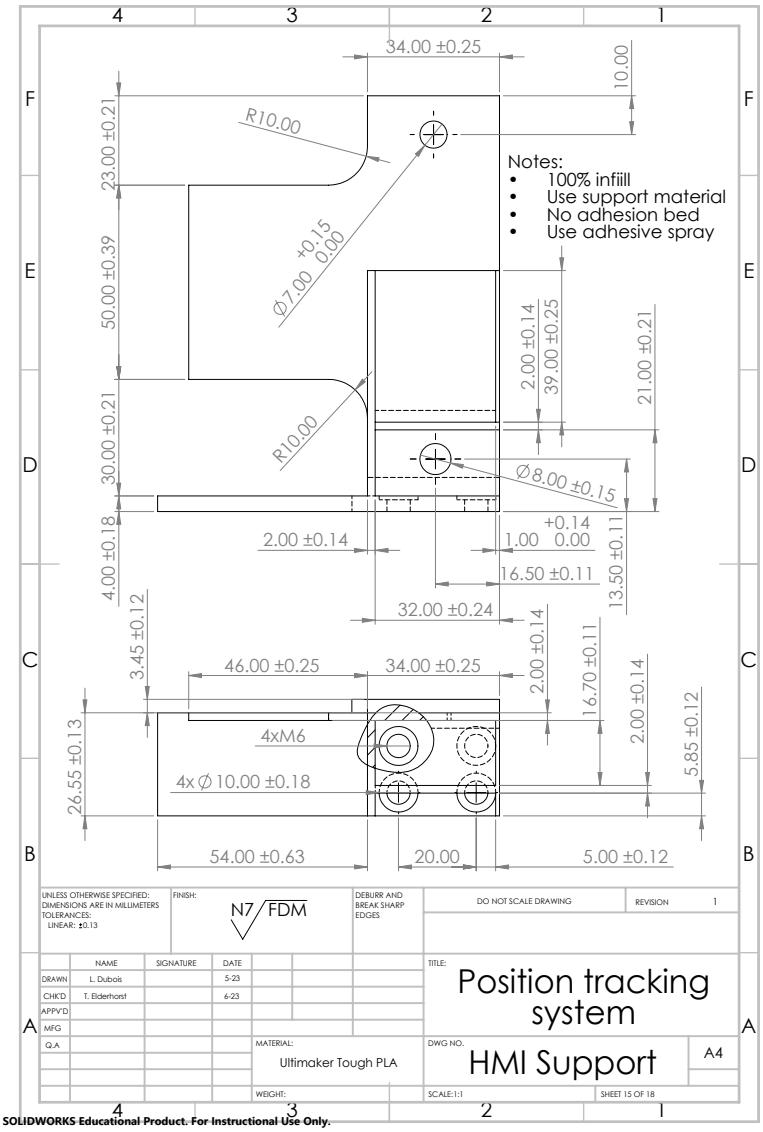

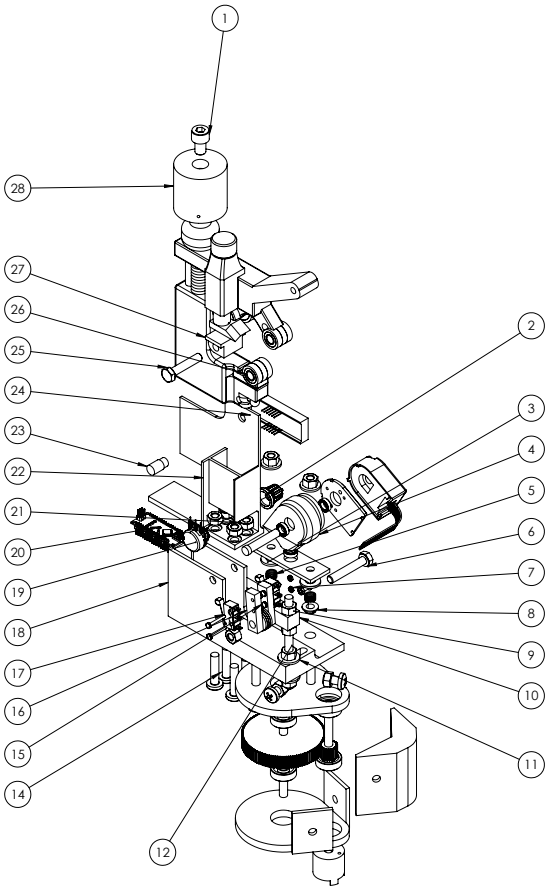

Notes:
- Arduino Nano is soldered into a perforated board
- 7 segment displays are soldered into a perforated board
- Perforated boards are glued onto their surfaces

ITEM NO.	PART NUMBER	Notes	QTY.
1	Steel M8 x 12 - 12N Screw		1
2	Rotary Knob		1
3	ISO 10673-7.4-S washer		2
4	Wheel assembly	Includes gearbox and measuring wheel system, seen in its own exploded viewin next sheet	1
5	Spring		2
6	Hex steel bolt M6		1
7	Steel M2 Nut		4
8	Iglidur Linear Bearing		2
9	Steel M6 Nut		3
10	Bracket for limit switch		1
11	ISO 10669-7.15-N Washer		6
12	80 mm threaded rod		1
13	Steel M6 Nut		2
14	Steel M6x25 Screw		4
15	Steel M2 x 16 screw		4
16	Mechanical switch holder		2
17	WLK-4MINI		2
18	Base carcass		1
19	Potentiometer		1
20	Arduino Nano		1
21	Narrow steel M6 Nut		4
22	HMI support		1
23	Button		1
24	Seven segment display		1
25	Steel M6 x 30 screw		1
26	US-7000		1
27	Holder		1
28	Torquewrench adaptor		1

UNLESS OTHERWISE SPECIFIED: DIMENSIONS ARE IN MILLIMETERS
FINISH:
DO NOT SCALE DRAWING
REVISION

	NAME	SIGNATURE	DATE
DRAWN	L. Dubois		6-23
CHK'D	T. Elderhorst		6-23
APP'VD			
MFG			
Q.A			

MATERIAL:
WEIGHT: 0.68 kg
SCALE:1:2
SHEET 16 OF 18

TITLE:
Position tracking system
Exploded view
DWG NO.
A2

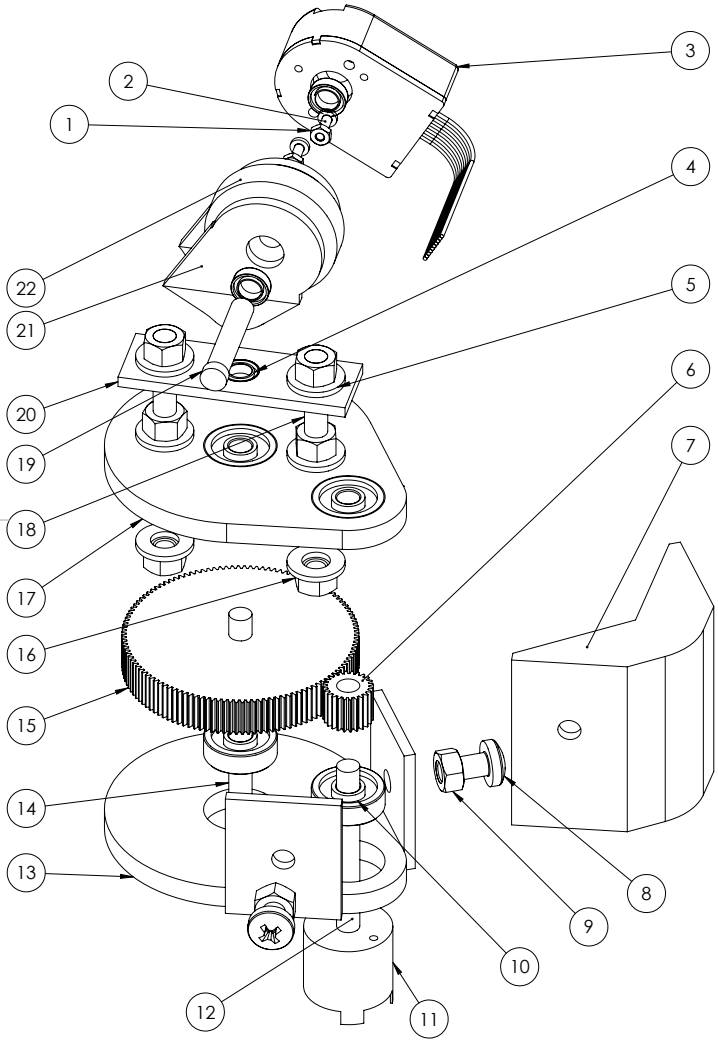

ITEM NO.	PART NAME	QTY.
1	Steel M2.5 nut	2
2	Steel M2.5 x 8 screw	2
3	Optical Encoder HEDL-5540-A12	1
4	NMB Radial Ball Bearing - Shielded End Type, 6mm I.D, 10mm O.D	3
5	ISO 10673-7.4-S washer	6
6	ISO - Spur gear 0.5M 24T 20PA 10FW	1
7	Gear cover	1
8	Steel screw M6 x 12	2
9	Steel M6 Nut	2
10	ISO 15 ABB - 026 - 8,SI,NC,8_68 Bearing	4
11	Broadcom Mechanical encoder 6mm shaft	1
12	Inbetween axis	1
13	Gearbox lid	1
14	Swivel axis	1
15	ISO - Spur gear 0.5M 120T 20PA 10FW	1
16	Steel M6 Nut	6
17	Wheel bracket spring support	1
18	Mobile threads	2
19	Wheel axis	1
20	Wheel bracket	1
21	Wheel swivel	1
22	Wheel	1

UNLESS OTHERWISE SPECIFIED:
DIMENSIONS ARE IN MILLIMETERS

DO NOT SCALE DRAWING | REVISION 1

	NAME	SIGNATURE	DATE
DRAWN	L. Dubois		6-23
CHK'D	T. Elderhorst		6-23
APPV'D			
MFG			
Q.A			

TITLE:

Position tracking system

DWG NO. Exploded view of wheel assembly | A3

WEIGHT: | SCALE:1:1 | SHEET 17 OF 18

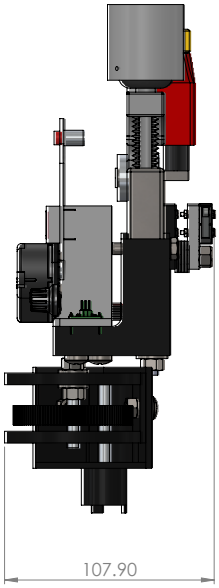

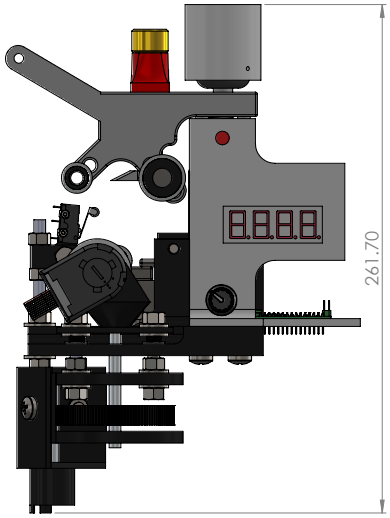

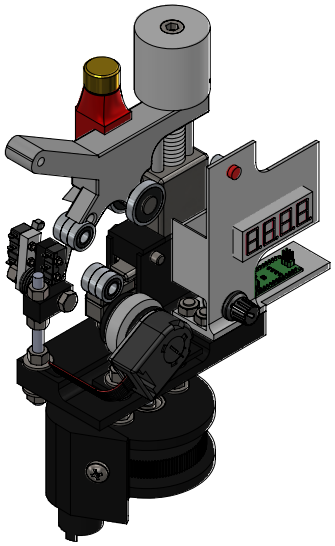

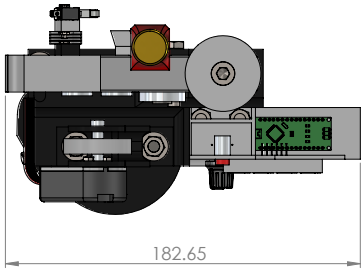

UNLESS OTHERWISE SPECIFIED: DIMENSIONS ARE IN MILLIMETERS						DO NOT SCALE DRAWING	REVISION 1
	NAME	SIGNATURE	DATE			TITLE: Position tracking system	
DRAWN	L. Dubois		6-22				
CHK'D	T. Elderhorst		6-23				
APPV'D							
MFG							
Q.A						DWG NO. Assembly	A3
				WEIGHT: 0.68 kg		SCALE:1:2	SHEET 18 OF 18